Elucidating mechanisms of action of bioactive substances by chemical-genetic profiling

by

Imelda Galván Márquez

A thesis submitted to the Faculty of Graduate and Postdoctoral

Affairs in partial fulfillment of the requirements for the degree of

Doctor of Philosophy

in

Department of Biology,
Ottawa-Carleton Institute of Biology

Carleton University
Ottawa, Ontario

General Abstract

The need for the development of antimicrobial agents has increased considerably due to emerging pathogens, bioterrorism and antimicrobial resistance (Spellberg et al., 2003). As antimicrobial resistance (AMR) is a worldwide public health concern, identification of inhibitory substances that effectively overcome this problem is urgently needed. This study aimed to investigate the modes of inhibitory activity of a variety of chemical species, the biopolymer chitosan, zinc oxide and silver nanoparticles (ZnONPs and AgNPs), the bacteriocin nisin, and a crude bacterial extract with a putative, uncharacterized bacteriocin. I used large-scale phenotypic screens performed with *Saccharomyces cerevisiae* and/or *Escherichia coli* for these functional genomics studies, followed by mechanistic studies to confirm the cellular pathways elucidated by the the large-scale phenotypic screens performed using non-essential gene deletion sets (*Saccharomyces cerevisiae* and *Escherichia coli*).

The antifungal mode of action of chitosan was investigated using the *S. cerevisiae* deletion mutant set (≈4600 mutants). This functional analysis supported the standing hypothesis that chitosan perturbs membrane functions and revealed an additional novel mode of action: mutants with deletions in a set of genes related to protein synthesis were very sensitive to chitosan. Disruption of protein synthesis was confirmed by a β-galactosidase expression assay suggesting that this is a primary mode of antifungal action by chitosan.

The antifungal and cytotoxic modes of action of ZnONPs and AgNPs were also investigated using the *S. cerevisiae* deletion mutant set. The large-scale phenotypic screen for ZnONPs showed that mutants lacking genes involved in transmembrane and membrane transport, cellular ion homeostasis and cell wall organization or biogenesis exhibited high sensitivity to ZnONPs. Secondary assays confirmed that ZnONPs cause disruption and depolarization of cell membrane and, in addition, alter cell wall integrity in yeast. In contrast, mutants lacking genes involved in transcription and RNA processing, cellular respiration, and endocytosis and vesicular transport were highly sensitive to AgNPs. For AgNPs, reduction of transcription, disruption of the electron transport chain performance and interference with endocytosis were confirmed by secondary assays.

The antibacterial mode of action of nisin was investigated using an *E. coli* mutant set (Keio) comprising ≈4000 mutants. Large-scale phenotypic screening indicated that nisin interferes with the following processes: cell wall/membrane/envelope biogenesis, cell cycle and DNA replication, recombination and repair. A DNA content assay based on flow cytometry suggested that nisin may interfere with DNA synthesis as a mode of action.

Finally, the antimicrobial mode of action of a fermented supernatant produced by *Bifidobacterium breve* was investigated using the *E. coli* Keio mutant set. Results from the large-scale phenotypic screen indicated that the bifidobacterial supernatant interferes with carbohydrate transport and metabolism, intracellular trafficking, secretion and vesicular transport, and energy production and conversion. Mechanistic studies are further required to confirm the affected cellular pathways revealed by this chemical-genetic profile.

Dedication

This dissertation is dedicated to my parents, Imelda Márquez and Víctor Galván who taught me the value of love, sacrifice, commitment and hard work in life. To my siblings Lorena, Víctor and Luis who always have supported me.

I would also like to dedicate this dissertation to my beloved family, my children Oscar, Alejandro, Daniela and Diego, and my husband Oscar. I like to thank them for all their support, encouragement, understanding, sacrifice and great love, you made possible this great achievement. Without you in this challenging journey I would not have been able to accomplish this important goal in my life. This is a special dedication to my life partner and best friend, my beloved husband who supported me unconditionally along this exciting journey.

Acknowledgements

I would like to express my immense gratitude to the best supervisors I could ever ask for, Dr. Myron L. Smith and Dr. Ashkan Golshani. I greatly and sincerely appreciate the opportunity they gave me to pursue this doctoral degree even knowing that I did not have a Science background and my knowledge of English was very basic. I am grateful for the trust they placed on me and for providing me the opportunity of acquiring scientific knowledge and academic skills.

There are not sufficient words to thank Dr. Myron L. Smith and Dr. Ashkan Golshani for their impressive patience, right advice even at the most difficult time, wise guidance, encouraging support, understanding, approachability and friendship. All my gratitude to the members of my committee, Dr. Alexandre Poulain, Dr. Anatoly Ianoul, Dr. Alex Wong and Dr. Catherine Carrillo, for their advice and time.

I like to extend my gratitude to the Dr. John Arnason, Dr. Jose Antonio Guerrero, Dr. Alex Wong, Dr. Bruce McKay, Dr. Farah Hosseinian, Dr. Apollinaire Tsopmo, Dr. Jayne Yack, Dr. Mihaela Flueraru, Dr. Kishore Murthy, Dr. Bill Willmore, Dr. John Vierula, Dr. James Cheetham, Dr. Dele Ogunremi and to all scientists that in at some point made significant contributions in different ways (knowledge, advice, equipment, material, chemicals, time, etc.) which allowed me to successfully complete my research goals and to continue until the end of this way.

I like to thank also to the Department of Biology for all the support I received. I like to express my gratitude to Laura Thomas, Darlene Moss, Lisa Chiarelli, Michelle O'Farrell, Caitlyn McKenzie and Ruth Hill-Lapensee who certainly provided great support with the administrative issues. Thanks to Ed Bruggink for his great support and for making himself available for all the unexpected technical issues.

I am very grateful to many other colleagues for their invaluable support, knowledge and skills sharing, and great friendship that made this challenging journey easier to continue in. Many thanks to Bahram Samanfar, Katie Omidi, Isabel Cruz, Dennis Lafontaine, Matthew James Meier, Ryan Reshke, Anatoly Belov, Mohsen Hooshyar, Le Hoa Tan, Houman Motesharei, Bodunde Olanike, Mergan Ghiyasvand, Jones Akuaku, Daniel Burnside, Maryam Karimloo, Chieu Anh Ta, Roberto Gutiérrez and my undergraduate students Fatima Haider, Melissa Graf, Jessica Parsons and Steven Bugiel for their hard work.

I like to express my gratitude also to all my friends for their understanding, love and for their words of encouragement and support that always gave me along my studies.

My great gratitude to Carleton University for this enriching learning opportunity and for offering a very welcoming and friendly environment to the students.

This work was partially funded by an Ontario Graduate Scholarship (OGS).

Statement of contribution

This dissertation "Elucidating mechanisms of action of bioactive substances by chemical-genetic profiling" is composed by four studies. I did the writing of the thesis with editing by Drs. Golshani and Smith.

Chapter 2: Disruption of protein synthesis as antifungal mode of action of chitosan. I collaborated in the design and development of the study. Jones Akaku under my training and supervision performed the phenotypic screening with the yeast mutant set. Isabel Cruz assisted us with the liposome assay. I carried out the β-galactosidase assay, and functional analysis of the GDA trials. This research work has been published in 2013 and I was the first author (Galván et al., 2013).

Chapter 3: Effects of zinc oxide and silver nanoparticles on [chemical-genetic profile in] Yeast (*Saccharomyces cerevisiae*). Andrey Massaskry did the chemical characterization of the nanoparticles used in this study. Mergan Ghiyasvand carried out the chemical-genetic profiles for ZnONPs and AgNPs, trypan blue assay and cell wall integrity assay; confirmatory assays for ZnONPs mode of action. Ardeshir Golshani did the preliminary phenotypic analysis (colony size determination). The liposome assay and cell membrane depolarization assay for ZnONPs, the endocytosis assay, the electron transport chain performance (MTT) assay and the β-galactosidase assay for AgNPs, and the functional analysis for ZnONPs and AgNPs were realized by myself.

Chapter 4: Mode of action of the bacteriocin nisin on the bacterium Gram-negative, *Escherichia coli.* Experimental design, development and data analysis were done by me. Under my supervision, Jessica Parsons contributed to this study by standardizing the positive control for the plasmid replication assay. Under my supervision, Melissa Graf realized the plasmid replication assay testing the *E. coli* deletion mutants and minimum inhibitory concentrations of nisin for ciprofloxacin-resistant mutants. The standardization of the nisin-citric acid antimicrobial assay with *E. coli* cells, the phenotypic and functional analysis, liposome assay, minimum inhibitory concentrations of nisin for DNA-related deletion mutants and DNA content analysis were done by myself.

Chapter 5: Antimicrobial factors produced by *Bifidobacterium breve*, a probiotic. Experimental design and development of this study and all experiments were executed by me.

Table of Contents

List of Tables

List of Figures

List of Appendices

List of Abbreviations

µg	Microgram
µl	Microliter
6-AU	6-azauracil
AMR	Antimicrobial resistance
ANOVA	Analysis of variance
ATP	Adenosine triphosphate
BHI	Brain heart infusion medium
CA	Citric acid
CCCP	Carbonyl cyanide 3-chlorophenylhydrazone)
CF	Carboxyfluorescein
CFS	Cell free supernatant
CFU	Colony forming unit
COG	Clusters of Orthologous Groups
cps	Centipoise (viscosity unit)
CTAB	Cetyl trimethylammonium bromide
$DiSBAC_2(3)$	Bis-(1,3-Diethylthiobarbituric Acid)Trimethine Oxonol
DMSO	Dimethyl sulfoxide
DNA	Deoxyribonucleic acid
DOPC	Dioleoylphosphatidylcholine
EDTA	Ethylenediaminetetraacetic acid
ENM	Engineered nanomaterials
ETC	Electronic transport chain
F6PPK	Fructose-6-phosphate phospho-ketolase
FC	Flow cytometry
FSC	Forward scatter
G418	Geneticin
GAL1	Galactokinase
GDA	Gene deletion array
Gyr	Gyrase
HIP	Drug-induced haplo-insufficiency profiling
HOP	Homozygous profiling
HSD	Honest significant difference
HTS	High throughput screening
KDa	Kilo Daltons
KOGs	Eukaryotic orthologous groups
l	Liter
LacZ	β-galactosidase
LB	Luria Bertani
LMW	Low molecular weight
LPS	Lipopolysaccharides
LUV	Large unilamellar vesicles
LY	Lucifer yellow
MDR	multi-drug resistance
MES	2-morpholinoethanesulfonic acid

mg	Milligram
MIC	Minimum inhibitory concentration
ml	Milliliter
MRS	De Man Rogosa and Sharpe
MRS-C	De Man Rogosa and Sharpe medium supplemented with cysteine hydrochloride
MSP	Multi-copy suppression profiling
MTT	3-(4,5-dimethylthiazol-2-yl)-2,5-diphenyltetrazolium bromide
MUB	4-methylumbelliferone
MUG	4-methylumbelliferyl-D-galactopyranoside
NaN_3	Sodium azide
NCBI	National Center for Biotechnology Information
nm	Nanometers
NPs	Nanoparticles
NTS	Non-typhoidal Salmonella
OD	Optical density
OM	Outer membrane
ONPG	ortho-Nitrophenyl-β-galactoside
PCR	Polymerase chain reaction
PI	Propidium iodide
RCM	Reinforced Clostridium medium
RNA	Ribonucleic acid
ROS	Reactive oxygen species
SC-URA	Synthetic medium lacking uracil
SDS	Sodium dodecyl sulfate
SGD	Saccharomyces genome database
SOL	Spot on the lawn assay
SSC	Side scatter
STEM	Scanning transmission electron microscope
TLC	Thin layer chromatography
Tris-HCl	Hydroxymethyl-aminomethane hydrochloride
TSB	Tryptic soy broth
WDA	Well diffusion assay
WT	Wild type
X-gal	5-bromo-4-chloro-3-indolyl-β-D-galactopyranoside
YKO	Yeast knockout collections
YPD	Yeast petone dextrose medium
λ	(lambda) wavelength

Chapter 1

General Introduction

The need for the development of antimicrobial agents has increased considerably in recent years due to immerging infectious diseases, bioterrorism and antimicrobial resistance (Spellberg et al., 2003). Emerging 'superbugs' such as methicillin-resistant *Staphylococcus aureus* (MRSA), fluoroquinolone-resistant *Escherichia coli*, *Pseudomonas aeruginosa* and non-typhoidal *Salmonella* spp. (NTS), among others, raises a great threat to the public health (WHO, 2014). Continuous discovery and development of novel drugs with distinct mechanisms of action or molecular targets is required to counteract this problem (Anderson, 2005).

The first uses of antibiotics in the 20th century had a great impact counteracting life-threatening infections and decreasing mortality rates (Powers, 2004). Since then, antibiotics have been successfully and widely used, and antimicrobial discovery was encouraged to continue. The initial stages of the antimicrobial discovery were based on fortuitous findings such as the discovery of penicillin by Alexander Fleming in 1928. Later on (1940-1960), systematic empirical screens of soil and fungal extracts were used to investigate potential antagonist substances (Waksman screening platform) through inhibition-of-growth-assays. Fungal, microbial, algal, animal and plant-derived substances as well as plant by-products have been exploited for antimicrobial discovery (Gyawali et al., 2014) and will continue providing leads for future antimicrobial investigations.

During this period the discovery of antimicrobials was very successful and this period was called the “Golden Age”. Microbial-derived antibiotics such as β-lactams, aminoglycosides, tetracyclines, macrolides, glycopeptides and streptogramins were discovered in this era; however some of their mechanisms of action and even their mode of action were elucidated decades later (Silver, 2011; Singh, 2014). “Mechanism of action” is defined in pharmacology as the effect of the direct interaction between the antagonic compound and the molecular target (blocking receptors, inhibiting specific enzymes, etc.). “Mode of action” is defined as the overall effect exerted by a drug after interacting with the molecular target (inhibition of cell wall synthesis, protein synthesis, etc.).

Unfortunately, the selective pressure due to the use of antimicrobials inevitably caused the emergence of antimicrobial resistance in pathogens. With the emergence of antimicrobial resistance, the discovery of new antimicrobial substances, with unique modes of action, was required.

In the 90’s, antimicrobial discovery changed from a phenotype-based approach to target-based approach and from screening natural substances to synthetic substances. The focus shifted to identification of novel targets (target-based approach) in pathogens and discovering or designing molecules able to inhibit the identified targets (Mecke and Mascher, 2011). The interest in generating synthetic antagonist substances such as quinolones was increased and through chemical modification, six generations of antibiotics with improved efficacy and potency were produced (Singh, 2014).

With the 'genomics era' that initiated with sequencing of the complete genome of the *Haemophilus influenzae*, identification of some potential antimicrobial targets was achieved, and it was assumed that essential, conserved bacterial proteins would be useful targets for high-throughput screening (HTS) assays which consisted of evaluating the drug target (protein) interaction with the chemicals under study (binding assay).

Unfortunately, in most cases, when promising substances were tested *in vitro* whole-cell assays, results were not satisfactory due to the fact that the majority of the molecules were not able to penetrate cells or were pumped out the cells. This failure discouraged pharmaceutical industry from continuing with antimicrobial development (Payne et al., 2007; Livermore, 2011; Lewis et al., 2013). Nevertheless, the problem of antimicrobial resistance and multi-drug resistance (MDR) continues to increase world-wide in some pathogens (Hughes and Karlén, 2014).

Other approaches such as RNA profiling and proteomics provided scientists with unique opportunities to investigate drug targets in a high-throughput manner. One of the early examples of such techniques is DNA/RNA microarrays. In this approach, changes in gene expression profiles in response to the presence of a bioactive compound or environmental stress were used to study the mode of activity of the target compound (Miller and Tang, 2009). Likewise, proteomic analysis provides insights into bacterial responses to antimicrobials. Similarities in protein expression profiles in response to antibiotic exposure could be used to study the mode of activity of unknown antimicrobials (Bandaw et al., 2003). However, the use of proteomics for drug discovery is limited due

to technical challenges such as proteome heterogeneity (unique proteome for a specific situation or within species variation), and low abundance of key proteins (sensitivity), or loss of protein during analysis/fractionation (Kopec et al., 2005).

The advances in chemical genetics, chemical genomics and informatics, provided important tools that allowed a genome-wide phenotype-screening approach for antimicrobial discovery, and perhaps more important, for the elucidation of mode of action of antimicrobial substances. The use of chemical-genetic profiling to gain insights into the mode of action of antagonists substances represents an advantage over the RNA profiles. The genome-wide transcription profiles do not reflect all regulatory processes in the cell such as, post-translation modifications that may alter the concentration of the synthesized active protein and translation regulatory processes (Freiberg et al., 2004).

Chemical genetics studies the effect of small molecules on biological processes in biological systems (Spring, 2004) and the produced data deliver robust substantiation for target engagement since it correlates the chemical action in a cellular or organism context (Nijman, 2015). The premise of chemical genetics is that, by modifying the gene expression of the potential drug target, the drug sensitivity would be modified too. The construction of genome-wide mutant libraries for different organisms (*S. cerevisiae, E. coli* and *B. subtilis*), has enabled functional genomic studies through chemical-genetic profiling.

The mutant collections have been generated through different techniques and with different outcomes. For example, some libraries have been created by deleting or

inactivating non-essential genes through replacement using a selectable marker such as kanamycin. Examples of these single-deletion mutant sets include *Saccharomyces cerevisiae, Escherichia coli K-12* (Keio), and *Salmonella enterica* serovar Typhimurium (Winzeler et al., 1999; Baba et al., 2006; Porwollik et al., 2014). Other collections have been developed by inactivating or decreasing function of essential genes. These libraries have been constructed as heterozygote deletion mutants in diploid microorganisms or by transposon insertion (*Saccharomyces cerevisiae, Candida albicans* and *Pseudomonas aeruginosas*), disruption of 3' noncoding sequence or antisense interference (*Staphylococcus aureus*) (Jacobs et al., 2003; Donald et al., 2009; Xu et al., 2011).

One of the first genome-wide mutant libraries completed was the yeast knockout collections (YKO), either as a heterozygous deletion mutant library or a haploid deletion library. Drug-induced haplo-insufficiency profiling (HIP) assay has been carried out with the diploid deletion strain library (genome-wide including essential genes), where a drug target may be directly elucidated by identifying supersensitive strains. Conversely, when homozygous deletion strains (non-essential genes) are used to investigate their response to a potential drug, the homozygous profiling (HOP) assay does not identify the direct drug target since it is not present but it does identify genes that buffer the gene deletion effect and that interact with the drug under study (Smith et al., 2010). Multi-copy suppression profiling (MSP) assays have been used to detect genes that, when overexpressed, confer resistance to the drug. Hoon and collaborators (2008) have

demonstrated that using the three strategies in an integrative way provides a suitable platform to predict target in a more precise manner (Hoon et al., 2008).

Developing new and effective antimicrobials that have unique mode of action is perhaps the main strategy to overcome the antimicrobial resistance problem. However, another important strategy is to develop combined chemical systems with synergistic properties such as a combination of substances (multi-drug cocktail) that exerts inhibitory activity on different cellular targets, inactivates mechanisms of antibiotic resistance, or permeabilizes pathogen's cell envelope. For example, using efflux pump inhibitors in combination with other antibiotics that target protein synthesis, using β-lactamase inhibitors in combination with β-lactam antibiotics (penicillin, methicillin, etc.), or by using antimicrobial peptides that regulate the macrophage response, etc. (Monaghan and Barret, 2006). Functional genomics can act as a tool to investigate chemical-chemical interactions in biological systems just as it is used to generate chemical-genetic profiles (Monaghan and Barret, 2006; Roemer and Boone, 2013).

Considering the need to relieve the problem of antimicrobial resistance, the main goal of the current study was to investigate the potential cellular processes/pathway targets (mode of action) for natural molecules such as chitosan, nisin and 'probiotic' bacterial supernatant, as well as engineered zinc oxide and silver nanoparticles. These bioactive compounds were evaluated using a chemical-genetics approach that utilized *S. cerevisiae* or *E. coli* gene deletion libraries. Clues based on chemical-genetic profiles into

the mode(s) of activity of the target compounds were then further explored via focused follow-up investigations to better elucidate the activity of these compounds.

This thesis is divided into four studies. In chapter 1, the antifungal activity of chitosan, a natural by-product of animal or fungal origin, was elucidated using the yeast gene deletion mutant set. Supersensitive yeast mutants were classified based on the function of the genes that, once deleted, result in high sensitivity of the cells to the target compound. Secondary assays confirmed that chitosan has several specific inhibitory targets in yeast. The second chapter focused on investigating the cytotoxic effects of zinc oxide and silver nanoparticles on yeast. The identified cytotoxic effects may also be considered as antifungal mode of action of the nanoparticles. Follow-up experiments were utilized to validate targets. In the third chapter, the mode of action of nisin, a polycyclic antimicrobial peptide of bacterial origin, and citric acid, used to control bacterial growth, on bacteria was explored using the *E. coli* gene deletion mutant set. The effect of nisin was confirmed using secondary assays that measured plasmid replication and the content of genomic DNA. In the fourth chapter, the potential mode of action of the fermented supernatant produced by the probiotic *Bifidobacterium breve* was investigated using the *E. coli* gene deletion mutant set.

Chapter 2

Disruption of protein synthesis as antifungal mode of action of chitosan

2.1 ABSTRACT

The antimicrobial activity of chitosan has been acknowledged for more than 30 years and yet its mode of action remains ambiguous. We analysed chemical-genetic interactions of low-molecular weight chitosan using a collection of ≈4600 *S. cerevisiae* deletion mutants and found that 31% of the 107 mutants most sensitive to chitosan had deletions of genes related primarily to functions involving protein synthesis. Disruption of protein synthesis by chitosan was substantiated by an in vivo β-galactosidase expression assay suggesting that this is a primary mode of antifungal action. GDA analysis and secondary assays also indicate that chitosan has a minor membrane disruption effect - a leading model of chitosan antimicrobial activity.

2.2 INTRODUCTION

Chitosan has gained attention as an abundant and inexpensive bioactive substance with potential applications in agricultural, food, pharmaceutical and textile industries (Raafat et al., 2008). It is produced by alkaline N-deacetylation of chitin, which is estimated to be the second most abundant biopolymer on earth after cellulose, owing to its prevalence in the exoskeletons of arthropods and the cell wall of most fungi (Cohen, 1987). Chitosan is a highly basic, linear polycationic heteropolysaccharide (β-1,4 linked N-acetylglucosamine units) comprised of about 6.9% nitrogen that has a molecular weight range of 50 to 2000 KDa. It has a slightly variable pKa of ≈6.0±0.3 depending on the degree of deacetylation, which ranges from about 75 to 95% (Costa et al., 2012; Goy et al., 2009). Native chitosan is water insoluble but can be dissolved in slightly acidic solutions at a pH lower than its pKa, when the amino groups are in their protonated form.

Chitosan exhibits a diversity of biological properties including antifungal, antibacterial and antiviral activities (Allan et al., 1979; Sudarshan et al., 1992; Chirkov, 2002). This wide-spectrum of antimicrobial activity is of particular interest for applications in the manufacture of wound dressings, coatings for perishable foods, in seed treatments, and in the manufacture of microbe resistant packaging materials, among others (Raafat et al., 2008). This spectrum of antimicrobial activity seems to be influenced by various determinants such as the developmental stage of the target microorganism, and physico-chemical properties of the chitosan used, including molecular weight, degree of

solubilisation, acetylation, and charge density, and environmental growth conditions such as pH, temperature, exposure time, etc. (Kong et al., 2010).

In spite of this well documented activity, the mechanism(s) of antimicrobial action of chitosan remains ambiguous (Raafat et al., 2008). Three main mechanisms of antimicrobial activity have been proposed: 1) Metal-chelation, which might destabilize the outer membrane in Gram-negative bacteria (Helander et al., 2001) or microbial cell walls; 2) Electrostatic interactions between negatively charged residues of cell surfaces and the amino protonated groups of chitosan that would lead to cell wall permeability (Raafat et al., 2008) and plasma membrane perturbation (Zakrzewska et al., 2007; Palma-Guerrero et al., 2010); and 3) Interaction between microbial DNA and the internalized chitosan that might interfere with gene expression (Goy et al., 2009).

The present study investigates the antifungal mode of action of low molecular weight (LMW) chitosan using a Gene Deletion Array (GDA) with the yeast *Saccharomyces cerevisiae*. The GDA system employs the exposure of about 4600 non-essential gene deletion mutants of yeast to a sub-lethal concentration of a compound (Galván et al., 2008; Mir-Rashed et al., 2010). Identification of the most susceptible (supersensitive) mutants gives an indication of the cellular pathway(s) perturbed by the compound, hence provides clues regarding its mode of action. Based on results of our GDA analysis, we used secondary assays to verify that chitosan can negatively affect protein synthesis and the cell membrane in yeast.

2.3 MATERIALS AND METHODS

2.3.1 Strains, growth conditions and antifungal assays

LMW chitosan with a degree of deacetylation between 75 and 85%, viscosity of 20-200 cps and average molecular weight (Mv) of ≈150 x 103 (repeat units) was purchased from Sigma-Aldrich (Oakville, ON, Canada). YPD (1% yeast extract, 2% peptone, 2% dextrose) agar (1.5% w/v) plates with different concentrations of chitosan (1.0, 1.25, 1.5, 1.75 and 2.0 g/l) were prepared in order to ascertain the minimum inhibitory concentration (MIC_{50}) using the drop-out assay as described by Chen et al. (2003), briefly as follows. Chitosan suspensions were prepared in 1% acetic acid, adjusted to a pH of 5.5 and added to the molten YPD medium. *S. cerevisiae* strain S288C was cultured from glycerol stocks in YPD medium at 30 °C with constant agitation (150 rpm) for 1-2 days and cell density was adjusted to ≈1.0 x 10^7 cells/ml. A 10-fold serial dilution of cell culture was done in a 96-well microplate to obtain 1 x 10^6 – 1 x 10^3 colony forming units (CFU)/ml and 10 µl of each dilution was spotted onto the YPD agar plates containing dilutions of chitosan. The plates were incubated 1-2 days at 30°C and MIC_{50} was determined as the chitosan concentration at which there was a ≈50% reduction in CFU compared to plates without chitosan. MIC_{50} determinations were done in triplicate.

2.3.2 Gene Deletion Array (GDA) Analysis

The molecular activity of LMW chitosan was investigated through a large-scale drug sensitivity screen by monitoring colony size reduction in a set of ≈4600 haploid deletion mutants of *S. cerevisiae* using methods similar to those of Parsons et al. (2004). This gene deletion array (GDA) was developed by Winzeler et al. (1999) using the strain BY4741, a derivative of S288C. In this large-scale screening, an increased sensitivity of a mutant strain to chitosan compared to the no-drug control indicates a chemical-genetic interaction that can be used to study mode of action. YPD agar plates with and without chitosan (1.75 mg/ml) were inoculated with deletion mutants by hand-pinning with a 384-floating pin replicator. After 1-2 days incubation at 30^{o}C, the plates were digitally photographed and the images were analyzed by visual inspection and by growth detector software (Memarian et al., 2007). The GDA screen was done in triplicate and each trial was independently analyzed. Sensitive mutant strains (hits) were identified by a colony size reduction of ≥50% in at least two of the three replicas. Susceptibility to chitosan of twenty mutant strains was confirmed by drop-out assays as follows. Randomly selected sensitive and non-sensitive mutant strains (based on the GDA) were inoculated in YPD broth and incubated overnight at 30^{o}C, 150 rpm. Cell cultures were adjusted to ≈10^3 CFU/ml and mixed with YPD-chitosan (1.5 mg/ml) or YPD-no chitosan, and incubated for 4-5 hrs at 30^{o}C, 150 rpm. A 10-fold serial dilution of each culture was performed as described (Chen et al., 2003) and 10 µl aliquots of each cell dilution were spotted on YPD

agar plates and incubated for 1-2 days at 30^{o}C. Colony counts were performed to estimate growth inhibition due to chitosan exposure.

The molecular functions of genes deleted in the supersensitive mutants were obtained from the Saccharomyces Genome Database (http://www.yeastgenome.org - accessed November 2012). The supersensitive mutants were grouped into functional categories according to KOG (eukaryotic orthologous groups; Tatusov et al., 2003).

2.3.3 Translation efficiency assay (β-galactosidase expression)

The β-galactosidase expression assay was performed to investigate the effect of chitosan on the efficiency of protein translation. The effect of the chitosan on the β-galactosidase efficiency biosynthesis was estimated through an enzymatic activity assay. This employs a GAL1 promoter/LacZ fusion (galactokinase/ β-galactosidase) that exerts an inducible expression of the functional enzyme in presence of galactose. The obtained catalytic activity on the substrate ONPG expressed in enzymatic units, has been indirectly considered as an estimation of the translated/expressed enzyme (Mumberg et al., 1994; Firoozan et al., 1991).

The vector p416 (Mumberg et al., 1994; Alamgir et al., 2008) with a galactose-inducible β-galactosidase gene was transformed into the yeast strain W303 (MATa/MATα{leu2-3, 112 trip1-1 can1-100 ura3-1 ade2-1 his 3-11,15}[phi+] . The transformed yeast cells were grown in synthetic medium lacking uracil (SC-URA) and incubated at 30 °C for 24 h, before resuspending in SC-URA (galactose). The cultures were

adjusted to an OD_{600nm} ≈0.7 and incubated for 8 hrs at 30°C in the presence of a range of sub-inhibitory concentrations of chitosan (0.35 – 1.25 mg/ml). The activity of the induced β-galactosidase on the substrate O-nitrophenyl-α-D-galactopyranoside (OPNG) was determined spectophotometrically (λ_{420nm}) as described previously (Stansfield et al., 1997). The reduction of the relative β–galactosidase activity compared to its respective control, cycloheximide (protein synthesis inhibitor) provides an approximate measurement of the inhibition of translation efficiency.

2.3.4 Membrane disruption (Liposome) assay

Membrane-disruption by LMW chitosan was investigated using carboxyfluorescein (CF) loaded liposomes (Cheetham et al., 2003). Carboxyfluorescein (Life Technologies Inc., Burlington, ON, Canada) was encapsulated in large unilamellar vesicles (LUV ≈ 100 nm diameter) of dioleoylphosphatidylcholine (DOPC, Avanti Polar Lipids, Alabaster, AL, USA). After having established the appropriate dilution of the LUV suspension, the membrane disruption assay was carried out in a 96-well microplate (black/clear Optilux™ flat bottom; BD Bioscience, San Jose, CA, USA). The threshold fluorescence intensity of the LUV suspension for each experimental well was measured (excitation 492 nm/emission 517 nm) with a FLUOstar microplate reader (OPTIMA BMG LABTECH Inc., Durham NC, USA) to obtain the fluorescence at time zero (F0). Chitosan (30 mg/ml) was two-fold serially diluted in HEPES buffer before adding to the LUV suspension (1:10) to obtain final concentrations of between 6 and 3000 μg/ml.

Fluorescence intensities were also determined after the addition of the chitosan carrier solvent (1% acetic acid) and HEPES buffer. After adding the chitosan, the microplate was incubated in darkness for one hour at room temperature and the fluorescent emission was measured to obtain F (fluorescent intensity of the vesicles after chitosan addition). The F100 (Fluorescence intensity with 100% leakage of CF) was read 10 minutes after triton X-100 (10% v/v) was added. The % leakage (%L) was calculated by the equation: %L = [(F-F0)/ (F100-F0)] X 100.

2.4 RESULTS AND DISCUSSION

2.4.1 Chitosan minimum inhibitory concentration

We initiated this study by determining that the chitosan MIC_{50} for *S. cerevisiae* strain S288C was 1.5 mg/ml. This value differs from some previous studies in which the chitosan MIC_{50} has been reported to be as low as 100 µg/ml for *S. cerevisiae* (Jaime et al., 2012). However, different MIC values for chitosan are noted, owing to variables such as molecular weight and degree of acetylation of the utilized chitosan and the identity of target microorganism and its cell surface properties (Mellegård et al., 2011). Our determination of MIC_{50} of LMW-chitosan for yeast strain *S288C* was necessary for subsequent GDA analyses.

2.4.2 Identification of *S. cerevisiae* deletion mutants most sensitive to chitosan

The antifungal activity of LMW-chitosan was investigated using a chemical-genomic screen by exposing the GDA of *S. cerevisiae* to 1.75 mg/ml of chitosan and detecting mutants with an increased sensitivity to the drug. Supersensitive mutants were identified by a significant colony size reduction (≥40%, Supplementary Table S1).

As shown in Figure 2-1A, among the top 2.5% most inhibited haploid deletion mutants, we distinguished 7 functional categories based on KOGs (eukaryotic orthologous groups). Four of the categories represent the majority (≈71%) of the supersensitive mutants and will be discussed briefly below. A fifth large category represents deletions of genes with unknown function.

We found a significant enrichment (*p-value* = 1.95 x 10^{-5}) of supersensitive mutants have deletions of genes involved in protein biosynthesis. For example, 18 of the 33 mutant strains in this category have deletions of genes that encode ribosomal proteins (Table S1). The second largest group of mutants supersensitive to chitosan comprises 18 strains that have deletions of genes involved in cell cycle and DNA processing (Table S1). The high sensitivity to LMW-chitosan of deletion mutants related to protein biosynthesis and processing, and cell cycle and DNA processing (first and second largest groups, respectively) is in agreement with the hypothesis that cationic chitosan can interact with DNA and/or RNA (Hardwiger et al., 1985) which may, in turn, inhibit protein synthesis.

The next largest groups represent deletions that effect non-vesicular ion trafficking and Golgi/endosomal transport (16 deletion mutants), and cell wall/cell

membrane biogenesis (9 mutants). Interestingly, this last group includes deletions of genes that are involved in sphingolipid (e.g. *IPT1, SKN1, LCB3*) and ergosterol (e.g. *ERG3*, *ERG5*) biosynthesis. Variations on the concentration of these cell membrane components affect the plasma membrane fluidity, which has previously been proposed to influence cell sensitivity to chitosan (Palma-Guerrero et al., 2010). The membrane topology and its dynamics affect the endosomal transport and trafficking. A drastic perturbation in the plasma membrane might produce defective invaginations impeding the proper trafficking (MacMahom and Gallop, 2005). It has been recently proposed that the plasma membrane in yeast is organized in domains (compartments) and networks which are involved in the regulation of processes such as cell polarity, signalling and membrane protein and lipid turnover (Ziólkowska et al., 2012). By extension, perturbation of the plasma membrane by chitosan may alter other cell processes as evident in our GDA analysis. Our observations that strains with deletions of genes effecting cell wall and cell membrane biogenesis are highly sensitive to chitosan support a leading hypothesis that the antifungal mode of action of chitosan is through perturbation of the plasma membrane (Zakrzewska et al., 2005; Yookyung et al., 2008).

2.4.3 Effect of LMW-chitosan on protein synthesis

To validate our results that indicate chitosan mainly affects protein biosynthesis, we investigated whether or not chitosan decreases the rate of β-galactosidase biosysnthesis using an inducible expression cassette (Figure 2-1B). In the figure, β-

galactosidase activity is plotted relative to the no-chitosan controls. When the yeast cells (strain W303 containing p416, see methods) were exposed to 0.35 mg/ml of chitosan the β-galactosidase activity was reduced to 32% of no-chitosan controls. β-galactosidase activity was further reduced with increasing chitosan concentrations of up to 1.25 mg/ml, the highest concentration tested in this assay, which resulted in 13% β-galactosidase activity compared to no-chitosan controls. The inhibitory effect of 1.25 mg/ml chitosan on protein synthesis was less pronounced than with the positive control; 10 μg/ml of cycloheximide resulted in 2% of control translation (data not shown). Nevertheless, the results clearly show that LMW-chitosan reduces the rate of translation at concentrations that are well below the MIC_{50} (1.5 mg/ml), and in a dose-dependent manner.

Previous studies showed that electrostatic interactions can occur between positively charged amino groups from the N-glucosamine forming-monomers of chitosan and negatively charged phosphate groups on DNA and RNA, or carboxyl groups on proteins (Ma et al., 2009; Souza et al., 2009). Such interactions between chitosan and DNA, RNA and protein could partly explain the effects of chitosan on translation efficiency and could also help explain our GDA results that found increased sensitivity of strains deleted for genes involved in protein biosynthesis, and DNA replication, recombination and repair (Figure 2-1A).

2.4.4 Membrane disruption assay

A membrane disruption assay was performed, since this is considered a main mode of antifungal action of chitosan and our GDA results also show high chitosan sensitivity by mutants with deletions in genes involved in cell wall/membrane functions. The membrane-disruptive properties of LMW chitosan were investigated using carboxyfluorescein (CF) loaded liposomes. Similar to what was reported by Yoonkyoung et al. (2008), we found that LMW-chitosan at 0.75 µg/µl caused moderate (≈7%) leakage of carboxyfluorescein contained in large unilamellar vesicles (Figure 2-1C). This finding is in accord with our GDA results that showed increased chitosan sensitivity of strains lacking genes involved in cell wall/membrane/envelope biogenesis and transport and secretion processes.

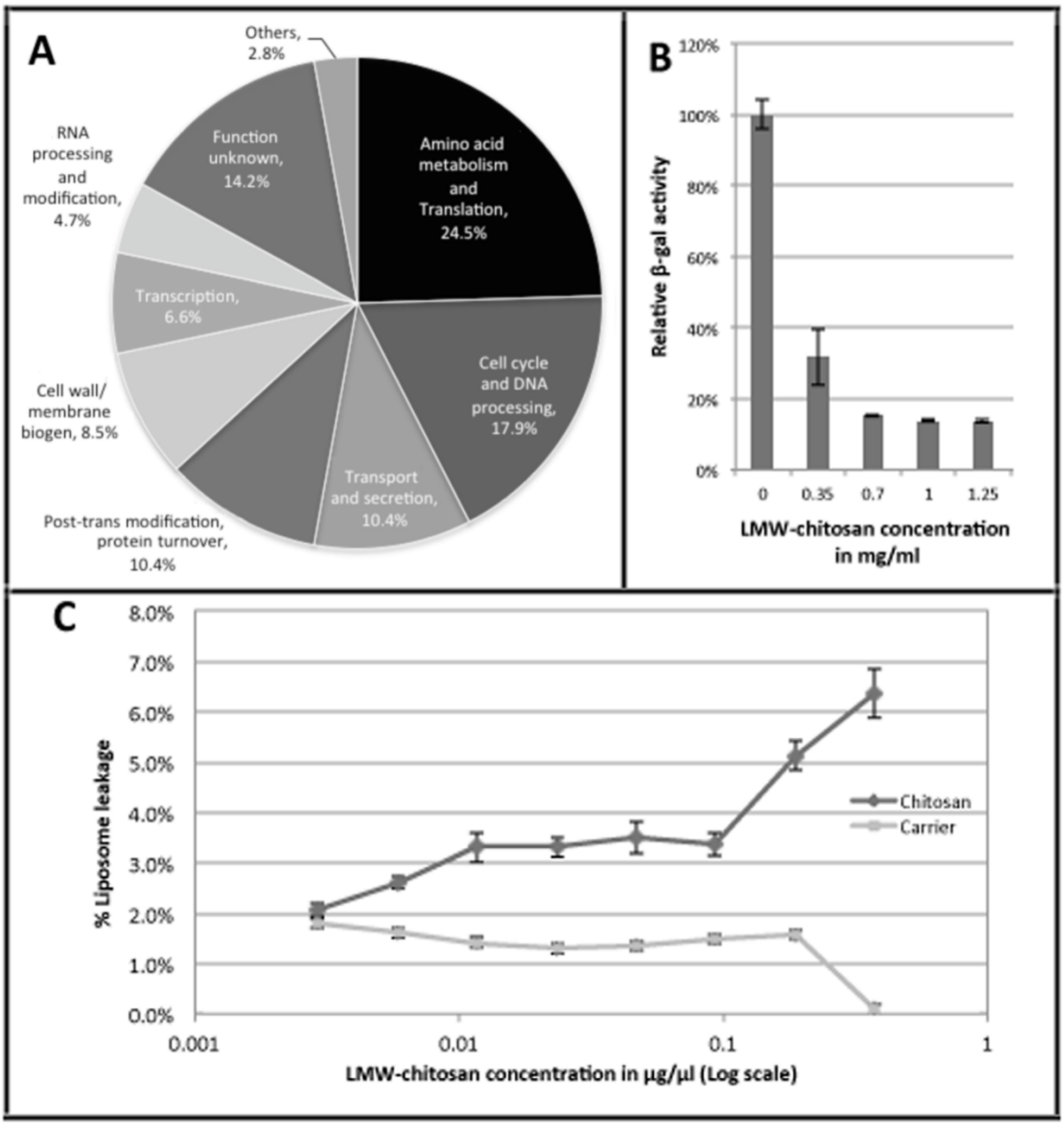

Figure 2-1. **Evidence that chitosan interferes with protein synthesis and membrane integrity.** **A)** Functional distribution of the 107 (2.5%) most sensitive gene deletion strains to 1.75 mg/ml chitosan. Deleted genes in supersensitive strains were classified by function using KOG. **B**) β-galactosidase expression assay indicates that chitosan inhibits protein biosynthesis efficiency in a dose-dependent manner. The efficiency of protein synthesis was evaluated using an inducible β-galactosidase reporter gene (p416 construct) and measuring enzyme activity spectrophotometrically based on ONPG conversion. Enzyme activity is plotted relative to no-chitosan controls. **C)** LMW-chitosan disrupted DOPC-LUVs based on carboxyfluorescein-loaded liposome leakage measurements. The disruptive effect of the carrier solvent is also presented.

2.5 CONCLUSIONS ON CHITOSAN MODE OF ACTION

Analysis of chemical-genetic interactions using the *S. cerevisiae* mutant collection provides insight into potential molecular targets of antifungals. This study shows that chitosan interferes primarily with protein synthesis. Disruption of such a fundamental process may account for some of the diverse additional effects of chitosan implicated by our GDA analysis, including cellular trafficking, secretion, and cell cycle progression. Alternatively, chitosan may interfere directly with multiple cellular targets.

Chapter 3

Effects of zinc oxide and silver nanoparticles on the baker's yeast, *Saccharomyces cerevisiae*

3.1 ABSTRACT

Metals and metalloids have been used as antimicrobials for thousands of years (Lemire *et al*. 2013). Metal nanoparticles (NPs), particles that are 1 – 100 nm in size, are used for a variety of commercial purposes and may also possess cytotoxic properties. Here, we used a collection of ≈4600 *Saccharomyces cerevisiae* deletion mutant strains to study the influence of zinc oxide nanoparticles (ZnONPs) and silver nanoparticles (AgNPs) on the model eukaryotic cell. Among the top most sensitive deletion mutants, we found *S. cerevisiae* strains lacking genes involved in transmembrane and membrane transport (19%), cellular ion homeostasis (17%) and cell wall organization or biogenesis (12%) exhibit highest sensitivity to ZnNPs. The strains most sensitive to AgNPs were enriched in deletions of genes involved in transcription and RNA processing (16%), cellular respiration (14%) and endocytosis and vesicular transport (12%). Secondary assays confirmed that ZnONPs affect cell wall functions and integrity. Similarly, secondary assays demonstrated that AgNPs decrease transcription, reduce endocytosis and provoke a dysfunctional electron transport system.

3.2 INTRODUCTION

Engineered nanomaterials (ENMs) are increasingly integrated into everyday life. ENMs possess unique physical, chemical and structural properties attributable to their small size (in range of ≤100 nm in one dimension). Nanomaterials may have different or improved properties compared with their conventional 'bulk' (microsize) counterparts, such as higher reactivity, conductivity and optical sensitivity (Nel et al., 2006). Due to these improved properties, ENMS have been incorporated into a variety of applications, including medical diagnostics and therapeutics, antimicrobials, food packaging, cosmetics, rubber manufacture, chemical fibers, and electronic conductors (Berardis, et al. 2010; Ji, et al., 2008). In fact, as of October 2013, 1628 consumer products were reported to contain ENMs (Nanotechproject, 2014).

Zinc oxide nanoparticles (ZnONPs) and silver nanoparticles (AgNPs) are among the most commonly used ENMs. ZnONPs are present in 36 reported consumer products, especially in ultraviolet (UV) blocking cosmetics (Sharma et al., 2011; Nanotechproject, 2014). ZnONPs effectively absorb UV-A and UV-B light through a process called band-gap absorption, and are less photoactive than titanium dioxide nanoparticles (TiO_2NPs), which are also used in sunscreens (Faure et al., 2013). In addition, ZnONPs were reported to have biocidal/antimicrobial properties (e.g. Zhang et al., 2007; Ivask et al., 2012) that are thought to be mediated by the release of zinc ions (Zn^{2+}) and generation of reactive oxygen species (ROS) (Espitia et al., 2012). Notably, the annual worldwide production of ZnONPs is estimated at 550 tons (Piccino et al., 2012). In contrast, the annual production

of AgNPs is estimated at 55 tons, but AgNPs are present in 383 consumer products (Nanotechproject, 2014). AgNPs are effective growth inhibitors of a wide range of Gram-positive and Gram-negative bacteria, and even some viruses (Massarsky et al., 2014). The antimicrobial action of AgNPs may involve (i) release of silver ions (Ag^+), which mainly bind to thiol-containing compounds thereby disrupting important cellular functions, including DNA replication, (ii) attachment to cell membranes, which disrupts the membrane potential, and (iii) generation of ROS (Massarsky et al., 2014).

Despite the potentially beneficial properties of ENMs, concerns about their safety have been raised over the past decade. Inevitably, ZnONPs and AgNPs will reach the environment. It has been estimated that sludge-treated soil would be the main environmental compartment for deposition of ZnONPs and AgNPs, and could accumulate 1.6-23.1 and 0.5-4.1 µg/kg/y of NPs, respectively (Gottschalk et al., 2009). This suggests that organisms in the soil would be at a greater risk to adverse effects of ENMs. The overall health of microorganism populations is of particular concern given that microbes have important environmental roles, including nitrogen fixation and nutrient cycling. Several studies have shown a plethora of effects by ZnONPs and AgNPs on various bacterial species, including oxidative stress and damage, as well as uptake and damage to various cellular components [reviewed by Ivask et al. (2014)]. However, very few studies have addressed the toxicity of ZnONPs and AgNPs in eukaryotic microorganisms. For example, Kasemets et al. (2009) examined the toxicity of ZnONPs in the budding yeast, *Saccharomyces cerevisiae* and reported that growth was inhibited by 80% at 250 mg ZnO/l

for both nano-scale and bulk forms. Moreover, it was suggested that growth inhibition was due to release of Zn^{2+} and possible induction of oxidative stress. In contrast, a lower concentration of 50 mg/l AgNPs was necessary to inhibit yeast growth (Debabrata and Giassudin, 2013). These authors reported that cellular proteins, amino acids, and RNA molecules, as well as the plasma membrane were possibly affected by AgNPs. Notably, generation of hydroxyl radicals and induction of apoptosis were suggested as toxicity mechanisms for AgNPs in another yeast species, *Candida albicans* (Hwang et al., 2012).

The present study uses a Gene Deletion Array (GDA) as a platform for a high-throughput functional genomic screening to enhance our understanding of ENM toxicity mode of action. This gene deletion array (GDA) comprises ≈4600 non-essential gene deletion strains of *S. cerevisiae*. The theory behind the screen is that strains with deletion of genes in a parallel, redundant pathway to that targeted by a bioactive compound will have increased sensitivity to treatment with that compound (Alamgir et al., 2008; Galván et al., 2008; 2013). For example, deletion mutant strains for protein synthesis genes show increased sensitivity to drugs such as paromomycin and cycloheximide that target the process of protein synthesis (Alamgir et al., 2008; 2010). Once a sensitivity profile is generated, highly sensitive strains are categorized according to the cellular activity and function of the deleted genes. The distribution of the sensitive strains can provide information on relevant cellular pathways affected by the compound under study. Here, we examined the chemical-genetic profiles of ZnONPs and AgNPs using the GDA platform and elucidated cellular pathways were validated using follow-up assays.

3.3 MATERIALS AND METHODS

3.3.1 Chemicals

Zinc oxide nanoparticles (ZnONPs) 50-70 nm (catalog #544906) were purchased from Sigma-Aldrich. Aqueous silver nanoparticles (AgNPs) stock solution at 2 mg/ml (31% silver) was purchased from Sciventions Inc. MTT (3-(4,5-dimethylthiazol-2-yl)-2,5-diphenyltetrazolium bromide), sodium azide, glucose, MES (2-morpholinoethanesulfonic acid), DMSO (dimethyl sulfoxide), geneticin (G418) and CCCP (carbonyl cyanide 3-chlorophenylhydrazone) were from Sigma-Aldrich (Oakville, ON, Canada). $DiSBAC_2(3)$ [Bis-(1,3-Diethylthiobarbituric Acid)Trimethine Oxonol] was purchased from Life Technologies (Carlsbad, California, USA).

3.3.2 Nanoparticle preparation and characterization

ZnONPs in powder form were suspended in ethanol at a concentration of 10 mg/ml and ultra-sonicated for 5 min to reduce agglomeration and obtain a homogeneous suspension. This solution was then diluted to 1 mg/ml in YPD medium. The aqueous stock solution of silver nanoparticles (AgNPs; 0.62 mg/ml total silver) was diluted to 0.095 mg/ml in YPD medium.

The size of ZnONPs and AgNPs was assessed using Dynamic Light Scattering (DLS). Briefly, 1 ml of nanoparticle solution was added to a clean 12 mm polystyrene cuvette (DTS0012) and DLS was measured using a Zetasizer NanoZS according to the manufacture guidelines (Malvern Instruments Ltd. Malvern, Worcestershire, UK). Each sample was

measured at least 3 times; obtained values were averaged and standard deviation (SD) was calculated. The size of silver nanoparticles was also verified using a scanning transmission electron microscope (STEM; JEOL JSM-7500F Field Emission Scanning Electron Microscope, Jeol USA, Inc. Peabody, MA, USA). For this, a drop of silver nanoparticle stock solution was applied to a carbon-coated grid and air-dried overnight at room temperature prior to visualization; images were captured by transmission electron diffraction (TED).

3.3.3 Strains and Growth conditions

Yeast cells, *S. cerevisiae* strains S288C (*MATα SUC2 gal2 mal2 mel flo1 flo8-1 hap1 ho bio1 bio6*) or W303 (*MAT*a*/MATα {leu2-3,112 trp1-1 can1-100 ura3-1 ade2-1 his3-11,15}*) were grown in YPD (1% yeast extract, 2% peptone, 2% dextrose) medium at 30°C for 1-2 days. Deletion strains were maintained in a solid array of YPD with 2% Agar, containing 200 µg/ml of geneticin (G418).

3.3.4 Nanoparticles minimum inhibitory concentrations and sensitivity analysis

The minimum inhibitory concentrations (MIC_{100}) for ZnONPs and AgNPs were investigated by broth microdilution assays (CLSI, 2008; Rex et al., 1993) and drop-out assays. An overnight culture of yeast (S288C) cells was 10-fold serially diluted to obtain 10^5 cells/ml. For microdilution assay, 100 µl of nanoparticle stock (10 mg/ml of ZnO or 0.2 mg/ml of AgNPs) was serially diluted 1:1 in YPD in microtitre plates and 100 µl of the cell

suspension was added into each well. Microtitre plates were incubated at 30°C and inhibitory activity was evaluated by reading OD_{600nm} in a FLUOstar Optima multi-mode microplate reader (BMG Labtech, Ortenberg, Hessen, Germany) after 48 hrs. The minimum inhibitory concentration (MIC_{100}) was calculated by the equation: 100-[(Abs_{exp}-Abs_{blank})/$Abs_{carrier}$-$Abs_{carrier\ blank}$)]*100. MIC_{100} was defined as the lowest concentration that resulted in complete inhibition of visible growth in liquid medium at 48 hrs.

The MIC values were used as a guide to determine sub-inhibitory concentrations of ZnONPs and AgNPs for GDA analyses with agar medium. Colonies from two plates, randomly chosen from the GDA mutant set, were replicated onto YPD + 2% agar plates containing a range of ZnONPs (0.1–1.5 mg/ml) or AgNPs (0.003 – 0.12 mg/ml). Plates were incubated at 30°C for 1-2 days and colony sizes were measured to identify ZnONPs and AgNPs concentrations at which approximately 5-10% of the strains had a colony size reduction of 30% or more compared to control medium with no NPs. The appropriate sub-inhibitory concentrations determined in this way were used for full scale GDA analyses.

3.3.5 High-throughput phenotypic screening (GDA analysis)

Approximately 4600 haploid gene deletion strains of *S. cerevisiae* were exposed to sub-inhibitory concentrations of ZnONPs and AgNPs nanoparticles (1 mg/ml and 0.095 mg/ml, respectively). Plates were incubated for 1-2 days at 30°C and digital images of these plates were acquired. Digital analysis was used to determine colony areas as

described by Memarian et al. (2007). The size of each colony was compared to the average size for all colonies on both experimental and control plates (Galván et al., 2008; Alamgir et al., 2010). Each experiment was carried out in triplicate. Colonies with size reduction of 50% or more in at least two replicate experiments were classified as positives hits (highly sensitive strains). Functional clustering of the highly sensitive mutants was performed according to eukaryotic orthologous groups (KOG; Tatusov et al., 2003), GeneMania (http://genemania.org/) and GO term finder through SGD (SGD, Hong et al., 2006).

Mutant strains identified as highly susceptible to AgNPs and/or ZnONPs by GDA analysis were verified using drop-out assays (Chen et al., 2003; Jessulat et al., 2008). In brief, selected mutant strains were incubated overnight in YPD at 30^{o}C, cultures were adjusted to contain 10^3 CFU/ml by 10-fold serial dilutions and incubated for 4-5 hr to reach mid-log phase (OD_{600} ≈0.6). Ten-fold serial dilutions (10^{-2} to 10^{-6}) of each culture were prepared and 15 µl aliquots of each cell dilution were spotted onto YPD agar plates with and without sub-inhibitory concentrations of 1 mg/ml ZnONPs or 0.095 mg/ml AgNPs. Plates were incubated at 30°C for 1-2 days and enumeration of colony forming units was performed to estimate growth inhibition.

3.3.6 Membrane disruption analysis

Membrane disruption potential by ZnONPs was examined using the method of Cruz et al. (2014). Liposomes were prepared as described by Cheetham and collaborators

(2003) with dioleoylphosphatidylcholine (DOPC) to encapsulate carboxyfluorescein (CF) in large unilamellar vesicles (LUV ≈ 100 nm diameter). LUVs were suspended in iso-osmotic buffer (100 mM NaCl, 10 mM HEPES, pH 7.4) and mixed with a series of 1:1 serial dilutions of ZnONPs (0.1 and 2 mg/ml) in the iso-osmotic buffer prepared in a 96-well microplate (black/clear Optilux flat bottom; BD Bioscience, San Jose, CA, USA) and distributed together with carrier solution (0.02 N HCl). Fluorescence threshold value was identified by the fluorescent signal of LUV suspension alone. Fluorescence intensity was measured with a μ=485 nm (excitation) and λ=528 nm (emission) using a Cytation 5 cell imaging multi-mode reader (BioTek, Winooski, VT, USA). After mixing, the compound and liposomes were allowed to interact for one hour at room temperature in dark prior to obtaining fluorescent emission reading. The percent leakage (%L) was calculated by the equation: %L = [(F-F0)/ (F100-F0)] X 100. F is fluorescent intensity of the vesicles after incubation of liposomes with ZnONPs or carrier. F0 is the fluorescence intensity of the liposomes in the buffer solution. F100 is fluorescence intensity with 100% leakage and measured 10 minutes after adding triton X-100 (10% v/v).

Membrane perturbation by ZnONPs was also examined using the method of (Freshney, 1994). Trypan blue is a negatively charged, cell membrane-impermeable dye (≈960 Da) that only penetrates cells with compromised membranes (Tran et al., 2011). Yeast cells were grown overnight in YPD medium to mid-log phase and adjusted to approximately 10^4 cells/ml based on optical density (OD_{600nm}). Two ml of yeast cultures were subjected to different concentrations of ZnONPs (0.1 - 1.5mg/ml). Controls for each

concentration were prepared with equivalent volumes of carrier solvent (ethanol) without nanoparticles. Overnight cultures of treated cells were adjusted to a density of 10^7 cells/ml, and mixed (1: 1) with a 0.4% trypan blue solution (Freshney, 1994). The numbers of viable (unstained) and non-viable (stained) cells were counted separately using a hemocytometer and/or a microscope (CARL ZEISS #4649608, Oberkochen, Ostalbkreis, Germany). Each experiment was repeated at least three times and the average and standard error of stained and unstained cells were determined. Percentage of stained (permeable cells) was calculated by dividing the number of stained cells by total number of cells, multiplied by 100.

A cell membrane depolarization assay via flow cytometry analysis (FC) was performed as follows. ZnONPs stock solution was prepared at 5 mg/ml in 50 mM citric acid. Yeast cells were incubated overnight and cell density was adjusted to $1x10^7$ cells/ml. This cell culture was treated with different concentrations of ZnONPs (0.25, 0.5 and 1.0 mg/ml) along with 10 mM citric acid (carrier control) and incubated for 3 hours. Twenty µM CCCP (carbonyl cyanide 3-chlorophenylhydrazone) was used as a positive control. Cells were then harvested by centrifugation (9300 *x g*, 2 min). Cells pellets were washed with PBS (phosphate buffer saline) 2-3 times and stained with 5 µM of $DiSBAC_2(3)$ [Bis-(1,3-Diethylthiobarbituric Acid)Trimethine Oxonol] for 30 min at room temperature.

Stained cells were subjected to flow cytometry analysis using a BD Accuri C6 instrument (BD Biosciences, East Rutherford, NJ, USA) with the following specifications: red laser with an excitation wavelength of 488 nm, emission detector of 585±40 nm (FL2),

and forward ($0^{o}\pm13^{o}$) and side scatter ($90^{o}\pm13^{o}$) detectors. Samples were injected at a medium speed of 36 µl/min, and 10-10000 events were measured per sample. Forward scatter (FSC) and side scatter (SSC) were simultaneously measured. An increase in fluorescence intensity was expected for cells with depolarized membranes (Tretter et al., 1998; Quaranta et al., 2011).

3.3.7 Cell wall disruption assay

Cell wall disruption assays followed previously established protocols (Cruz et al., 2014). Yeast cells were grown in YPD with different sub-inhibitory concentrations of ZnONPs (0.5, 0.75, 1, 1.25 and 1.5 mg/ml) overnight at 30^{o}C with constant shaking at 150 rpm. Cell density for all the cultures was adjusted to $\approx10^{7}$ cells/ml and a 2 minute sonication treatment was done using a 3 mm microtip probe with amplitude set to 20%, a 15 s pulse and 3 s intervals between pulses (Vibra Cell VCX130, SONICS & MATERIALS INC., CT, USA). To evaluate the effect of ZnONPs on sonicated (S) and non-sonicated (NS) cells, cell viability was measured by colony counts using drop-out assay analysis. Each experiment was done at least in triplicate.

3.3.8 β-galactosidase fluorescent assay

Effect of AgNPs on transcription was examined by the method of Vidal-Aroca et al. (2006). The yeast cells (strain W303) were transformed with the expression vector p416, which contains a galactose inducible β-galactosidase gene (Mumberg et al., 1994).

Transformed cells were grown in a synthetic medium lacking uracil (SC-URA) with 2% glucose. Cells were harvested at cell density of approximately 0.3-0.6 OD and washed 2 times before adding SC-URA medium containing 2% galactose. Cell density was adjusted to 10^7 cells/ml (OD 0.3) and cultures were aliquoted in 96-well microtitre plates where yeast cells were exposed to a range of sub-inhibitory concentrations of AgNPs (0.9 to 9.0 µg/ml). The transcription inhibitor 6-azauracil (48 µg/ml) was used as a positive control. Plates were incubated at 30°C for 6 and 10 hrs. 20 µl from each well was transferred into a black/clear 96-well microplate (black/clear Optilux flat bottom; BD Bioscience, San Jose, CA, USA) containing 80 µl of Z-buffer. OD_{600} of each well was determined with a Cytation 5 cell imaging multi-mode plate reader (BioTek, Winooski, VT, USA). 25 µl of 4-methylumbelliferyl-D-galactopyranoside (MUG, 1 mg/ml in DMSO) was added to each well and the mixtures were incubated for 15 min at room temperature. The reaction was stopped by adding 30 µl of 1M Na_2CO_3. β-galactosidase activity was quantified by measuring fluorescence at λ=475 nm (emission) with a µ=390 nm (excitation). MUB units for each replica (samples and controls) were calculated with the equation: $F_{390/475}$ /t × A_{595}. Each experiment was repeated at least 3 times. Where $F_{390/475}$ is the sample fluorescence at the end of the reaction, t is the time of reaction in minutes (min), and A_{595} is the absorbance of the cell suspension.

3.3.9 MTT assay

MTT (3-(4,5-dimethylthiazol-2-yl)-2,5-diphenyltetrazolium bromide) assay was executed to study deficiencies in cellular respiration. In this assay, formazan salts are formed upon reduction by succinate dehydrogenase. This reduction is detected as a colour change and is an indirect measurement of mitochondrial activity (Sánchez et al., 2005).

Yeast cells (S288C) were pelleted from overnight cell cultures and resuspended in distilled water. Cell suspensions were incubated overnight at 30^{o}C to starve the cells. Cells were pelleted and resuspended in distilled water in 1:2 ratio. 15 µl of cell suspension was added to 1.5 ml microcentrifuge tubes containing 10 mM MES, 100 mM glucose and 0.5 mg/ml MTT. Sub-inhibitory concentrations of AgNPs (0.75, 1, 5, 10, 15 and 17.5 µg/ml) were added and total volumes were adjusted to 1 ml using distilled water. 2.5 mM sodium azide was used as an electron transport chain inhibitor (positive control) and 100 mM glucose was used as a negative control. Samples were incubated at 30^{o}C for 60 min, incubated on ice for 5 min and cells were pelleted and resuspended in DMSO to dissolve the formazan salt. Samples were recentrifuged and 100 µl of each supernatant was transferred to a microtitration plate. MTT reduction was determined using a FLUOstar plate reader (BMG Labtech; Ortenberg, Hessen, Germany) measured at 595 nm. Each experiment was repeated five times.

3.3.10 Lucifer yellow intake assay

Lucifer yellow (LY) intake assay was performed as described previously (Dulic et al., 1991; Wiederkehr et al., 2001). In brief, yeast cells were grown to mid-log phase (OD_{600}=0.2-0.5) in YPD supplemented with 30 mg/l each of uracil, adenine and tryptophan (YPUAD). Cell cultures were concentrated 10-fold by centrifugation. 100 µl aliquots of concentrated cell suspensions were mixed with 100 µl of treatment solution containing sub-inhibitory concentrations of AgNPs of 40 or 80 µl/ml. For a positive control a buffer (pH 7) containing 12.5 mM sodium phosphate, 2.5mM sodium fluoride and 2.5 mM of the endocytosis inhibitor sodium azide (ATPase inhibitor) was used. Samples were incubated at 30^{o}C for 15 min before addition of LY for a final concentration of 40 mg/ml. Samples were incubated at 30^{o}C for an additional hour. Cells were then pelleted and washed 3x with 1 ml of ice-cold buffer (50 mM succinic acid, 20 mM NaN_3 pH 5.0). Pellets were resuspended in 200 µl of the same buffer and observed by fluorescence microscopy (Axiophot, model, objective 40x and 100x, FITC optics; Zeiss, Germany). The percentage of fluorescent cells was calculated by analyzing at least six different fields of view, each with >20 cells.

3.4 RESULTS AND DISCUSSION

3.4.1 Characterization of nanoparticles

The average size of ZnONPs was 278 nm based on DLS measurements (Figure 3-1A). This is much larger than 50-70 nm size range listed by the manufacturer, suggesting that these particles aggregate under our experimental conditions. Based on DLS measurements, the average size of AgNPs was 9 nm (Figure 3-1A), which agreed with the 1-10 nm size range indicated by the manufacturer. Furthermore, STEM images confirmed that AgNPs were ≈10 nm in size (Figure 3-1B).

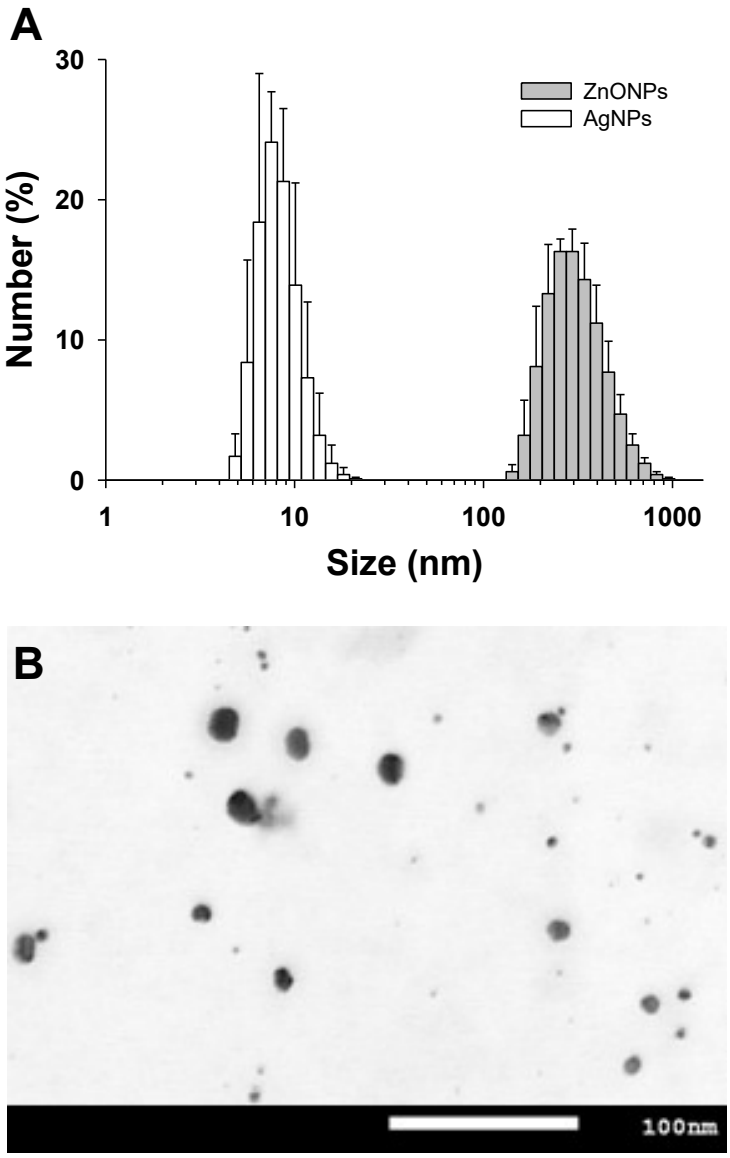

Figure 3-1. Size characterization of nanoparticles. A. DLS was used to assess the size of ZnONPs (1 mg/ml in YPD medium) and AgNPs (0.095 mg/ml in YPD medium). Size distribution and standard deviation (error bars) are presented (n ≥3). B. STEM was used to assess the size of AgNPs using the aqueous stock solution.

3.4.2 Identification of highly sensitive mutants to ZnONPs and AgNPs

The minimum inhibitory concentration (MIC_{100}) was defined as the lowest concentration that resulted in complete inhibition of visible growth of cells. The MIC_{100} of ZnONPs and AgNPs for yeast in solid (agar) medium was determined to be $1.3 < MIC_{100} \leq 1.5$ and $0.10 < MIC_{100} \leq 0.12$ (mg/ml), respectively. Concentrations in agar medium of 1 mg/ml for ZnONPs and 0.095 mg/ml for AgNPs caused about 30% reduction in colony size and were selected for the high-throughput GDA phenotypic screenings. Mutant strains showing high sensitivity to drug treatment (50% of reduction in colony size or more) were identified as potential candidates. In this manner, 60 and 98 mutant strains (from a total of ≈4600) were identified as highly sensitive to ZnONPs and AgNPs, respectively (Supplementary Tables S2 and S3).

The highly sensitive mutants were clustered into functional categories (Figure 3-2). The highly sensitive ZnONPs mutant strains, formed 3 functional categories with significant enrichment (Figure 3-2A). Transmembrane and membrane transport genes (*p-value* = 1.3×10^{-3}) form the most populated group (19%) of mutants highly sensitive to ZnONPs. Cellular ion homeostasis genes form the second most populated group (*p-value* = 7.9×10^{-6}), representing 17% of the hits. Genes involved in cell wall organization/biogenesis formed another major group, representing 12% of the mutants (*p-value* = 9.8×10^{-3}). Similarly, mutants sensitive to AgNPs could be categorized into several functional groups (Figure 3-2B); the largest groups were transcription and RNA processing (16%, *p-value* = 1.3×10^{-3}), cellular respiration (14%, *p-value* = 5.7×10^{-4}), and

endocytosis and vesicular transport (12%, vesicle coat, *p-value* = $1.4x10^{-5}$). The above functional groups provide potential insights into the modes of action of ZnONPs and AgNPs that were further tested by secondary assays.

Drug sensitivity drop-out assay was used in order to confirm the sensitivities of mutant strains identified in the primary large scale screens. The results of our drop-out analysis confirmed the sensitivity of the *yjl095wΔ, ycl058cΔ,* and *yjl080cΔ* strains to ZnONPs and sensitivity of *yjr104cΔ, yn1037cΔ* and *ybr085wΔ* to AgNPs.

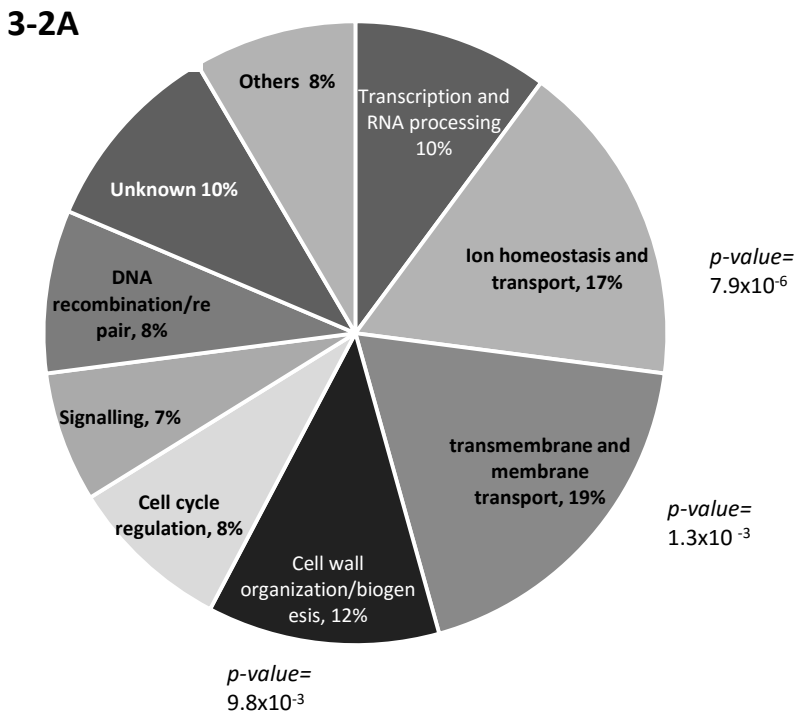

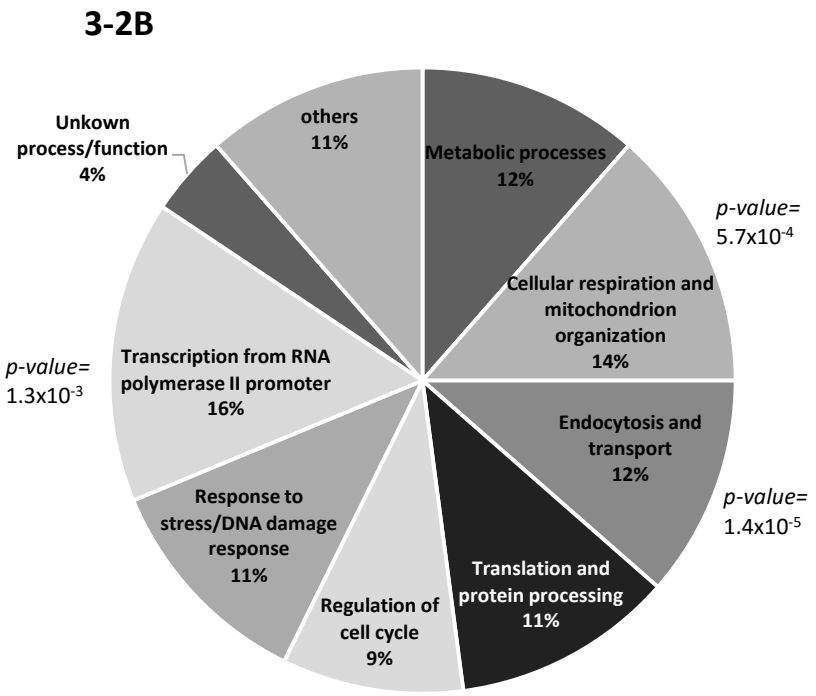

Figure 3-2. Functional distribution of deletion mutants that are highly sensitive to ZnO and Ag nanoparticles. A) Clustering of the 59 most sensitive deletion mutant strains to 1 mg/ml of ZnO nanoparticle. Mutants lacking genes involved in membrane and transmembrane transport, ion homeostasis and transport, and cell organization of biogenesis encompass the major represented groups. B) Clustering of the 96 most sensitive deletion mutant strains to 0.095 mg/ml of Ag nanoparticle. Mutants lacking genes involved in transcription, cellular respiration and, endocytosis and vesicular transport represent the significantly enriched groups.

3.4.3 Membrane disruption property of ZnONPs

In our phenotypic large-scale screening for sensitive mutants against ZnONPs, we observed a significant enrichment (19%, *p-value* = $1.3x10^{-3}$) of mutant strains with deletions of genes involved in transmembrane and membrane transport/organization. These genes include *PKR1*, which codes for an ER associated V-type ATPase assembly factor involved in vacuolar transport, and *ERG2* and *ERG28* which code for proteins involved in ergosterol biosynthesis. Defective composition in the cell membrane such as deficiency in ergosterol may alter the plasma membrane fluidity. Previous studies suggested that ZnONPs may exert its antibacterial activity by permeabilizing the *E. coli* cell membrane due to nanoparticle accumulation on the cell surface causing leakage of cell content, and ultimately resulting in cell death (Huang et al., 2008; Sharma et al., 2010). This is in accord with the results obtained from our phenotypic screening, where mutants with defective cell membranes showed high sensitivity to ZnONPs, and suggested that ZnO nanoparticles interact with cell membrane components in yeast.

To further test ZnONPs effect on membranes, liposomes containing carboxyfluorescein (CF) were exposed to different concentrations of ZnONPs (0.05 mg/ml-0.2 mg/ml). Leakage of CF from DOPC-liposomes was observed to increase in a dose-dependent manner as ZnONPs concentration increased, to a point where 0.20 mg/ml of ZnONPs resulted in 23.87% leakage (Figure 3-3A). Note that this pronounced disruption of liposomes occurred at concentrations that were well below the yeast MIC_{100} of 1.5 mg/ml. The influence of ZnONPs on DOPC lipid may be attributed to the release of

Zn^{2+} ions that alter liposome conformation by an electrostatic interaction to modify permeability (Jitao et al., 2012; Mu et al., 2014).

Membrane perturbation effect of ZnONPs was further investigated using trypan blue stain analysis (Figure 3-3B). Intact cells do not take up the dye and, consequently, the trypan blue dye exclusion assay is used to test cell viability (Strober, 2001) and also to estimate cell membrane perturbation (Tran et al., 2011). The numbers of non-stained and stained cells were quantified after exposure to different concentrations of ZnONPs compared to the control (no-ZnONPs treatment). Results are presented in Figure 3-4B as percentages of stained cells over total cells examined. It was observed that membrane permeability to trypan blue increases in a dose-dependent manner as ZnONPs concentration increases.

The results of the trypan blue assay are consistent with liposome assays that indicate ZnONPs permeabilizes membranes. Altogether our observations validate the inference from chemical-genetic profile analysis that the cell membrane and membrane transport are altered by ZnONPs in yeast. Previously it was hypothesized that ZnONPs disrupt the *E. coli* cell membrane (Zhang et al., 2010). Therefore, it appears that this mode of activity for ZnONPs may be conserved in both bacterial and fungal cells.

3-3A

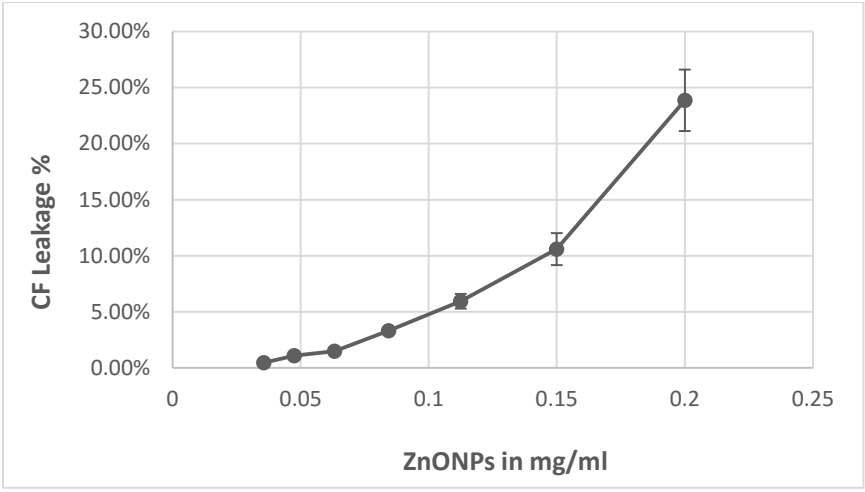

3-3B

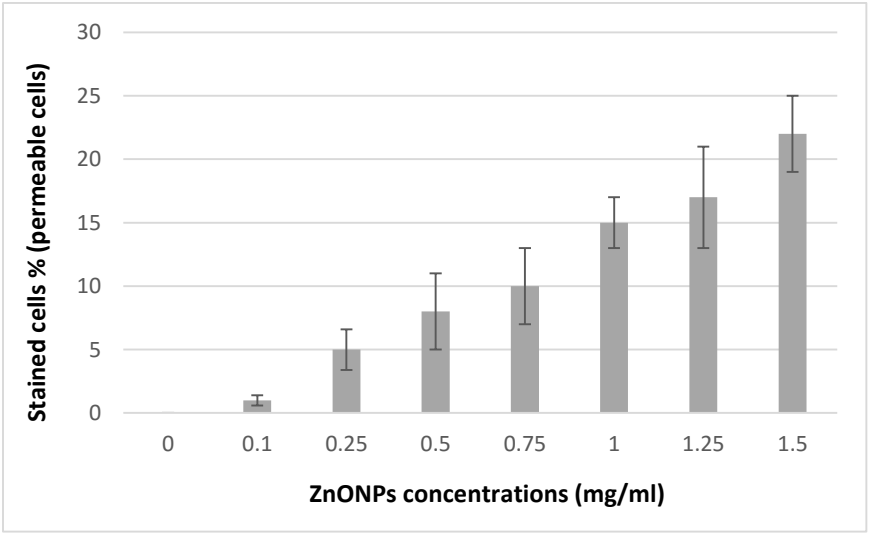

Figure 3-3. Testing the membrane-disruptive properties of the ZnONPs.
A) Investigating the activity of ZnONPs on cell membrane using a liposome assay. Carboxyfluorescein-DOPC liposomes were exposed to different concentrations of ZnONPs (0.05 to 0.2 mg/ml). After incubation for 30 minutes fluorescent signal was recorded (μ=485 nm, and λ=528 nm) and Leakage % was calculated. Data points represent the average value for at least 3 independent investigations. Error bars represent standard errors. B) Investigating the activity of ZnONPs on cell membrane using trypan blue assay. Yeast cells grown to mid-log phase were treated with eight different concentrations of ZnONPs (0, 0.1, 0.25, 0.5, 0.75, 1.0, 1.25 and 1.5mg/ml) and incubated at 30^{o}C for 2 hours. Cell suspensions were adjusted to a final density of 10^{7} cells/ml and subjected to 0.4% trypan blue staining. Data points represent means (±S.E.) for at least 3 independent investigations normalized to that of no- ZnONPs control.

3.4.4 Ion homeostasis alteration caused by ZnONPs

In our high-throughput screen for ZnONPs hyper-sensitive strains, we also observed an enrichment of mutants with deletions in genes involved in ion homeostasis (17%, *p-value* = $7.9x10^{-6}$) such as *FTR1*, which codes for an ion transporter, *GEF1*, which is involved in cation homeostasis, and *SPF1*, which mediates Ca^{2+} homeostasis. A membrane depolarization assay was performed to confirm the effect of ZnONPs on ion homeostasis. In this assay an electrical potential-sensitive fluorescent dye ($DiSBAC_2(3)$) was utilized (Quaranta et al., 2010). This dye can only penetrate cells with depolarized cell membranes and provides a fluorescent signal when it binds to intracellular proteins. Therefore, cells displaying an ionic imbalance in the cell membrane will depict an increase in fluorescence. Yeast cells were exposed to 0.25 and 1.0 mg/ml of ZnONPs and the level of fluorescent signal was then measured (Figure 3-4). The depolarizing effect of the ZnONPs was observed in samples exposed to 1 mg/ml of ZnONPs. This ZnONPs effect was comparable to that of the proton ionophore CCCP (a depolarizing agent) used as a positive control. Both samples showed a second peak in the fluorescent region (10^4 - 10^5) on the FL2-H axis indicating that the dye was able to enter the cell due to membrane depolarization. The results suggest that ZnONPs depolarizes the cell membrane and validate the results from our phenotypic screening, where an enrichment for homeostasis related genes was observed. This membrane depolarization effect may be linked to the observed membrane destabilizing effects of ZnONPs.

This observed influence of ZnONPs on ion homeostasis in yeast mirrors the mode of action suggested by Kao and collaborators (2011), who reported that ZnONPs disturb the ion homeostasis in human cells. It was proposed that ZnONPs enter the cell via endocytosis and the acidic pH of the endosomes facilitates ZnO dissolution thus increasing the cytosolic and mitochondrial Zn^{2+} concentrations, leading to depolarization of the mitochondrial membrane which triggers programmed cell death (Kao et al., 2011).

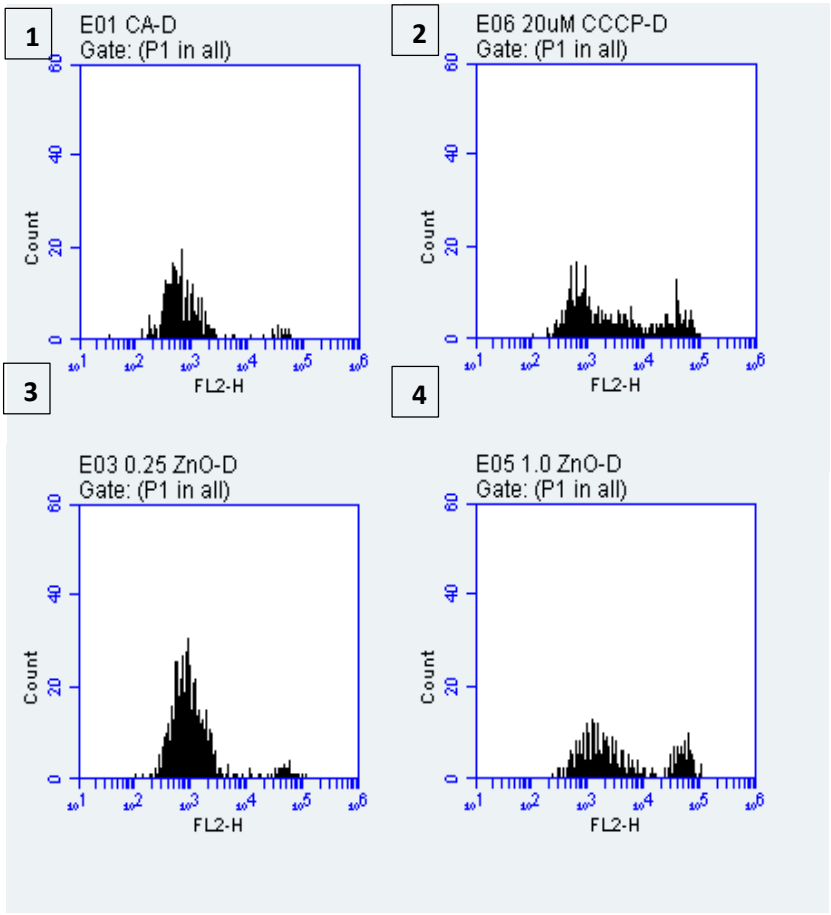

Figure 3-4. Effect of ZnONPs on cell membrane depolarization. Yeast cells (10^6 cells/ml) were subjected to: (1) 0.01 mM of citric acid, as a carrier-control, (2) 20 µM of CCCP (Carbonyl cyanide 3-chlorophenylhydrazone) used as a positive control, (3) 0.25 mg/ml of ZnONPs, (4) 1 mg/ml of ZnONPs. The histograms represent the fluorescent signal (X axis, FL2-H) emitted by yeast cell counts (Y axis). ZnONPS at the concentration of 1 mg/ml (4) caused an effect similar to CCCP (positive control) by showing a second peak in the fluorescent region 10^4 - 10^5 on the FL2-H axis, suggesting that membrane depolarization enabled the dye to enter the cell.

3.4.5 ZnONPs disrupt cell wall integrity

The third major group of mutants highly sensitive to ZnONPs have deletions in cell wall organization and biogenesis genes (*p-value* = 9.8×10^{-3}), and represent 12% of the most sensitive mutant strains (Figure 3-2A). Included in this group were gene deletions such as *KRE6, HOC1* and *BCK1* (involved in glucan biosynthesis, cell wall mannan biosynthesis and control of cell integrity, respectively). Any alteration in cell wall composition caused by gene deletions may modify cell wall rigidity and lead to a higher sensitivity to chemicals that target cell wall integrity. To test the results from our large-scale screening analysis, that suggested that ZnONPs interfere with cell wall functions, a cell wall integrity assay was carried out by exposing ZnONPs-treated cells to mild sonication. The perturbation of the cell wall architecture caused by a physical agent such as sonication can be enhanced by exposing cells to chemicals that interfere with cell wall integrity (Mir-Rashed et al., 2010). Cell viability was estimated by drop-out analysis following 10-fold serial dilutions (10^{-2}-10^{-6}) for each treatment with and without sonication. Figure 3-6 indicates that exposure to ZnONPs enhances the sonication-induced disruption of yeast cell wall functions in a dose-dependent manner. For example, samples exposed to 0.5 mg/ml of ZnONPs and sonicated showed a 0.50 survival ratio compared to control (non-ZnONPs-treated sonicated cells), 1.0 mg/ml ZnONPS yielded a ratio of 0.38, and 1.5 mg/ml ZnONPs yielded a ratio of zero (no survival of ZnONPs-treated sonicated cells) (Figure 3-5C). These results provide evidence of the intensifying effect of ZnONPs on cell wall sensitivity to sonication. This experiment supported our inference

from the GDA analysis that ZnONPs interact with cell wall functions in yeast. This effect of ZnONPs on yeast cell wall corresponds to findings by Hassan et al. (2013), based on Scanning Electron Microscopy with *Aspergillus* spp., that indicate ZnONPs electrostatically interact with cell wall biomolecules to alter the spatial configuration of the cell wall.

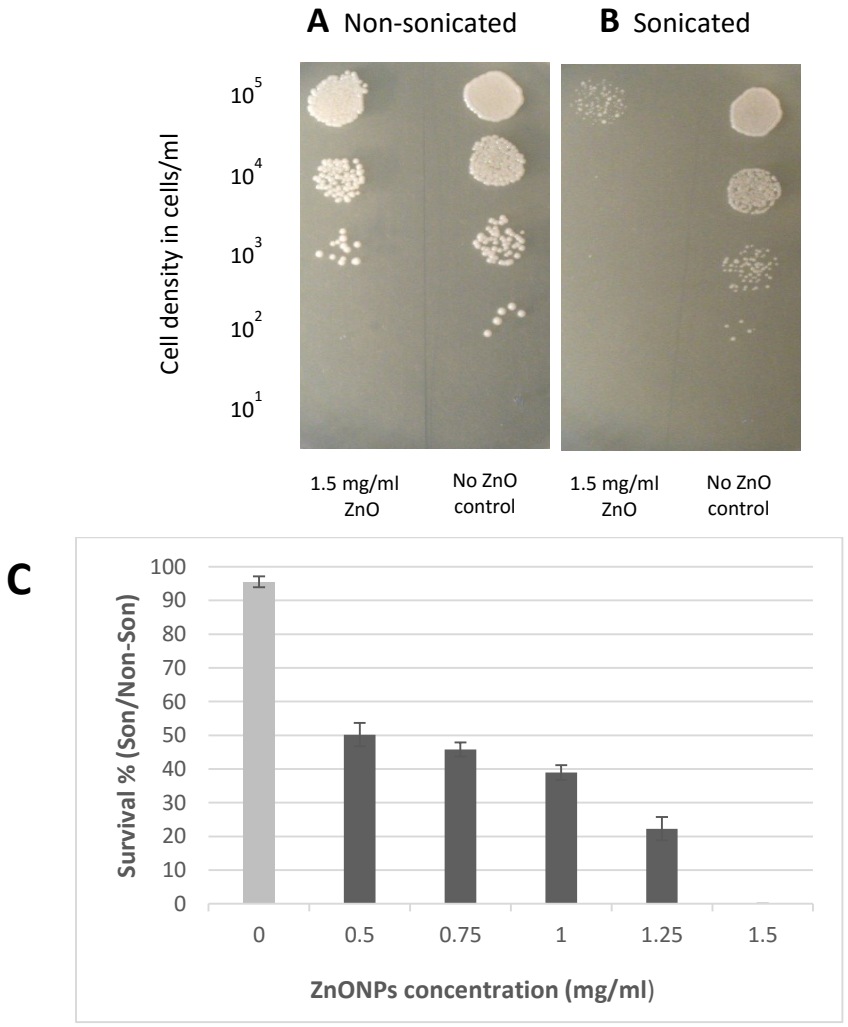

Figure 3-5. Effect of ZnONPs on cell wall integrity. Disruptive effect of sonication was intensified by exposing yeast cells (10^5 - 10^1 cells/ml) to increasing concentrations of ZnONPs. 10-fold serial dilutions of treated cell suspensions were spotted onto YPD: **(A)** without sonication, and **(B)** with sonication. Panel **(C)** represents the quantification of yeast cells sensitivity to ZnONPs with and without sonication. Cell survival rate (% survival sonicated/non-sonicated cells) decreases with increasing concentrations of ZnONPs in a dose-dependent manner indicating that ZnONPs compromise cell wall functions.

3.4.6 β-gal assay indicates that AgNPs decreases transcription rates

Based on GDA analyses, we found that 16% of the most sensitive deletion mutants to AgNPs were in the transcription and RNA processing category (*p-value* = $1.3x10^{-3}$). Mutants lacking genes that encode for transcription elongation factors such as THP2, THO2 and RNA processing proteins such as CTK1 are found in this functional category. To test the effect of AgNPs on transcription, a reporter β-galactosidase expression-based assay was carried out. This assay has been used previously to investigate transcription rates in *Salmonella* (Kutsukake et al., 1990) and in yeast (Rohde et al., 2000; Krogan et al., 2003). Yeast (W303) cells were transformed with plasmid p416 and cells were exposed to different sub-inhibitory concentrations of AgNPs (0.9 to 9.0 μg/ml). The effect of AgNPs on the β-galactosidase enzymatic activity was evaluated as an indirect measure of transcription (Krogan et al., 2003). Enzymatic activity was estimated in terms of the MUB (4-methylumbelliferon fluorescent product) release after MUG was hydrolyzed by expressed β-galactosidase. The assay showed that AgNPs reduce gene expression in a dose-dependent manner (Figure 3-6). For example, exposure of 2.14 μg/ml AgNPs resulted in a 36% decrease in β-galactosidase activity compared to the negative control (non-AgNPs), and a concentration of 9 μg/ml caused a decrease of 64% in activity, which is comparable to the effect of 48 μg/ml 6-azauracil, a known inhibitor of transcription.

The effect of AgNPs on transcription may be explained by the 'hard-soft acid base theory (HSAB)' which states that 'soft' acids such as Ag^{+}, among other metals, can bind sulphur or phosphorous in 'soft' bases, altering protein structure or function (Pearson,

1963; Lemire et al., 2013; Higa et al., 2013). Another potential explanation is that silver ions could be indiscriminately incorporated as metal cofactors into enzymes (ion mimicry), interfering with regular metabolic functions (Clarkson, 1993; Lemire et al., 2013). It is our understanding that AgNPs effect on transcription has not been previously reported. More studies are required to determine the specific target of AgNPs in the transcription process.

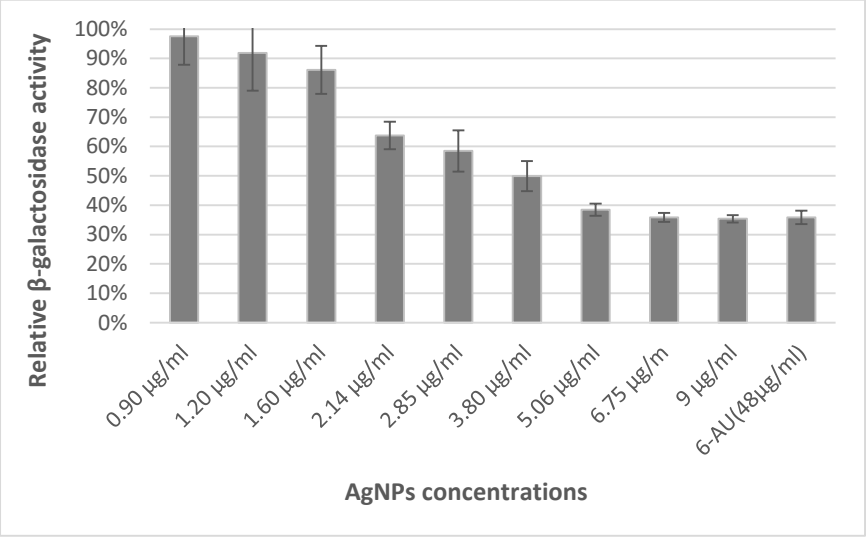

Figure 3-6. Changes to the expression of β-galactosidase in response to treatment with AgNPs. Expression assay was performed on yeast cells transformed with plasmid p416 containing a galactose inducible β-galactosidase reporter gene. Yeast cells (10^7 cells/ml) were grown in 2% galactose-supplemented SC-URA medium containing AgNPs concentrations between 0.9 and 9.0 µg/ml or 6-azauracil (positive control). Fluorescent units were obtained based on the amount of MUB generated after MUG hydrolysis. MUB units for each replica (samples and controls) were calculated with the equation: $F_{390/475}$ /t × A_{595}. µ=390 nm and λ=475 nm. Mean values (±SE) are related to that for the control and based on at least 3 independent experiments.

3.4.7 AgNPs influence electron transport chain (ETC) performance

The second largest functional group that resulted in high sensitivity to AgNPs in the GDA analysis comprised mutants lacking genes that code for proteins involved in

cellular respiration (14%, *p-value* = $5.7x10^{-4}$) such as IDH1 which catalyzes the oxidation of isocitrate to alpha-ketoglutarate, SOD1 which is cytosolic copper-zinc superoxide dismutase that detoxifies superoxide, and ETR1 (YBR026C), a 2-enoyl thioester reductase that is involved in aerobic respiration. We tested the effect of AgNPs on cellular respiration with 3-(4,5-dimethylthiazol-2-yl)-2,5-diphenyltetrazolium bromide (MTT) assay. MTT monitors electron transport chain performance since it is reduced by mitochondrial succinate dehydrogenase to the formazan salt [(E,Z)-5-(4,5-dimethylthiazol-2-yl)-1,3-diphenylformazan that can be measured spectrophotometrically (Sánchez and Konigsberg, 2006). To this end, yeast cells were exposed to different concentrations of AgNPs (0.75-17.5 μg/ml). Sodium azide is an ETC inhibitor that blocks complex IV in the ETC and was used as a positive control. Figure 3-7 shows that 57.7% of MTT was reduced when the yeast cells were exposed to 5 μg/ml of AgNPs representing ≈42% decrease in activity. With exposure to 10 μg/ml of AgNPs, a 64% decrease in activity was observed. The results indicate that the MTT reduction by ETC is inhibited by AgNPs in a dose-dependent manner.

Of interest, the level of ETC inhibition by AgNPs is greater than that by our positive control, sodium azide. This might be due to the fact that sodium azide inhibits the Heme groups of oxidases including the cytochrome oxidases (complex IV), but it does not affect the reducing potential from other sources such as oxido-reductases anchored in non-mitochondrial membranes (Montellano et al., 1988; Berridge and Tan, 1993). It was previously speculated that AgNPs inhibition of *E. coli* is due to the interaction of Ag ions

with the thiol groups frequently encountered in membrane and antioxidant proteins including thioredoxin reductase and superoxide dismutase (Holt and Bard, 2005). Alteration of mitochondrial membrane proteins can trigger permeabilization of membranes and depolarization in mitochondria, provoking an impaired electron transfer causing oxidative stress (Costa et al., 2010; Lemire, 2013; Massarsky et al., 2014; Zhang et al., 2014). In our studies, an experiment was carried out with the antioxidant histidine, and it was observed that the inclusion of the histidine reduced growth inhibition of yeast by AgNPs, indicating that antioxidants can sequester ROS produced during cellular respiration (data not shown).

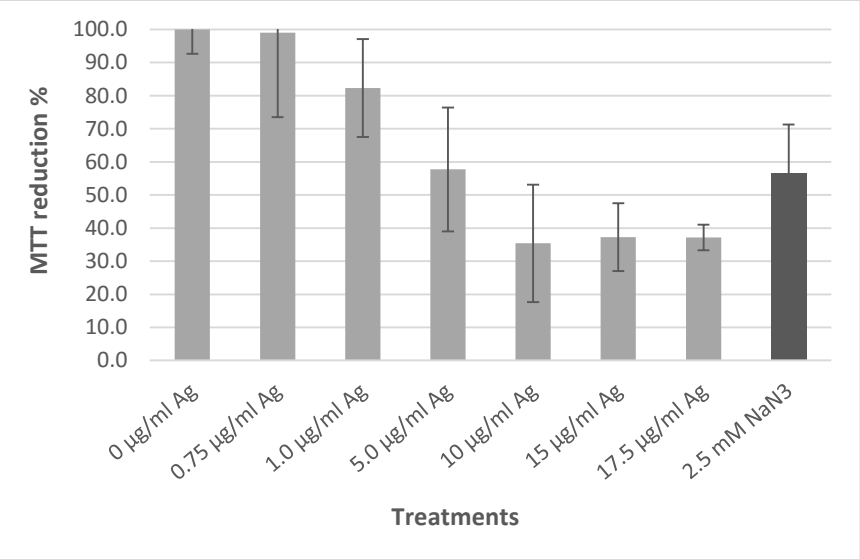

Figure 3-7. AgNPs inhibits the yeast electron transport chain (ETC) in a dose-dependent manner. Upon reduction, MTT is transformed to the purple coloured formazan salt that can be quantified spectrophotometrically. Yeast cells were exposed to 0.75, 1, 5, 10, 15 and 17.5 µg/ml of AgNPs. Each experiment was repeated at least 3 times and the average was normalized to the control. Sodium azide was used as a positive control. Error bars represent standard error.

3.4.8 Fluid-phase endocytosis assay supports the effect of AgNPs on endocytosis

In our high-throughput GDA study the group representing endocytosis and vesicular transport was also highly enriched. This category represents 12% (*p-value* = $1.4x10^{-5}$) of highly sensitive mutant strains comprising deletions of genes involved in clathrin-mediated endocytosis and vesicular transport such as *ENT3, APM4, APL1, APL2* and *AAC1.* To further study the effect of AgNPs on endocytosis a fluid-phase endocytosis assay was done based on Lucifer Yellow intake. Lucifer Yellow (LY) is a highly hydrophilic dye which is unable to cross the cell membrane but it is internalised through endocytosis (Wiederkehr et al., 2001). Its accumulation can be investigated by fluorescence microscopy and it has been used as a measure of endocytosis performance (Riezman, 1985) where defects in endocytosis can be observed as differences in fluorescence localization and intensity (Dulic et al., 1991; Munn, 2000). To this end yeast cells (10^7 cells/ml) were exposed to sub-inhibitory concentrations of AgNPs (40 and 80 µg/ml) and incubated in the presence of 4 mg/ml of LY. The buffer containing sodium azide (2.5mM NaN_3/2.5mM NaF/12.5Mm sodium phosphate), an endocytosis inhibitor, was used as positive control. Samples were observed under microscope and percentage of fluorescent cells was calculated after counting cells. The percentages of LY-stained yeast cells exposed to 40 µg/ml and 80 µg/ml of AgNPs were 37.1% and 22.6%, respectively (Figure 3-8). These values are comparable to that for the positive control treatment with 13.1% NaN_3 (Figure 3-8). NaN_3 inhibits ATP hydrolysis which may interfere with the vacuolar pH balance and thus perturb endocytosis (Bowler et al., 2006; Dettmer et al., 2006). These

observations validate the results of the GDA screening that suggest that AgNPs affect endocytosis.

This effect of AgNPs on endocytosis can be explained by the capability of metal ions to generally impair membrane function. Previous studies demonstrated that AgNPs affected the cell membrane morphology in *E. coli* and *V. cholera*, leading to defective transmembrane transport and increased permeability (Le et al., 2012). Similarly, Kim and co-workers (2009) found that AgNPs altered the membrane dynamics of *Candida albicans*, changing the chemi-osmotic potential and causing lipid peroxidation. It is well established that modification of membrane dynamics can affect vesicular membrane trafficking (Mayinger, 2012). These perturbations can be attributed to the capability of metal-nanomaterials like AgNPs to electrostatically interact with negatively charged functional groups such as COO-, SH- or phosphorous. These functional groups are found in proteins and phospholipids, including those in cellular membranes.

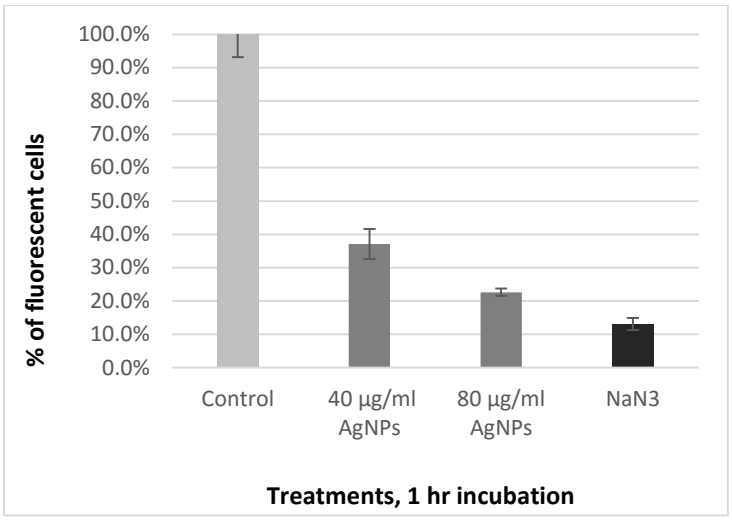

Figure 3-8. AgNPs interfere with endocytosis. Integrity of endocytosis was evaluated by Lucifer Yellow (LY) accumulation in cells. Yeast cells were incubated for 1 hour at 30°C in YPUAD in presence of 4 mg/ml of LY, without or with 40 or 80 µg/ml of AgNPs. A buffer containing 12.5 mM sodium phosphate, 2.5mM sodium azide and 2.5 mM sodium fluoride buffer, pH 7 was used as a positive control. Percentage of fluorescent cells relative to no-AgNPs-control was determined by examining at least 6 different fields, each with >20 cells, using a fluorescent microscope (Axiophot, model, objective 40x and 100x, FITC optics; Zeiss, Germany). Results represent mean values (±SD).

3.5 CONCLUDING REMARKS

ZnONPs and AgNPs among other engineered nano-materials (ENMs) demonstrate a broad spectrum of toxic effects against bacteria, fungi, viruses and algae. It is thought that the antimicrobial and cytotoxic properties of NPs depend on their chemical composition, surface structure/charge, surface/volume ratio, solubility, shape and aggregation properties (Nel, et al., 2006). Antimicrobial activities of ENMs seem to be correlated to the type of cells, presence and composition of cell wall, cell membrane composition and the developmental stage of the cell (Niazi et al., 2011). The toxic effects of NPs on microorganisms appears to also extend to higher eukaryotes including

mammalian cells (Nel et al., 2006). A growing number of studies are focusing on the mechanisms of action of NP toxicity to evaluate the potential risk of NPs to human health and environment (Marambio-Jones and Hoek, 2010). In this study we report on the potential mode of action of both ZnONPs and AgNPs on the baker's yeast, *S. cerevisiae*, an eukaryotic model organism. Our results indicate that the antifungal activity of ZnONPs contribute to altering ion homeostasis, depolarizing and disrupting cell membrane, and disturbing cell wall. We infer that AgNPs, on the other hand, inhibit yeast growth by reducing rates of transcription, cellular respiration and endocytosis.

This study provides additional evidence for the usefulness of large-scale genomics screening to study of nanoparticles and other biologically active compounds. It demonstrates that chemical-genetic profiling provides insights into the mode of induced cytotoxicity. The speed and ease of use, coupled with relatively simple data analysis makes chemical-genetic analysis using GDA an ideal tool for the preliminary investigation of nanoparticle mode of activity.

Chapter 4

Mode of action of the bacteriocin nisin on the Gram-negative bacterium, *Escherichia coli*

4.1 Abstract

We investigated the inhibitory activity of nisin in combination with a membrane disrupting chelator, citric acid, against the Gram-negative bacterium, *E. coli*. Nisin is a well-characterized bacteriocin that is known as an effective inhibitor of a variety of Gram-positive bacteria. As such, nisin is used as a natural food preservative and in veterinary medicine. Study of nisin's inhibitory activity against Gram-negative bacteria may provide new insights into the mode of action of this compound and its suitability for treating infections caused by Gram-negative bacteria. We analyzed chemical-genetic interactions to identify nisin-sensitive *E. coli* strains in the Keio library of deletion mutants. The most sensitive mutants fell into two main groups: cell wall/membrane/envelope biogenesis and cell cycle and DNA replication, recombination and repair. Further analyses were used to test nisin's effects on DNA replication. These assays indicated that nisin exposure causes a small decrease in replication of the low copy number plasmid, pFZY1, in *E. coli*. However, a flow cytometry-based assay revealed a significant decrease in genomic DNA content in *E. coli* strains exposed to sub-inhibitory concentrations of nisin-citric acid. The effect of nisin-citric acid on ciprofloxacin-resistant *E. coli* mutants was also investigated and it was observed that the majority of those tested (*CipR2*, *CipR6* and *CipR8*) showed

increased sensitivity to nisin compared to wild type. This research indicates that nisin interferes with Gram-negative bacterial cell wall/membrane functions and reveals an additional, previously unknown mode of action whereby nisin inhibits DNA replication in Gram-negative bacteria. Our findings indicate that nisin is a multi-targeted antimicrobial, a feature that provides advantages over single-target antimicrobials in repressing bacterial resistance mechanisms.

4.2 INTRODUCTION

Bacteriocins are low-molecular weight peptides of between 30 – 60 amino acids that are ribosomally synthesized by many Bacteria and Archaea (Klaenhammer, 1988; Riley, 1998). Bacteriocins can exhibit either a narrow or a wide spectrum of bacteriostatic or bactericidal activity and are usually classified according to structure into class I (lanthionine-containing bacteriocins), class II (non-lanthionine containing bacteriocins) or class III (bacteriolysins) (Cotter et al., 2005). In this chapter, I investigated the mode of action of a well-characterized class I bacteriocin, Nisin, which is produced by the lactic acid bacterium, *Lactococcus lactis* subps. *lactis*.

Nisin was first isolated in 1928 by Rogers and Whittier and characterized by Mattick and Hirsch in 1947 (Delves-Broughton et al., 1996; Juncioni de Arauz et al., 2009). It was originally used as a food preservative in processed cheese in 1957 and was later approved as a food additive by the Food and Agriculture Organization of the United Nations in 1969 (Delves-Broughton et al., 1996). Nisin is an amphiphilic and cationic peptide containing 34 amino acids and is 3500 Da in size. Nisin, like other class I bacteriocins, is post-translationally modified to generate the lanthionine rings that are likely functionally important for antibacterial activity (Juncioni de Arauz et al., 2009). Nisin is encountered in two variants: nisin A and nisin Z; both molecules possess a similar structure but they differ in a single amino acid residue at position 27, being a histidine in nisin A and an asparagine in nisin Z (Cheigh and Pyun, 2005).

Nisin has demonstrated an efficient antagonist activity towards a variety of food spoilage, food poisoning and pathogenic Gram-positive bacterial strains of *Lactobacillus*, *Pediococcus, Bacillus, Micrococcus, Lactococcus, Streptococcus, Staphylococcus*, *Listeria, Enterococcus,* and *Clostridium* among others (Delves-Broughton, et al., 1996; Coma et al., 2001; Sobrino-Lopez et al., 2008; Juncioni de Arauz, 2009; LeBel et al., 2013; Tong et al., 2104; Chai et al., 2015). This broad spectrum activity has enabled the use of nisin to improve food quality (i.e., nutraceutical foods, food spoilage prevention), food safety (anti-listeriosis, *Listeria monocytogenes*), as a veterinary medicine (anti-mastitis application against *Staphylococcus aureus*), and as a human medicine (treatment for dermatitis, dental caries, respiratory and vaginal infections) (Cotter et al., 2005; Juncioni de Arauz et al., 2009).

The antimicrobial mode of action of nisin has been associated with its ability to depolarize the cytoplasmic cell membrane through its high affinity for the cell wall precursor lipid II (undecaprenyl-pyrophosphyoryl-MurNAc-(pentapeptide)-GlcNAc). Nisin recruits lipid II molecules, building up very stable channels in the cytoplasmic membrane (8 nisin and 4 Lipid II molecules/channel). Formation of these channels results in leakage of cellular contents, efflux of ions that dissipate the cell's proton motive force, and depletion of intracellular ATP, which further perturbs the cell membrane and other biochemical processes. Nisin binding to lipid II also prevents peptidoglycan synthesis and thus disrupts cell wall biogenesis and functions (Wiedemann et al., 2004; Hasper et al., 2004; Bauer and Dicks, 2005; Christ et al., 2007).

In contrast, Gram-negative bacteria tend to be resistant to nisin due to the outer membrane (OM) that impedes the movement of hydrophobic molecules such as nisin to targets in the cytoplasmic cell membrane. Metal-chelators can destabilize the OM by removing Ca^{+2} and Mg^{+2} from the cell wall and increase OM permeability, allowing nisin to reach its target in the cytoplasmic cell membrane. Previous studies have demonstrated that a combination of nisin and permeabilizing agents such as EDTA, disodium pyrophosphate, sodium hydrogen orthophosphate, citric acid, or lactic acid can efficiently inhibit growth of Gram-negative bacteria such as *Escherichia coli, Salmonella* sp., and *Pseudomonas* sp. (Delves-Broughton et al., 1996; Boziaris et al., 1999; Helander et al., 2000; Alakomi et al., 2000). Despite studies on the primary molecular targets of nisin in Gram-positive bacteria, the mode of action of this bacteriocin on Gram-negative bacteria has not been investigated. It is assumed that nisin exerts its inhibitory activity on Gram-negative bacteria through the same mode of activity as in Gram-positive bacteria through the depolarization of cell membrane and cell wall synthesis inhibition (Cotter et al., 2005), however this has not been adequately tested.

In this study, a high-throughput chemical-genetic interaction analysis was done using a set of *E. coli* deletion mutants with medium containing sub-inhibitory concentration of nisin (and citric acid as a chelator). The 'Keio' library of strains with non-essential gene deletions used in this study was developed by Baba and co-workers (2006) and contains approximately 3900 mutant strains of *Escherichia coli* (K-12). Previously, deletion libraries such as this have enabled stimulus-response studies at a genome-wide

level and have provided information on gene-gene and gene-drug interactions, as well as gene function discovery (Babu et al., 2009; Babu et al., 2011; Brochado and Typas, 2013; Kumar et al., 2016). From our analysis of the genetic profile of mutant strains that were super-sensitive to nisin we obtained molecular mechanistic insights into nisin mode of action. As expected from previous work with Gram-positive bacteria, the functional clustering of the phenotypic analysis showed that nisin interacts with factors involved in cell membrane transport systems and cell wall biosynthesis. In addition, strains with deletions in genes involved in DNA-replication-repair were also very sensitive to nisin, and we further investigated this potentially novel mode of action of nisin.

4.3 MATERIALS AND METHODS

4.3.1 Chemicals

Nisin A was purchased from Santa Cruz Biotechnology (2.5 % purity, 1000 IU/mg; Santa Cruz, Dallas, TX, USA). Citric acid and Luria-Bertani medium (LB, 1% peptone, 0.05% yeast extract and 1% NaCl) were from Bioshop (Burlington, ON, Canada). NaOH, HCl (37%), ethanol (95%), triton-X, ciprofloxacin and kanamycin were from Sigma (Oakville, ON, Canada). Carboxyfluorescein, propidium iodide and RNAase were purchased from Life Technologies (Life Technologies Inc., Burlington, ON, Canada) and lipids were from Avanti Polar Lipids (DOPC, Avanti Polar Lipids, Alabaster, AL, USA).

4.3.2 Strains and growth conditions

Escherichia coli strain *JCM1649* (NR_112558, Table 4-1), referred to as wild type in this study, was provided by Dr. A. Wong (Department of Biology, Carleton University) and it was routinely grown in LB broth at 37^{o}C with constant agitation (150-200 rpm) unless otherwise specified. The Keio collection of about 3900 deletion mutants was kindly provided by the National BioResource Project (National Institute of Genetics of Japan, NIG). The Keio set was grown at 32^{o}C on LB agar (2% agar) containing 30 µg/ml of kanamycin, and stored long term in LB broth + kanamycin with glycerol (16% v/v) at -80^{o}C.

The list of *E. coli* mutants from the Keio collection used in plasmid replication and flow cytometry assays is presented in Table 4-1. These mutants were cultured in LB broth supplemented with 30 µg/ml of kanamycin at 32^{o}C unless otherwise specified. The low-copy-number plasmid pFZY1 was propagated using *E. coli* in LB broth containing 100 µg/ml of ampicillin. Ciprofloxacin-resistant strains (Table 4-1) were obtained from A. Wong (Department of Biology, Carleton University).

Table 4-1. Selected *E. coli* strains

Strain	Gene/Mutation	Sensitivity test
Wild type strains		
JCM1649	Wild type control for deletion mutant strains	Nisin, Nisin-CA, novobiocin
MG1655	Wild type control of Cip-resistant strains	Nisin-CA
Selected nisin-sensitive Keio mutants with deletions of DNA replication/repair genes		
ΔdnaQ	deletion of DNA polymerase III epsilon subunit	Nisin-CA, novobiocin
ΔdnaG	deletion of DNA primase	Nisin-CA, novobiocin
ΔtatD	deletion of *tatD*, Mg-dependent cytoplasmic DNase	Nisin-CA, novobiocin
ΔparC	deletion of DNA topoisomerase IV, subunit A	Nisin-CA, novobiocin

Ciprofloxacin (Cip)-resistant mutants		
CipR1	*gyrA*/S83A	Nisin-CA
CipR2	*marR* deletion of amino acids 72-82	Nisin-CA
CipR3	*gyrA*/D87Y	Nisin-CA
CipR5	*gyrA*/D87G	Nisin-CA
CipR6	*marR*/R94C	Nisin-CA
CipR8	*marR*/R77H	Nisin-CA

4.3.3 Nisin and Nisin-Citric acid (nisin-CA) sensitivity tests

To determine a suitable citric acid concentration in combination with nisin, drop-out and microdilution tests were performed. For the drop-out test, an overnight culture of *E. coli* WT grown in LB at 37^{o}C was diluted to adjust cell density to 10^5 cells/ml. This cell suspension was distributed into culture tubes containing different concentrations of nisin (0, 0.25, 0.5 and 1.0 mg/ml) and citric acid (10 and 20 mM, pH adjusted to 5.0 with NaOH) to test for growth inhibition. Negative controls of citric acid (0, 10 or 20 mM, pH 5.0±0.02) were also tested. All culture tubes were incubated for 3 hours at 37^{o}C. After incubation, 10-fold serial dilutions (10^{-3} to 10^{-8}) of each culture were prepared and 10 µl of each dilution was spotted onto LB agar plates and incubated for 16-24 hrs at 37^{o}C to subsequently count colonies.

For the microdilution analysis, the MIC_{90} and MIC_{50} were defined as the lowest concentration of nisin that caused a 90% or 50% growth inhibition, respectively. Working solutions of the substances under study (nisin, nisin-citric acid or novobiocin) were prepared according to Table 4-2 and filter-sterilized with a 0.2 µm membrane (novobiocin and citric acid) or heat-treated (nisin) at 80^{o} C for 10 min. A 1:1 serial dilution of the

corresponding working solution was done in a 96-well microtitration plate containing LB broth. Carrier control and non-drug controls were included in the test-plate (Table 4-2). An overnight culture of the *E. coli* strain under study (Table 4-1) was serially diluted to adjust cell density to 10^3 cells/ml and 100 μl of cell suspension was added to each well of the microtitre plate. Assays testing the effect of the citric acid in combination with nisin, included citric acid evenly distributed at a final concentration of 20 mM (pH adjusted to 5.0±0.02 with NaOH). Inhibitory effect was assessed after 16-24 hr incubation (35-37^{o}C) based on optical density measurements at 600 nm (OD_{600}) with a Cytation 5 cell imaging multi-mode reader (BioTek, Winooski, VT, USA). Inhibition was calculated using the formula: $I\% = 100-[(Abs_{exp}-Abs_{blank})/Abs_{carrier}-Abs_{carrier\ blank})]* 100$. Every concentration was tested at least in triplicate, results of the inhibition % were averaged and SE was calculated.

Table 4-2. Antimicrobials used in the sensitivity test and their corresponding working concentrations.

Chemicals	Working solution concentration	Range of tested concentrations	Carrier	Other chemicals
Nisin	20 mg/ml	0.07 - 10 mg/ml	0.02 N HCl	
Nisin-citric acid	16 mg/ml	0.01 - 8 mg/ml	0.02 N HCl	20 mM CA[1]
Novobiocin[2]	6.4 mM	0.05 - 3.2 mM		
Citric acid	200 mM	20 mM		

[1] Citric acid (CA) was used as chelator. 20 mM citric acid was evenly distributed in all the wells including the negative control and carrier control (0.02 N HCl)

[2] Novobiocin was used as a positive control for inhibition of DNA replication (Hardy et al., 2002)

4.3.4 High throughput chemical-genetic profiling

A suitable sub-inhibitory concentration of nisin in agar medium was required for a chemical-genetic profile experiment with nisin and the Keio deletion mutant set. Based on the MIC assays in liquid medium, nisin (1.2 and 2.0 mg/ml) was combined with 20 mM citric acid (pH 5.0 $\pm$ 0.02) in LB + 2% agar medium. Control plates were prepared that contained the same proportion of carrier (0.02 N HCl) and citric acid. Colonies from two randomly chosen plates from the Keio set were inoculated onto the nisin-CA and CA-control media using a 384-floating replicator. The plates were incubated at 32^{o}C for 16 hours and the colony sizes were visually examined. The concentration at which approximately 5-10% of the strains showed increased sensitivity identified by a colony size reduction of between 30 to 50% compared to control (Galván et al., 2013) was selected for experiments with the complete Keio mutant set.

The Keio deletion mutant collection of about 3900 mutants on 24 plates was simultaneously inoculated by pinning onto experimental (with nisin-CA) and control (with CA) plates, incubated at 32^{o}C for 16-24 hrs and then digital images were acquired and analyzed by growth detector software (Memarian et al., 2007). Digital analysis was verified by visual examination. Four replica experiments with the entire Keio set were done. From each experiment, the percent inhibition of each mutant strain was calculated based on colony size measurements on control and experimental plates (colony size reduction% = [(Area $_{(control)}$-Area $_{(experimental)}$)/Area $_{(control)}$] (100). Mutants showing a high sensitivity (60-100% colony size reduction) to nisin-CA were identified. High sensitivity

mutants on at least 2 of the 4 replica experiments were then selected and categorized into functional clusters according to COG (Clusters of Orthologous Groups, http://www.ncbi.nlm.nih.gov/COG/; http://www.compsysbio.org/bacteriome/).

4.3.5 Membrane disruption assay (liposomes assay)

The liposome assay is a cell-free assay where lipid membrane disruption by the substance under study is made evident through the release of fluorescent content from the liposome. Liposomes used in this study were prepared as previously described (Cruz et al., 2014). Liposomes were made with dioleoylphosphatidylcholine (DOPC) encapsulating carboxyfluorescein (CF) in large unilamellar vesicles (LUVs ≈ 100 nm diameter; Cheetham et al., 2003). LUVs were suspended in iso-osmotic buffer (100 mM NaCl, 10 mM HEPES, pH 7.4) and mixed with a 1:1 serial dilution series of nisin (1.5 to 6.0 mg/ml) in the iso-osmotic buffer in a 96-well microplate (black/clear Optilux flat bottom; BD Bioscience, San Jose, CA, USA). As a control, the nisin carrier (0.02 N HCl) was also serially diluted across the plate in parallel with the nisin suspension.

Fluorescence intensity was measured with an excitation wavelength (μ) of 485 nm and an emission wavelength (λ) of 528 nm using a Cytation 5 cell imaging multi-mode reader (BioTek, Winooski, VT, USA). Threshold fluorescence (F0) was determined by reading the fluorescent signal of the LUV suspension without additives. After mixing, the compound and liposomes were allowed to interact for one hour at room temperature in dark prior to obtaining fluorescent emission readings, F (fluorescent intensity of the

vesicles after incubation of liposomes with nisin/carrier). F100 (Fluorescence intensity with 100% leakage of CF) was obtained 10 minutes later by adding triton X-100 (10% v/v). The % leakage (%L) was calculated by the equation: %L = [(F-F0)/ (F100-F0)] X 100.

4.3.6 Plasmid replication assay

E. coli W3110 (WT) and selected DNA replication/repair mutants (Table 4-1) were transformed with the plasmid pFYZ1. The pFZY1 is a low-copy plasmid (1-2 copies/cell) containing an ampicillin resistance cassette and a β-galactosidase-coding *lacZ* gene (Koop *et al.* 1987). Chemically competent *E. coli* WT and DNA replication/repair mutant strains were transformed separately through heat-shock (Tu, 2010). Transformants (blue colonies) were selected on LB-ampicillin agar plates (1.5% agar, 100 μg/ml ampicillin) containing 40 μl of X-gal solution (5-bromo-4-chloro-3-indolyl-β-D-galactopyranoside, 40 mg/ml). Single blue colonies were cultured and stored as glycerol stocks (16%) at -80^{o}C for future use.

pFZY1-transformants were grown overnight in LB-ampicillin (100 μg/ml) broth and the cell density of each culture was adjusted to 10^3 cells/ml by dilution. Aliquots of 100 μl of these adjusted cultures were plated on LB agar plates (1.5% agar) containing different concentrations of nisin-CA (0.1- 0.9 mg/ml) or novobiocin (0.05 – 2.0 mM). Control plates were also inoculated with each strain to test the potential effect of carrier solvents (0.02 N HCl) and chelator (20 mM citric acid) on plasmid replication. Plates were incubated for 16-24 hr at 37^{o}C and after incubation plates were stored at 4^{o}C to allow

blue color to develop before colonies were counted and scored as blue (with plasmid) or white (without plasmid). Assays were done independently at least three times and values are presented as means ± SE.

4.3.7 Flow cytometry analysis (DNA content)

Wild type *E. coli* strain JCM1649 and selected DNA-Keio mutants (Table 4-1) were each grown at 32^{o}C, 150 rpm, to mid-log phase and diluted to a cell density of 10^7 cells/ml. The cultures were combined with sub-inhibitory nisin-CA concentrations, HCl-CA (carrier solvent control), novobiocin (positive control), or no-drug (negative control). Nisin concentrations were selected according to the corresponding MIC_{90} for each strain (Table 4-3): *ΔdnaQ* and *K-12* were exposed to 0.25 and 0.50 mg/ml of nisin; *ΔdnaG* and *ΔtatD* were exposed to 0.75 and 1.0 mg/ml of nisin. All the nisin treatments were combined with citric acid and adjusted to 20 mM (pH 5.0±0.02). DNA mutants and wild type were subjected to 0.2 mM novobiocin (positive control), to the equivalent volume of carrier and chelator (HCl and 20 mM Citric acid) and to the no-nisin control.

After 30 and 120 minutes of incubation at 35^{o}C, 1 ml aliquots were withdrawn (in duplicate) from each culture-treatment, centrifuged to pellet the cells and washed with ice-cold PBS (pH 7.4). Cells were fixed by resuspension in 1 ml of 70% ice-cold ethanol and stored overnight at 4^{o}C. After overnight fixation, cells were centrifuged and ethanol was discarded. Cells were again washed with ice-cold PBS, pelleted by centrifugation prior to discarding supernatant, and stained by addition of 200 µl of fresh propidium iodide (PI)

solution (0.1 % v/v Triton X-100 in PBS, containing 0.2 mg/ml of RNAse and 20 µg/ml of PI). PI is a cell membrane-impermeable, fluorescent dye that intercalates into DNA and fluoresces in proportion to PI-DNA complex formation. Prior to staining, cells were permeabilized by adding ethanol to allow PI penetration into the cell (Riccardi and Nicoletti, 2006). Then cells were dispersed in the stain solution by pipetting and vortexing and incubated at 37^{o}C for 15 min in the dark. Stained cells (200 µl) of each treatment were transferred into wells of a 96-well plate, flat bottom (black/clear Optilux™ flat bottom; BD Bioscience, San Jose, CA, USA) to subsequently be analyzed by the flow cytometer.

The flow cytometry assay was performed using a BD Accuri C6 (BD Biosciences, East Rutherford, NJ, USA), instrument provided with a red laser with a µ (excitation) = 488 nm, emission detector of 585±40 nm (FL2), and forward (0^{o}±13^{o}) and side scatter (90^{o}±13^{o}) detectors. Samples stained with PI were injected at medium speed (36 µl/min), and 10000 events were measured per sample. Forward scatter (FSC) and side scatter (SSC) were simultaneously measured. Bacterial populations were gated in FSC-SSC-Dot Plots and stained cell counts (DNA content) were observed in a single-parameter histogram (PI relative fluorescence VS cell count).

4.4 RESULTS AND DISCUSSION

4.4.1 Sensitivity tests

4.4.1.1 Nisin and nisin-citric acid sensitivity

Nisin minimum inhibitory concentrations for *E. coli* WT (*K-12*) were determined by performing microdilution assays as described in section 4.3.3 and as illustrated in Figure 4-1. As expected, *E. coli* was relatively resistant to high concentrations of nisin; addition of 2.5 mg/ml nisin caused only 50% growth inhibition (data not shown). Based on a previous report by Boziaris et al. (1999), inhibition of Gram-negative bacteria with nisin can be improved using metal chelators, such as EDTA and citric acid, among others, presumably due to disruption of the outer membrane (OM). We investigated inhibition of *E. coli* growth using combinations of four different concentrations of nisin (1.0, 0.5, 0.25 and 0.125 mg/ml) with three different concentrations of citric acid (5, 10, and 20 mM, adjusted pH to 5.5).

The results from this assay indicate that citric acid destabilizes the *E. coli* outer membrane and enhances the antimicrobial effects of nisin (Figure 4-2). Relatively little inhibitory activity was observed on *E. coli* with exposure to nisin at or below 0.5 mg/ml, with or without citric acid (data not shown). However, compared to controls with no inhibitor, 1 mg/ml of nisin combined with 5 mM CA results in ≈2-fold reduction of *E. coli* growth and 1 mg/ml of nisin with 10 mM CA yields more than a 10-fold growth reduction. Similar to our results, Stevens and collaborators (1991) demonstrated that nisin (50 µg/ml) in combination with 20 mM EDTA inhibited growth of *Salmonella* species. Fang

and co-workers (2002) observed a reduction of the microbial count of *E. coli O157:H7* in ground beef treated with calcium alginate immobilized nisin in combination with EDTA.

Lipopolysaccharides (LPS) in the OM are negatively charged, divalent cations such as Mg^{+2} or Ca^{+2} are necessary to neutralize this charge and allow polysaccharide units to cross-link and maintain an effective barrier. LPS integrity becomes compromised when these cations are chelated (Adams et al., 2014). The use of citric acid as a chelator to destabilize the *E. coli* OM and enhance nisin effect on this Gram-negative bacterium enabled us to use a high-throughput screen with the Keio deletion set and this chemical system (nisin-CA) and investigate potential (or alternative) mode of action of nisin in *E. coli* as a Gram-negative bacterium model.

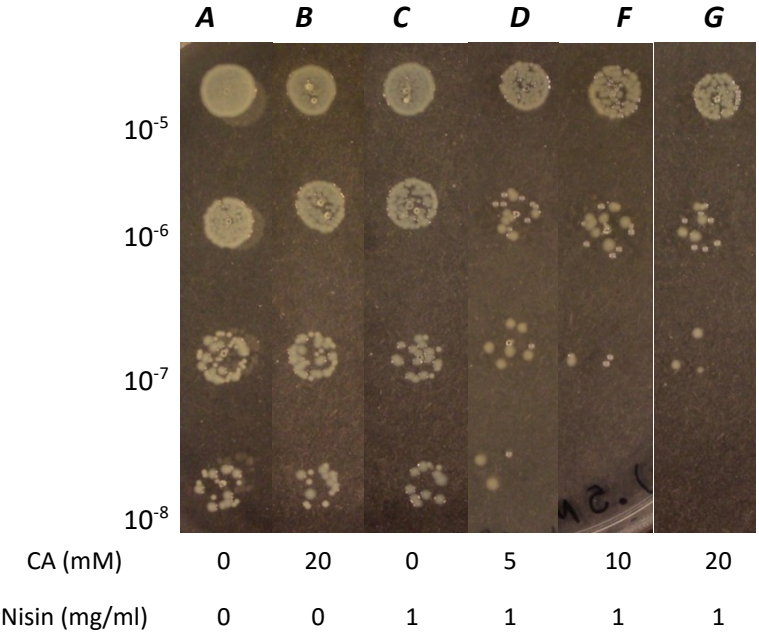

Figure 4-1. Drop-out assay analysis for *E. coli* sensitivity to nisin and citric acid. The different treatments are specified at the bottom of the figure; CA is citric acid adjusted pH to 5.5. At left, serial cell dilutions used for the analysis are indicated. Lane B shows that CA alone does not inhibit *E. coli* growth. Lane C shows that nisin, in the absence of CA, has no appreciable antimicrobial effect on *E. coli*. Lanes D, E and F show inhibitory effect of nisin in the presence of CA in increasing concentrations. Drop-out tests were performed in triplicate.

4.4.2 Identification of highly sensitive mutants to nisin-CA through a high-throughput phenotypic screening using the Keio deletion set.

The inhibitory effect of nisin-CA on *E. coli* was investigated through high-throughput phenotypic screening using the Keio set of *E. coli* mutants with non-essential gene deletions. The set of 3900 deletion mutants was grown on control (CA) and experimental media [sub-inhibitory concentration of nisin (1.56 mg/ml) in combination with CA (20mM citric acid with pH adjusted to 5.0±0.05)]. Mutants showing a colony size reduction of 60% or more on the experimental plate in comparison to the citric acid control plate were selected as candidates to infere the mode of nisin in a Gram-negative bacterium (Figure 4-2, supplementary Table S4).

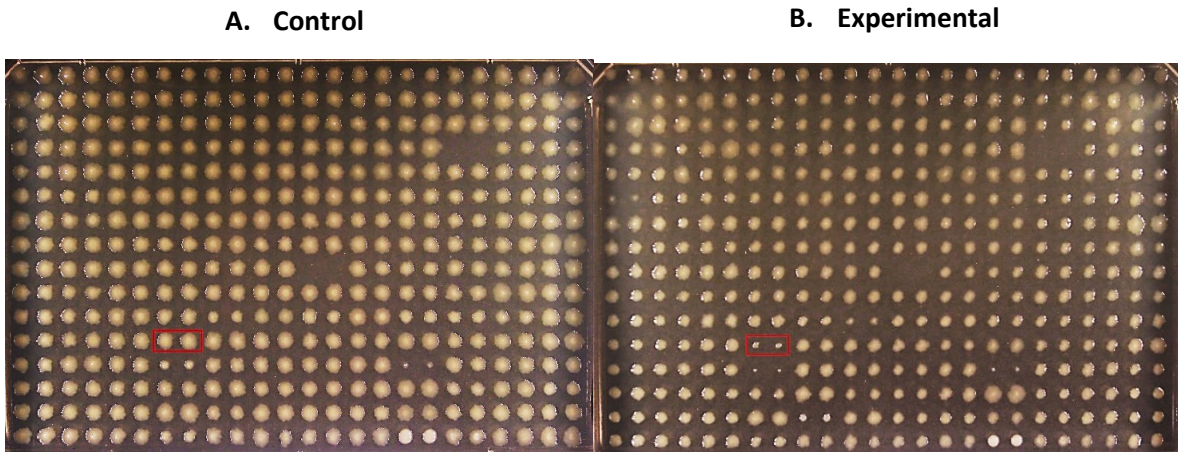

Figure 4-2. Example of a mutant strain that is significantly inhibited (boxes) when exposed to 1.56 mg/ml of nisin and 20 mM of citric acid (right) compared to control (left) with no nisin. Note: mutant colonies are printed in duplicate at adjacent positions (e.g. within red box).

The phenotypic screening was replicated four times and deletion strains showing high sensitivity (60-100% colony size reduction compared to CA control) in at least two trials were selected as potential candidates. The percent inhibition of the selected mutant candidates were averaged and results are presented in Table S4. Under our experimental conditions, 1.7% of the Keio set was found to be highly sensitive to nisin-CA.

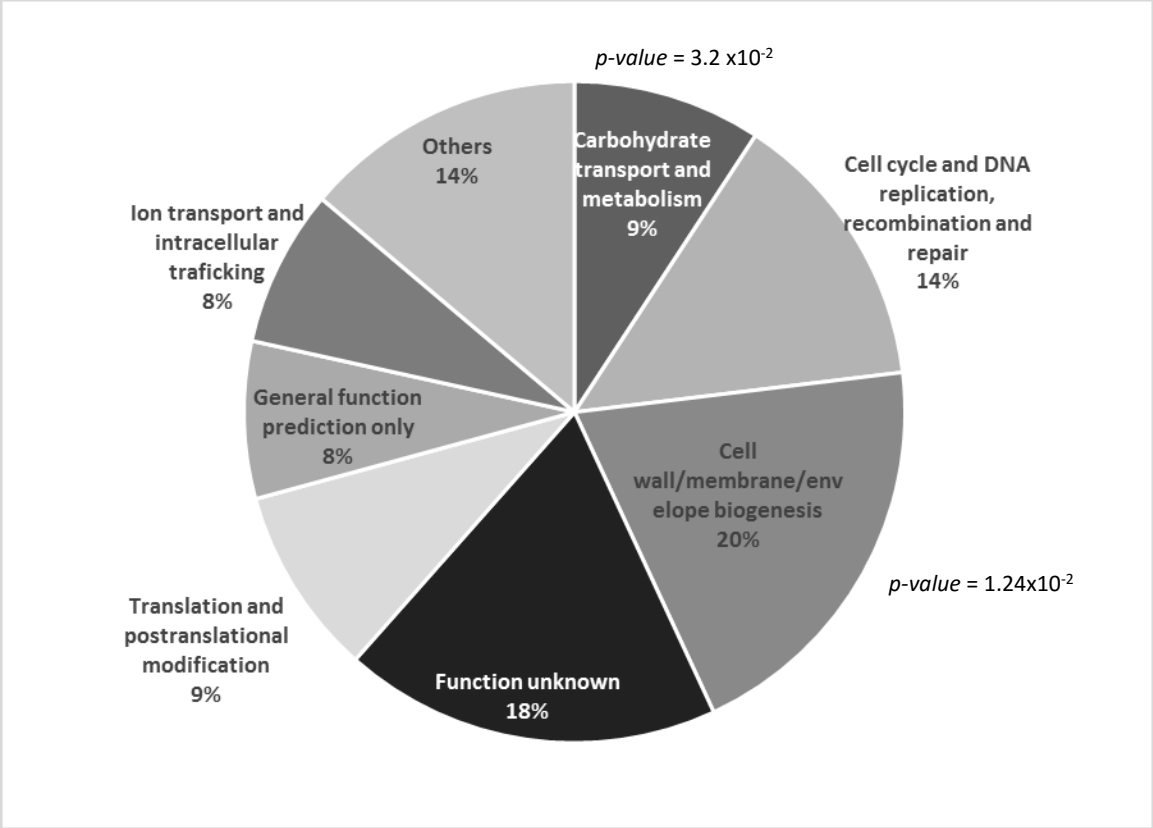

Figure 4-3. Functional distribution according to COG for genes deleted in the most sensitive mutant strains. Major known function COG groups include cell wall/membrane/envelope biogenesis (20% of sensitive mutants) and cell cycle/DNA replication, recombination and repair (14%).

Genes deleted in the sensitive mutants were classified according to cellular process (COG). In this way, 6 functional categories were identified as the most outstanding (Figure 4-3). The major functional category encompassed mutants lacking non-essential genes involved in cell wall/membrane/envelope biogenesis, representing 20% of the most sensitive mutants (*p-value* = 1.24×10^{-2}). The second largest category comprises mutants with deleted genes that are of unknown function. Our strain sensitivity analysis may provide some insights into the function of these uncharacterized genes since they may belong to other COG groups identified here. The third largest functional category (14 % of sensitive mutants) encompassed mutants lacking genes related to cell cycle and DNA replication, recombination and repair. Additional categories include translation and post-translational modification (9%), carbohydrate transport and metabolism (9%) and ion transport and intracellular trafficking (8%).

The effect of nisin on cell wall/membrane/envelope biogenesis (major group) and on DNA replication, recombination and repair (third major group) were further investigated by carrying out secondary assays.

4.4.3 Nisin effect on membrane disruption (liposomes assay)

The major functional category revealed by our high-throughput screen incorporated genes involved in cell wall/membrane/envelope biogenesis such as *rffH* (antigen O biosynthesis), *rffA* (antigen ECA biosynthesis), *rfaP* and *rffE* (lipopolysaccharide biosynthesis). These genes encode proteins that contribute to the maintenance and stabilization of the OM. Other mutants in this group lack genes involved in cell wall

organization and OM stabilization such as *amiA* and *amiC*. The fact that mutants with deletions of genes involved in cell wall synthesis and outer membrane functions are more susceptible to nisin-CA supports the prevailing dual mode of action for nisin on Gram-positive bacteria; pore formation in cell membranes and inhibition of cell wall synthesis (Cotter et al., 2005). In addition, two other groups, carbohydrate transport and ion transport, support the same mode of action of nisin proposed for Gram-positive bacteria since disturbing the cell membrane structure and function will likely impact carbohydrate and ion transport processes.

To further test this mode of action by nisin, a cell membrane disruption assay (liposome assay) was carried out. DOPC liposomes encapsulating CF dye were exposed to different concentrations of nisin (0.15-0.6 mg/ml). Fluorescence at $\lambda_{528\ nm}$ (emission) was recorded and percent leakage (%L) was calculated. This assay confirmed that nisin disrupts DOPC membranes. The lowest concentration of nisin tested (0.15 mg/ml) resulted in 40% leakage of CF from liposomes and the highest concentration of nisin tested (0.6 mg/ml) resulted in 87% leakage, in comparison to the carrier control trials where there was negligible disruption of liposomes (Figure 4-4). Liposomes act as artificial membranes and the leakage of the liposome is detected by an increase in the fluorescence intensity (CF released).

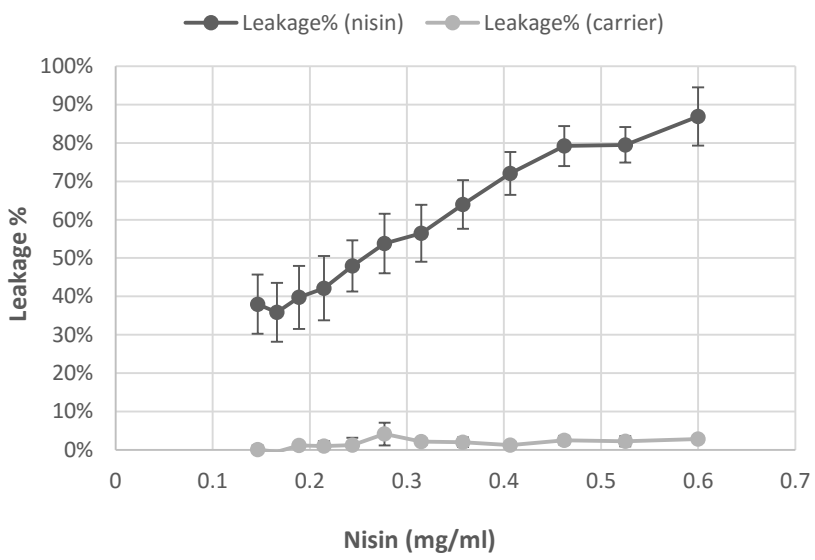

Figure 4-4. DOPC liposomes encapsulating CF (carboxyfluorescein) were exposed to different concentrations of nisin (0.15 to 0.6 mg/ml) prepared in 0.02 N HCl or to a carrier control (0.02 N HCl). After 30 min, fluorescent signal was recorded and leakage % was calculated. The trials were done in triplicate and results are presented as mean and standard error (±SE).

It is claimed that nisin binds the lipid II molecule as a first step in its mode of action. However, the results of our liposome assay indicate that the peptidoglycan precursor may not be essential to disturb the cell membrane since the liposomes do not contain lipid II. This observation is supported by a study carried out to investigate factors involved in resistance to nisin, where spheroplasts of nisin-resistant and wild type strains of *Micrococcus flavus* (Gram-positive) were equally sensitive to nisin in the absence of the cell wall. This suggests that nisin is able to perturb the cell membrane even when lipid II is compromised or absent, and indicates a potential interaction of nisin with other lipids present in the cellular environment (Kramer et al., 2004). Nisin is a cationic peptide that may interact electrostatically with the hydrophobic and negatively charged side of the

DOPC. The observed results corroborate that nisin makes pores in the cell membrane by lipid interaction disrupting the cell membrane and causing cell content leakage.

4.4.4 Plasmid replication assay

The third largest mutant group of the Keio set that was highly sensitive to nisin-CA encompassed mutants lacking genes involved in DNA replication, recombination and repair, representing 14% of the most inhibited mutants. Mutants lacking genes such as *dnaQ* (DNA polymerase III epsilon subunit), *dnaG* (DNA primase), *parC* (DNA topoisomerase IV, subunit A) and *tatD* (quality control of Tat-exported FeS proteins and Mg-dependent cytoplasmic DNase) were highly sensitive to nisin-CA. Nisin effects on DNA replication, recombination or repair has not been reported to date. To investigate this possible interaction, a plasmid replication assay was performed to test the potential effect of nisin-CA on DNA replication. Plasmid-containing *E. coli* cells were exposed to different concentrations of nisin and compared to a positive control (novobiocin, inhibitor of DNA synthesis). White and blue colonies were enumerated for each treatment to examine for interuptions in plasmid replication, where white colonies were assumed to have lost the plasmid. Blue colonies maintain the plasmid through DNA replication, and thus express the β-galactosidase enzyme that cleaves X-gal to yield the blue-coloured 5-bromo-4-chloro-3-hydroxyindole. We tested the effect of nisin on plasmid replication in WT and selected mutants that were super-sensitive to nisin-CA and had deletions of genes associated with DNA replication (*ΔdnaQ, ΔdnaG, ΔtatD,* and *ΔparC*) and *ΔmalS* as a nisin-

sensitive control (*malS* gene encodes an alpha-amylase, not related to DNA replication). The average percentage of white colonies in each group as well as standard error of the mean was calculated from at least three replicates in three separate experimental trials (Figure 4-5).

Table 4-3. Minimum Inhibitory Concentrations (MIC_{90}) of Nisin, Nisin-Citric acid (CA) and novobiocin, for *E. coli* WT and selected K-12 Keio deletion strains.

Strain	Nisin-CA[1] MIC_{90} (mg/ml)	Novobiocin MIC_{90} (mM)
K-12 (pFZY1)	0.50 < MIC ≤ 1.0	0.24 < MIC ≤ 0.32
K-12-ΔdnaQ (pFZY1)	0.70 < MIC ≤ 1.0	0.1 < MIC ≤ 0.2
K-12-ΔdnaG (pFZY1)	0.70 < MIC ≤ 1.0	0.05 < MIC ≤ 0.1
K-12-ΔtatD (pFZY1)	0.70 < MIC ≤ 1.0	0.05 < MIC ≤ 0.1
K-12-ΔparC (pFZY1)	0.15 < MIC ≤ 0.25	0.05 < MIC ≤ 0.1
K-12-ΔmalS (pFZY1)	0.94 < MIC ≤ 1.88	0.1 < MIC ≤ 0.2

[1] 20 mM citric acid (pH 5.0±0.2)

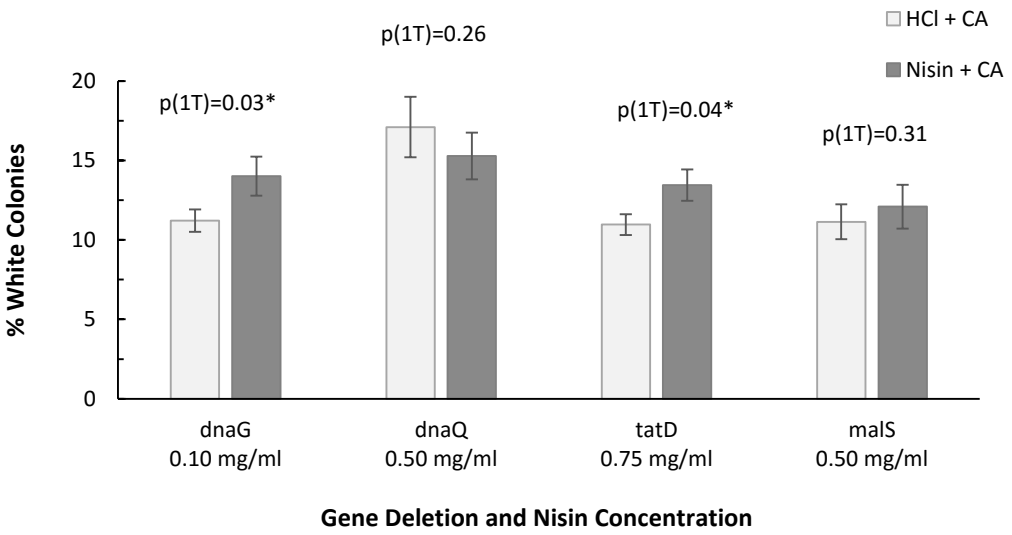

Figure 4-5. A pFZY1 replication assay was used to study the effect of nisin on plasmid DNA replication. *ΔmalS* was used as a control strain since the activity of *malS* is not related to DNA replication, recombination or repair. Dark grey columns represent the percent white colonies in strains that were exposed to nisin-CA. The sub-inhibitory concentrations used in the assay were based on the previously determined MIC_{90}, where the mutant strains showed different sensitivities (Table 3-3). Light grey columns represent percent of white colonies in strains that

were exposed to the HCl – CA carrier control (0.02 N HCl and 20 mM CA, pH 5.0 ± 0.02). Data is based on three replicate experiments and values presented are means ± SE. P-values are based on 1-tailed student's t-tests of arcsin square root transformed percentages to test for significantly more white colonies resulting from nisin exposure.

Based on a one-tailed student's t-test of arcsin square root transformed percentages, a significantly greater proportion of white colonies was observed when *ΔdnaG* (*p-value* = 0.03) and *ΔtatD* (*p-value* = 0.02) mutants were exposed to nisin-CA than when no nisin was present in the medium. This suggests a possible chemical-genetic interaction between the deleted genes and nisin (Parsons et al., 2004; Alamgir et al., 2008). In this way, it is thought that nisin interferes with parallel, and partially redundant, pathways to the one(s) involving *dnaG* and *tatD*. The *dnaG* gene encodes DNA primase that is involved in the synthesis of RNA primers that facilitate the initiation of DNA replication (Mitkova et al., 2003). The TatD protein functions as a 3'- 5' magnesium-dependent exonuclease of ssDNA and RNA that might be involved in repair of DNA damage induced by peroxide (Chen et al., 2014). Taken together, the synergy between nisin and the mutations *ΔdnaG* and *ΔtatD* indicates that nisin interferes with DNA synthesis and/or DNA repair.

Nisin exposure resulted in a non-significant difference in the abundance of white colonies in *ΔdnaQ* and *ΔmalS*. The *malS* gene encodes an alpha-amylase, which is not related to DNA replication, recombination or repair and is used as a negative control). The *dnaQ* gene encodes DNA polymerase III Ɛ subunit (required for speed and processivity of DNA replication), a subunit of DNA polymerase III (Pol III). Pol III is one of the five polymerases described in *E. coli* and is responsible for the majority of genomic DNA

replication. It should be noted that it is Pol I that plays a key role in plasmid replication (along with lagging-strand replication and DNA repair of chromosomal DNA; Sutton and Walker, 2001; Camps et al., 2003; Fijalkowska et al., 2012). The fact that polymerases besides the Pol III are involved in the DNA replication and that the plasmid replication is an independent and distinct process from the genomic DNA replication (Lilly and Camps, 2015), may explain why significant results were not seen with this particular mutant strain (*ΔdnaQ*), despite its apparent sensitivity in the chemical-genetic screening.

Overall, the data indicate an interesting chemical-genetic interaction between nisin and genes or gene-products of *dnaG* and *ΔtatD* that results in compromised plasmid DNA replication. To further investigate the involvement of nisin in DNA replication, we analyzed genomic DNA content using flow cytometry.

4.4.5 Flow cytometry (DNA content analysis)

The effect of sub-inhibitory concentrations of nisin-CA on genomic DNA replication was investigated by analyzing the DNA content in selected *E. coli* deletion and WT strains by flow cytometry. Intracellular DNA can be quantified in terms of fluorescence intensity when it is labeled with a fluorochrome such as propidium iodide (PI). PI molecules stoichiometrically intercalate into DNA and, when excited (535 nm), yield a fluorescent signal at 617 nm which is utilized to estimate DNA content (Suzuki et al., 1997). In brief, deletion mutants (*ΔdnaQ*, *ΔdnaG* and *ΔtatD*) and wild type cells were exposed (experimental) or not exposed (control) to sub-inhibitory concentrations of nisin

(section 4.3.7), or novobiocin (positive control). Then cells were fixed and permeablized with ethanol and stained with PI. Stained cells were analyzed with a flow cytometer and the results are presented in histograms (left) and dot plots (right, Figures 4-6 to 4-9) and a statistical summary is presented in Table 4-4.

The histograms show DNA content measures in strains *ΔdnaG* (Figure 4-6), *ΔdnaQ* (Figure 4-7), *ΔtatD* (Figure 4-8) and JCM1649 (WT) (Figure 4-9), following exposure to each of HCl-CA, nisin, novobiocin and negative control. In each case the Y-axis shows the count or number of analyzed events (0-500) and the X-axis shows the pulse-area (FL2-A) generated by the fluorescent light emitted (10^0-10^6). When the peak is found between 10^3 and 10^4 (X-axis), it is considered to be fluorescent light emitted by the DNA-PI complex (previously determined). The regions below 10^3 are considered as non-fluorescent.

The dot plots found on the right side of each panel show the emitted fluorescence (FL2-A) on the Y-axis and the scattered light (SSC-A) on the X-axis, which provides information on cell size. The dot plots represent the bacterial population containing PI-DNA. The dot density correlates to the number of events (peak height) observed in the fluorescent region (10^3-10^4) on the FL2-A axis in the h

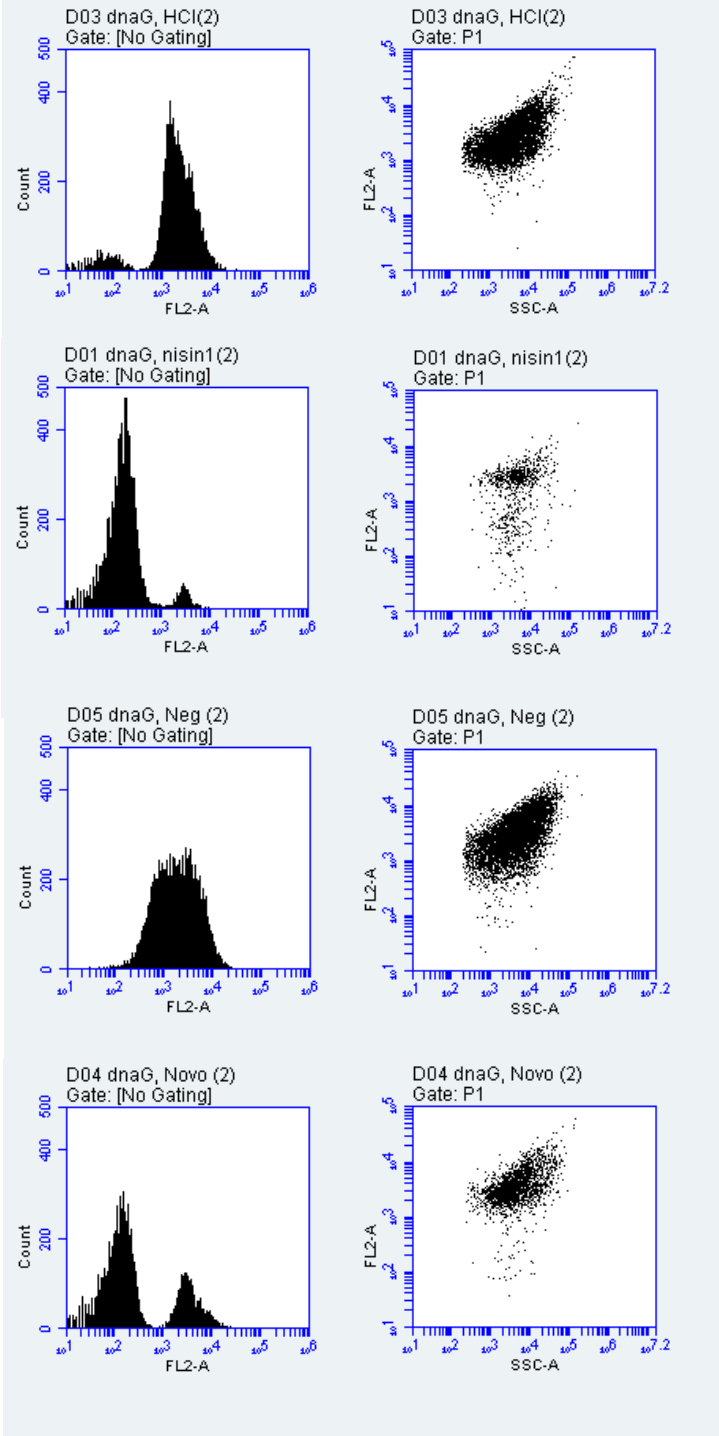

Figure 4-6 DNA content analysis in the deletion mutant *ΔdnaG.* Mutant cells were exposed for 120 min to nisin or to the corresponding controls. A) Carrier-CA control, B) 0.75 mg/ml nisin, C) non-treatment/novobiocin negative control, and D) positive control, novobiocin. At left, histograms (Count VS FL2-A) show the proportion of the bacterial cells emitting fluorescence (PI-DNA) and proportion of the cells not emitting fluorescence. At right, the bacterial subpopulation (gated) that shows fluorescent signal (on FL2-A, 10^2-10^3).

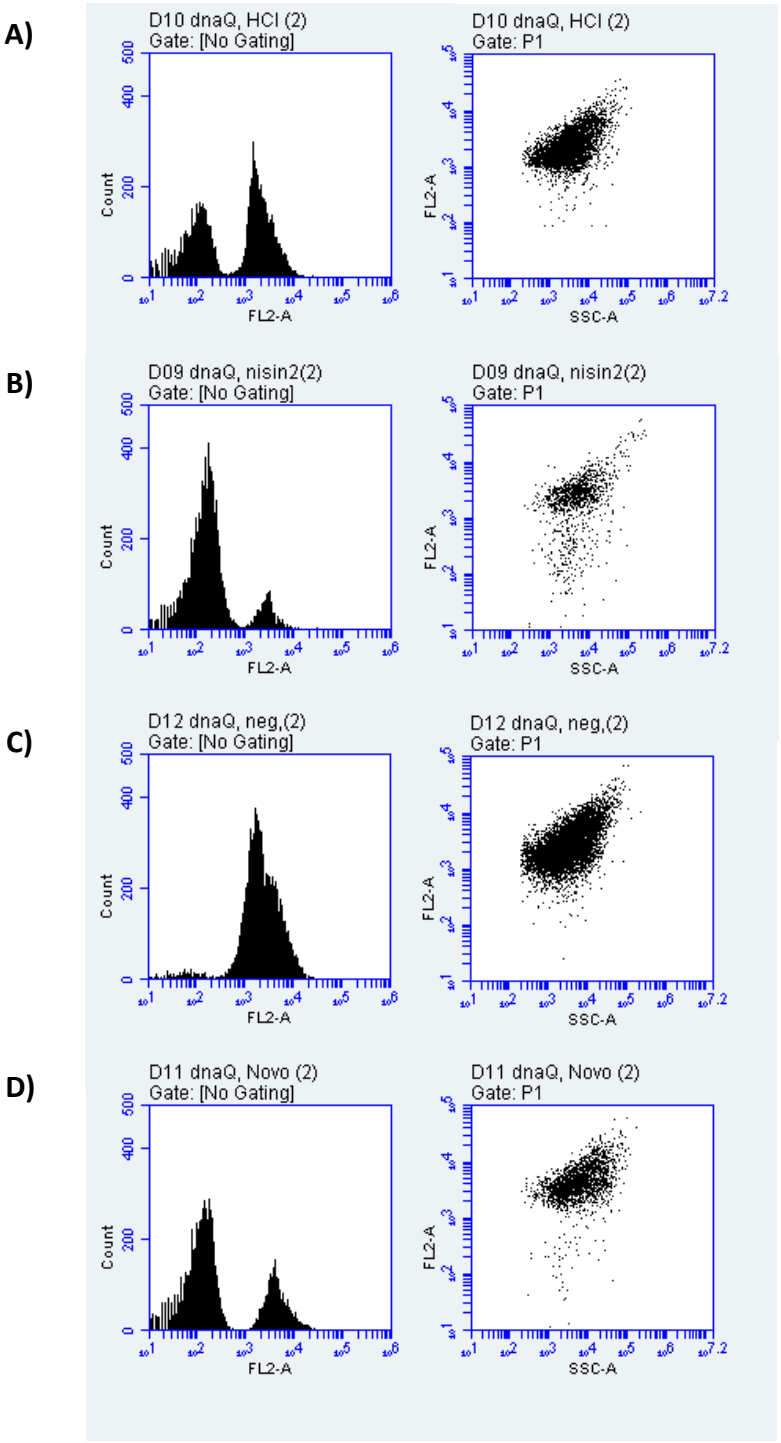

Figure 4-7 DNA content analysis in the deletion mutant *ΔdnaQ*. Mutant cells were exposed for 120 min to nisin or to the corresponding controls. A) Carrier-CA control), B) 0.5 mg/ml nisin, C) non-treatment/novobiocin negative control, and D) positive control, novobiocin. At left, histograms (Count VS FL2-A) show the proportion of the bacterial cells emitting fluorescence (PI-DNA) and proportion of the cells not emitting fluorescence. At right, the bacterial subpopulation (gated) that shows fluorescent signal (on FL2-A, 10-10^3).

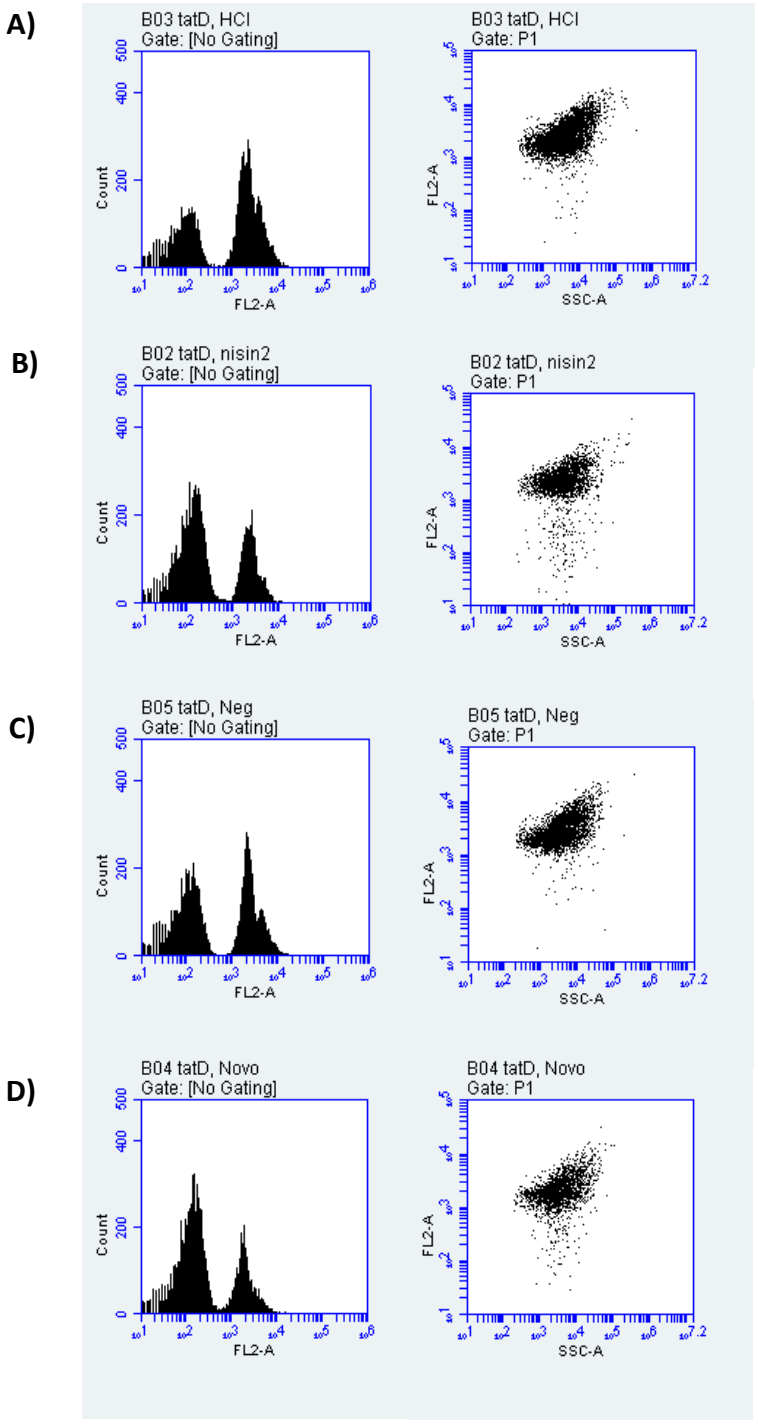

Figure 4-8. DNA content analysis in the deletion mutant *ΔtatD.* Mutant cells were exposed for 30 min to nisin or to corresponding controls. A) Carrier-CA control), B) 1.0 mg/ml nisin, C) non-treatment/novobiocin negative control, and D) positive control, novobiocin. At left, histograms (Count VS FL2-A) show the proportion of the bacterial cells emitting fluorescence (PI-DNA) and proportion of the cells not emitting fluorescence. At right, the bacterial subpopulation (gated) that shows fluorescent signal (on FL2-A, 10^2-10^3).

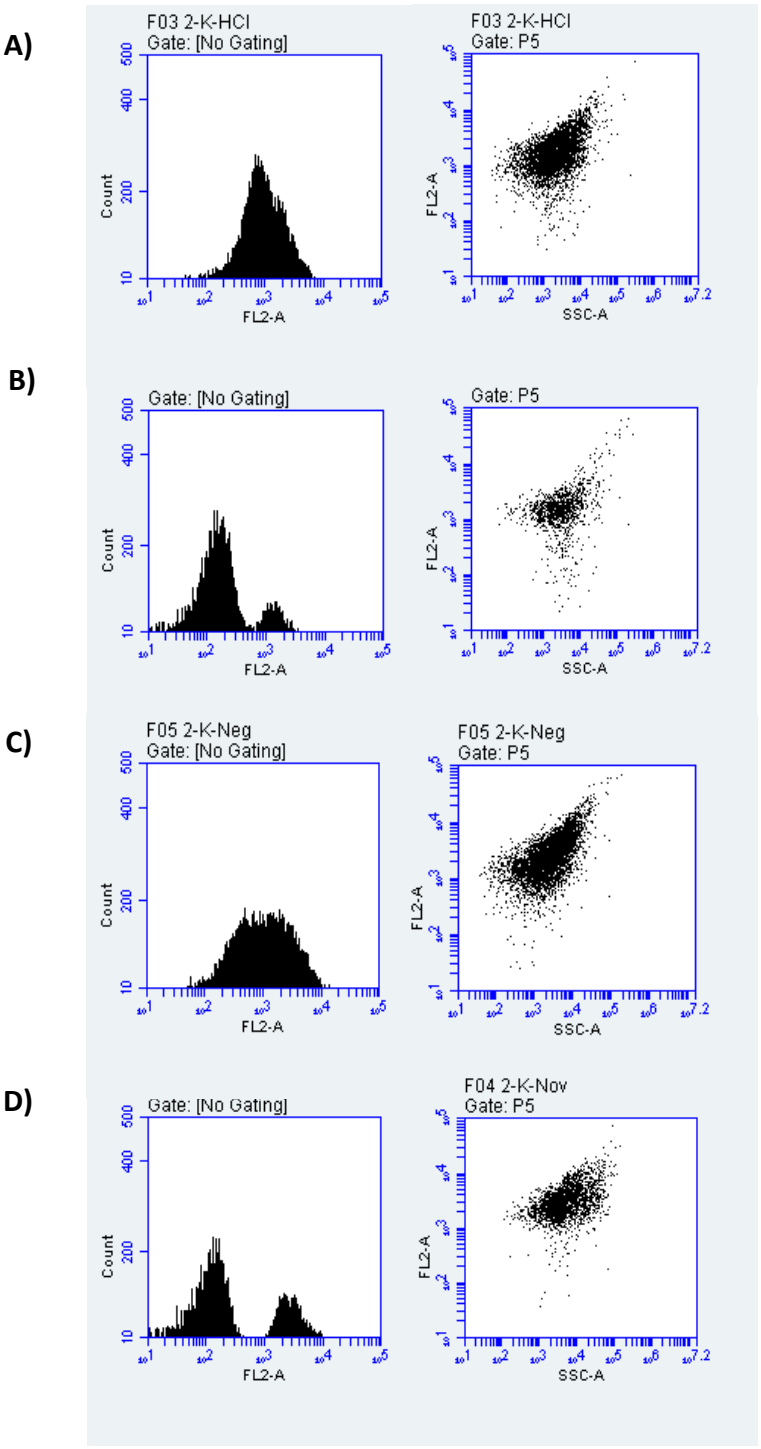

Figure 4-9 DNA content analysis in the WT *K-12. E. coli* cells were exposed for 120 min to nisin or to corresponding controls. A) Carrier-CA control), B) 0.5 mg/ml nisin, C) non-treatment/novobiocin negative control, and D) positive control, novobiocin At left, histograms (Count VS FL2-A) show the proportion of the bacterial cells emitting fluorescence (PI-DNA) and proportion of the cells not emitting fluorescence. At right, the bacterial subpopulation (gated) that shows fluorescent signal (on FL2-A, 10^2-10^3)

Table 4-4. Summary of the flow cytometry assay to determine the effect of nisin-CA on cellular DNA content in *E. coli* deletion mutants and WT strains.

***E. coli* cells**	**Count**	**Events / µl**	**% of This Plot**	**% of All**	**Mean SSC-A**	**Mean FL2-A**
Figure 4-6						
ΔdnaG (120 min incubation)						
7.A HCl-CA carrier control	6,593	3297	100.00%	65.93%	5,691.60	3,033.94
7.B 0.75 mg/ml nisin	918	459	100.00%	9.18%	7,027.38	2,084.39
7.C Non-treatment	6,638	3319	100.00%	66.38%	7,421.10	3,818.40
7.D 0.2 mM Novobiocin	2,242	1121	100.00%	22.42%	8,051.62	4,174.40
Figure 4-7						
ΔdnaQ (120 min incubation)						
8.A HCl-CA carrier control	4,054	2027	100.00%	40.54%	5,266.50	2,712.11
8.B 0.5 mg/ml nisin	1,436	718	100.00%	14.36%	9,465.79	2,649.08
8.C Non-treatment	6,824	3412	100.00%	68.24%	5,729.51	3,575.92
8.D 0.2 mM Novobiocin	2,304	1152	100.00%	23.04%	9,729.60	4,971.46
Figure 4-8						
ΔtatD (30 min incubation)						
9.A HCl-CA carrier control	4,456	2228	100.00%	44.56%	6,701.89	2,947.86
9.B 1.0 mg/ml nisin	2,731	1366	100.00%	27.31%	6,617.32	2,411.04
9.C Non-treatment	3,354	1677	100.00%	33.54%	5,951.40	3,146.31
9.D 0.2 mM Novobiocin	2,328	1164	100.00%	23.28%	5,648.40	2,268.03
Figure 4-9						
K-12 (120 min incubation)						
10.A HCl-CA carrier control	4,621	2311	100.00%	46.21%	3,674.21	2,146.98
10.B 0.5 mg/ml nisin	1,319	660	100.00%	13.19%	6,782.98	2,043.65
10.C Non-treatment	4,890	2445	100.00%	48.90%	4,095.62	3,270.93
10.D 0.2 mM Novobiocin	2,481	1241	100.00%	24.81%	9,122.56	3,485.13

It can be observed in the histograms (left side of figures 4-6 to 4-9) that when *E. coli* strains (*ΔdnaG, ΔdnaQ, ΔtatD* and K-12) were exposed to nisin the DNA content (PI-DNA complex) represented by the peak in the fluorescent region (10^3-10^4) is lower than

the peak of the corresponding carrier control (HCl-CA). A similar effect is observed when *E. coli* strains were exposed to novobiocin (positive control for inhibition of DNA synthesis) when compared with the corresponding novobiocin negative control.

The dot plots (right side of the figures 4-6 to 4-9) depict the proportion of the population that have PI-stained DNA, which is related to the peak height of the histograms previously mentioned. It is evident that, for all strains, when cells were subjected to nisin-CA or novobiocin the percent of stained cells is lower than the percent of cells exposed to the nisin carrier-control or the novobiocin carrier control, respectively (see "% of All" in Table 4-4). For example, for *ΔdnaG* trials, 9.18% of the cells treated with nisin exhibit DNA-PI fluorescence compared to 65.93% of cells that exhibit DNA-PI fluorescence after exposure to the nisin carrier control (HCl-CA). Interestingly, the decrease in DNA-PI signal associated with both nisin-CA and novobiocin treatments is less dramatic in the *ΔtatD* strain than in the other 3 strains examined. The *tatD* gene is implicated more in DNA repair than in DNA replication (Chen et al., 2014). These results lead us to infer that nisin might interfere with the DNA replication (initiation) more than with DNA recombination and repair.

Overall, the flow cytometry experiments indicate that nisin-CA acts in a similar way as novobiocin in reducing the DNA content of *E. coli* cells. Novobiocin is a coumarin produced by *Streptomyces* species, which is known to inhibit DNA gyrase. DNA gyrase requires energy in ATP form to introduce negative supercoils and relieve the torsional strain occurring during DNA replication (Hardy and Cozzarelli, 2003; Fàbrega et al., 2008;

Collin et al., 2011). DNA gyrase is composed by two subunits, gyrase A (GyrA) which contains an active site for DNA cleavage and the subunit B (GyrB) which contains an ATPase active site. Topoisomerase IV disentangles daughter chromosomes after replication, and also contains two subunits, ParC and ParE with similar functions to GyrA and GyrB, respectively (Hardy and Cozzarelli, 2003). Novobiocin obstructs DNA gyrase by competitively inhibiting the nucleotide binding site (GyrB) and ciprofloxacin (quinolone) targets the subunit A of gyrase (GyrA) impeding the DNA cleavage in the DNA replication process (Collin et al., 2011). These connections led us to investigate the sensitivity of ciprofloxacin-resistant mutants to nisin to obtain additional insight into its mode of action.

4.4.6 Sensitivity to nisin of ciprofloxacin-resistant mutants

Inhibition of ciprofloxacin-resistant mutants by nisin-CA was tested and results are presented in Table 4-5. Interestingly, all but one of the ciprofloxacin-resistant mutants tested were more sensitive to nisin-CA than the wild-type. The exception was the *CipR5* (D87G) mutant of *gyrA* which had a MIC_{90} similar to that of the wild-type strain, in the range of 1.00 - 0.50 mg/ml. Interestingly, *CipR1* (S83A) and *CipR3* (D87Y) *gyrA* mutants had MICs in the range of 0.50 - 0.25 mg/ml. This difference may reflect the different amino acid substitutions in these *gyrA* mutants and should be studied further to provide additional insights into nisin's mechanism of action. The mutations on the GyrA subunit carried by the ciprofloxacin-resistant mutants *CipR1, CipR3* and *CipR5*, render resistance

to ciprofloxacin by decreasing its affinity for the antibiotic. Nevertheless, it seems that these mutations do not provide resistance to nisin. These findings lead us to conclude that, unlike ciprofloxacin, nisin does not disturb DNA replication by interacting with the GyrA subunit or, that these mutations do not prevent the interaction of nisin with GyrA.

Remarkably, all the *marR* mutants showed the highest degree of sensitivity to nisin, (MIC_{90} range = 0.25 - 0.13 mg/ml). MarR, encoded by the gene *marR*, is a negative regulator of the marRAB operon, a multiple antibiotic resistance operon in *E. coli* and other bacteria. MarA is a transcriptional activator that controls expression of many genes in *E. coli*. Mutations that inactivate or suppress MarR function result in resistance to a variety of antibiotics by increasing chemical efflux and decreasing influx (Alekshun et al., 2000; Jacoby, 2005). The ciprofloxacin-resistant mutants *CipR6* (R94C) and *CipR8* (R77H) carry mutations in *marR* that suppress its activity, permitting MarA to activate *acrAB* and *tolC*, (genes encoding proteins involved in efflux pump system), and a gene that decreases translation of *ompF* (encoding an outer membrane porin, transmembrane transport) to decrease influx and increase efflux of quinolones (Jacoby, 2005; Du et al., 2015). Our results showed that these mutations in the ciprofloxacin-resistant strains did not provide resistance to nisin and, in fact, *marR* mutant strains are more sensitive to nisin than the *E. coli* WT or *gyrA* mutant strains. This indicates that nisin does not require the influx system and may penetrate bacterial cells by way of the pores it creates in the cell membrane. On the other hand, it is known that bacterial effux systems may be selective, and structural characteristics of the molecule to be expelled determine their affinity for

the transporters and efflux pumps (Chollet et al., 2004). We assume that the increased activity of the efflux pump system induced by the mutations on *marR* did not render resistance in the mutants to nisin because the AcrAB-TolC efflux machinery does not have an affinity for nisin. In addition, mutations in *marR* provoke a decrease in *ompF* translation, which encodes a porin that allows the intake of antibiotics but also some nutrients. We hypothesize that a potential cause of the hypersensitivity to nisin is that bacterial cells received less nutrients due to the presence of less OmpF porins making the cells more sensitive to external perturbations. However, these potential interactions should be further explored.

Table 4-5. Minimum inhibitory concentrations (MIC_{90}) of nisin-CA determined for ciprofloxacin-resistant mutants.

Strain	**Nisin-CA mg/ml)**
Wild-Type (*MG1655*)	0.50 < MIC ≤ 1.0
gyrA mutant (*CipR 1*)	0.25 < MIC ≤ 0.50
gyrA mutant (*CipR 3*)	0.25 < MIC ≤ 0.50
gyrA mutant (*CipR 5*)	0.50 < MIC ≤ 1.0
marR mutant (*CipR 2*)	0.13 < MIC ≤ 0.25
marR mutant (*CipR 6*)	0.13 < MIC ≤ 0.25
marR mutant (*CipR 8*)	0.13 < MIC ≤ 0.25

4.5 CONCLUDING REMARKS

Obtaining antimicrobial substances with different or alternative modes of action has been pointed out as an important pathway to overcome the phenomenon of antimicrobial resistance and developing effective antimicrobials. In this study, we investigated the mode of activity of the bacteriocin nisin against the Gram-negative bacterium *E. coli.* Our high-throughput phenotypic screening on the Keio set exposed to sub-inhibitory concentration of nisin in combination with citric acid, revealed that nisin's mode of action may be related to cell wall/membrane/envelope biogenesis which confirmed nisin's mechanism of action, perturbing cell membrane creating pores. However, the functional analysis also revealed that nisin may affect DNA replication, recombination or repair, indicating a second mode of activity such as macrolides (i.e. azithromycin) and berberine (Silver, 2007; Karaosmanoglu et al., 2014).

After analyzing the DNA content in *E. coli* deletion mutants (*ΔdnaQ, ΔdnaG* and *ΔtatD*) and wild type using a flow cytometry (FC) analysis, it was observed that nisin exposure caused a decrease in the DNA content similar in magnitude to novobiocin, an anti-gyrase and DNA replication inhibitory drug. Of interest, there is evidence that the peptide microcin B17 (MccB17, 3.1 KDa), a bacteriocin produced by enterobacteria, perturbs gyrase activity in DNA replication (Yang et al., 2014). This toxin slows down the super-coiling and relaxation of gyrase; and does not require the DNA-cleavage domain from the gyrA or the ATPase domain from the gyrB. It has also been observed that some quinolone-resistant mutants are sensitive to this peptide. Interestingly, similar to nisin (3.5 KDa), this

peptide undergoes post-translational modifications in which oxazole-thiazole fused rings are formed through cysteine residues (Collin et al., 2011). Nisin similarly undertakes post-translational modifications in which lanthionine rings are formed. That both peptides possess similar structural rings is very interesting in this context. The evidence that this MccB17 is toxic to DNA replication may support our results that indicate nisin perturbs DNA replication. Furthermore, Joo and co-workers (2012) found that nisin prevents cancer cell growth, reduces cell proliferation, arrests cell cycle and increases the DNA fragmentation in squamous cell carcinoma. Despite the fact that our study did not clarify the precise mode of action of nisin, our results and supporting evidence from the literature lead us to believe that nisin does affect DNA replication. It should be stressed that based on our DNA content analysis, it cannot be determined what specific step of the DNA replication process is affected by nisin. DNA replication is a complex process that involves many stages and proteins. Therefore, additional mechanistic studies would be required to detect the specific reaction(s) or molecular target(s) that nisin is affecting.

Remarkably, we observed that nisin-CA is an effective inhibitor of ciprofloxacin-resistant mutants. As a consequence, it is likely that nisin may have a role in treating diseases caused by pathogens commonly exhibiting resistance to quinolones such as *Pseudomonas aeruginosa*.

Chapter 5

Antimicrobial Factors Produced by *Bifidobacterium breve*, a Probiotic

5.1 ABSTRACT

The ability of *Bifidobacterium breve* to produce antimicrobial metabolites was investigated. The fermented bifidobacterial supernatant effectively inhibited some Gram-positive and Gram-negative bacteria. The effect of different carbon sources on antimicrobial production was also studied and revealed that medium supplemented with lactose as the main carbon source enhances antimicrobial activity by *B. breve*. A chemical-genetic screen using the *E. coli* Keio set of deletion mutants was used to examine the cellular processes affected by the uncharacterized antimicrobial substance(s) produced by *B. breve*. *E. coli* strains with deletions of genes involved in carbohydrate transport and metabolism, intracellular trafficking, secretion and vesicular transport, and energy production/conversion were among the most sensitive mutants. Additional mechanistic studies are required to confirm the pathways targets revealed by this chemical-genetic profile.

5.2 INTRODUCTION

Humans and other mammals host a vast and complex variety of microorganisms in the gastrointestinal tract. The composition of the collection of microorganisms comprising the gut microflora may differ in every human or animal and depends on environmental, genetic and physiological factors (Davis and Milner, 2009). Bacterial species considered as health promoting are referred to as 'probiotics' (Gibson & Roberfroid, 1995). Probiotic bacteria perform diverse roles to provide beneficial effects to the host, such as nutrient production (vitamin B complex, nicotinic and folic acids), constipation relief or modulating the microflora population by inhibiting pathogenic bacteria (Mussato and Mancilha, 2006). The most representative genera in the human gut are *Bifidobacteria* and *Lactobacilli. Bifidobacterium spp.* constitute between 3 and 7% of the microbiota in adults and up to 91% in newborns (Ballongue, 2004; Chekhoyoussef et al., 2009a), and include *Bifidobacterium breve*, *B. longum, B. dentium, B. adolescentis, B. infantis* (Pokusaeva and Fitzgerald, 2010). *Bifidobacteria* are anaerobic, Gram-positive, non-spore forming and non-catalase producing bacteria that have the ability to ferment a variety of carbohydrates (saccharolytic) such as gastric mucin, plant-derived oligosaccharides such as raffinose, and various monosaccharides. While fermentative capabilities vary between species and this may provide different attributes for adaptation to the host, all *Bifidobacteria* exhibit the "bifid shunt" which makes use of the enzyme fructose-6-phosphate phospho-ketolase (F6PPK) to convert monosaccharides to intermediate products of the fermentation pathway. The carbohydrates are subsequently

catabolized to produce short chain organic acids such as acetate, propionate and butyrate, intermediate products including succinate, lactate and ethanol, and gases such as hydrogen, methane, carbon dioxide and hydrogen sulphide (Ventura et al., 2007; Mussato and Manciha, 2007; Pokusaeva and Fitzgerald, 2010).

The production of organic acids such as acetate and lactate obtained through fermentation in *Bifidobacteria* species are partially responsible for the antagonist activity toward other microbes (Makras and De Vuyst, 2006). Nevertheless, some *Bifidobacteria* strains are capable of producing additional antimicrobials including peroxide and bacteriocins. Bacteriocins are low-molecular weight peptides produced by bacteria that have inhibitory effects on other bacteria (Cotter et al., 2005; Castillo Martínez et al., 2013). Bacteriocins and other secondary metabolites are not essential for growth but they may provide advantages for the producer in a competitive environment.

Secondary metabolite production may be affected by genetic, environmental and development stage factors. The production of secondary metabolites is usually induced by an environmental stress caused by changes in physical and chemical growth conditions (changes in pH, temperature, oxygen availability, depletion of nutrients, and increases in ethanol, lactic and/or acetic acid). Therefore, the production of bacteriocins or other antimicrobial compounds might be also influenced by these factors (Ruiz et al., 2010)

Bacteriocins are produced by a majority of bacterial species but only a few *Bifodobacteria* strains have been found to be bacteriocinogenic (Riley, 1998). For instance, the bacteriocins bifidin, bifidocin, bifilong, bifilact Bb-46, thermophilicin and

bifidin I have been isolated from spent supernatants fermented by strains such as *B. bifidum* NCDC 1452, *B. bifidum NCFB 1454*, *B. longum, B. longum* Bb-46, *B. thermophilum* RBL67 and *B. infantis* BCRC 14602, respectively (Anand et al., 1984, 1985; Kang et al., 1989; Yildirim et al., 1999; Saleh and El-Sayed, 2004; von Ah, 2006 and Cheikhyoussef et al., 2010). Other *Bifidobacteria* strains have shown antagonist effects against potential pathogens or food-spoilage bacteria, where the inhibitory factor has not been identified or characterized as a bacteriocin or bacteriocin-like substance (Bevilacqua et al., 2003; Touré et al., 2003).

The search for new antimicrobial substances with diverse or novel mechanisms of action has gained a lot of interest due to the phenomenon of pathogen resistance to common antibiotics. New bioactive compounds have been isolated and characterized from a wide variety of organisms. However, the elucidation of their mechanisms of action or identification of cellular targets represents a challenge. Genome-wide collections of single-mutants (*Saccharomyces cerevisiae* and *Escherichia coli* K-12) allow for the generation of drug-hypersensitivity and drug-resistance profiles that may provide key information to understand the mode of action of inhibitory compounds (Parsons, et al., 2004).

In this study, selected Bifidobacterial species were screened and antimicrobial activity was identified in *Bifidobacterium breve* supernatant. The potential cellular processes affected by the crude extract were examined through a chemical-genetic profile using the *E. coli* Keio mutant set.

5.3 MATERIALS AND METHODS

5.3.1 Chemicals

Sources of reagents were as follows. Bacteriological media such as MRS (de Man, Rogosa and Sharpe), TSB (Tryptic soy broth), and RCM (Reinforced Clostridium Medium) were purchased from Sigma (Oakville, ON, Canada). LB (Luria-Bertani), L-cysteine-HCl and beef extract were purchased from Bioshop (Burlington, ON, Canada). Lactic acid, glacial acetic acid, ampicillin, kanamycin, glucose, fructose, lactose, raffinose, maltose, EDTA (Ethylenediaminetetraacetic acid), Tris-HCl [(hydroxymethyl)-aminomethane hydrochloride)], CTAB (Cetyl trimethylammonium bromide), SDS (Sodium dodecyl sulfate), NaCl, proteinase K (≤30 units/mg of protein), ethanol (95%) and ethidium bromide were purchased from Sigma (Oakville, ON, Canada). Nisin was purchased from Santa Cruz Biotechnology (Dallas, TX, USA).

5.3.2 Bacterial strains and growth conditions

Bacterial strains used in this study are listed in Table 5-1. *Bifidobacterium* strains were grown in MRS-C (De Man Rogosa and Sharpe medium supplemented with 0.05% w/v of cysteine hydrochloride), and/or in modified RCM with 2% glucose or other carbon source, at 37 ^{o}C in anaerobic jars containing an Oxoid Anaerogen sachet (Fisher Scientific, Waltham, Massachusetts, USA). All other bacteria were grown in aerobic conditions: *Lactobacillus* strains, *Bacillus cereus* and *Pediococcus acidilactici* were grown in MRS at 37^{o}C; *E. coli* and *P. fluorescens* were grown in LB (Luria-Bertani) at 37^{o}C and 29^{o}C,

respectively. The Keio set of deletion mutants was maintained as an array of colonies on LB agar plates (2% agar containing 30 µg/ml of kanamycin) or in LB broth at 32°C without shaking. Food pathogen bacterial strains used to assess the inhibition spectrum of the bifidobacterial fermented supernatant were grown in Brain Heart Infusion (BHI) broth at 37°C for 12-16 hrs unless otherwise specified.

Table 5-1. Bacterial strains used

Type/ source	Strain name	Strain use	Strain ID[6]
Probiotics			
NRRL[1], B-41405	*Bifidobacterium animalis* subspecies *lactis*	Producer	BCL1
NRRL, B-41406	*Bifidobacterium animalis* subspecies *animalis*	Producer	JCM1190
NRRL, B-41410	*Bifidobacterium bifidum*	Producer/indicator	
NRRL, B-41408	*Bifidobacterium breve*	Producer	ATCC15700
NRRL, B-41661	*Bifidobacterium longum*	Producer	ATCC15697
NRRL, B-4495	*Lactobacillus acidophilus*	Indicator	
NRRL, B-548	*Lactobacillus delbrueckii subspecies bulgaricus*	Indicator	
NRRL, B-1932	*Lactobacillus fermentum*	Producer/indicator	
NRRL, B-41522	*Pediococcus acidilactici*	Producer/indicator	DSM20284
Commercial[2]	*Lactobacillus casei*	Indicator	ATCC334
Non-probiotics			
NRRL, B-4288	*Bacillus cereus*	Producer/indicator	ATCC14579
A. Wong[3]	*Pseudomonas aeruginosa*	Indicator	
A. Wong	*Pseudomonas fluorescens*	Indicator	
A. Wong	*Escherichia coli (*K-12 substr. W3110)	Indicator	W3110
NIG[4]	*Escherichia coli* gene knockout library	Genetic analysis	
Food pathogens			
CFIA[5]	*Salmonella enterica* ser. Typhimurium	Indicator	
CFIA	*Salmonella enterica* ser. Enteritidis	Indicator	
CFIA	*Salmonella enterica* ser. Heidelberg	Indicator	
CFIA	*Escherichia coli*	Indicator	
CFIA	*Listeria monocytogenes (005)*	Indicator	
CFIA	*Listeria monocytogenes (017)*	Indicator	
CFIA	*Enterococcus faecalis*	Indicator	
CFIA	*Klebsiella pneumoniae*	Indicator	
CFIA	*Staphylococcus aureus*	Indicator	
CFIA	*Streptococcus suis*	Indicator	

[1] NRRL = Northern Regional Research Laboratory (Agricultural Research Service, United States Department of Agriculture, Peoria, Illinois, USA)
[2] Strain isolated from probiotic supplement (Swiss, Toronto, ON, Canada)
[3] Dr. Alex Wong (Carleton University, Ottawa, ON, Canada)
[4] NIG = National Institute of Genetics, Japan
[5] Canadian Food Inspection Agency, Ottawa, ON, Canada
[6] Strain identification based on 100% identity from BLAST search of 16S sequences.

5.3.3 Confirmation of bacterial strains identity.

To confirm the identity of selected bacterial strains, PCR (polymerase chain reaction) of a 16S rDNA fragment was carried out and amplicons were sequenced and analyzed. Bacterial cells were grown in liquid media, centrifuged at 5000 *g* and supernatant was discarded. Bacterial cell pellets were resuspended in TE (10 mM Tris-HCl and 1 mM EDTA, pH 8.0±0.02) and 0.1 mm glass beads were added (10% of total volume) and cells were ruptured in a bead beater Mixer Mill MM200 (Retsch Ltd., Haan, Germany) at 30 Hz for 8 min. The cell suspensions were then mixed with 0.5% SDS and 0.3 mg/ml proteinase K for 60 min at 55^{o}C. After incubation, 5 M sodium chloride solution was added to a final concentration to 0.7 M. CTAB and NaCl solution was also added to the cell suspensions (final concentration 1.25% and 0.09 M, respectively) and the suspensions were thoroughly mixed and incubated at 65^{o}C for 10 min. Chloroform/isoamyl alcohol (24:1) was then added at a 1:1 ratio and mixed thoroughly prior to centrifugation at 9300 *g* for 5 min. The aqueous supernatant was recovered and mixed with 0.6 volumes of isopropanol, stored at -20^{o}C for 24 hrs prior to centrifugation at 9300 *g* for 5 min. The supernatant was discarded and precipitate was washed with 70% ethanol and centrifuged as before to recover the DNA precipitate, which was then air-dried and finally

resuspended in TE for storage at -20°C until use. DNA concentration and purity of the extracts were estimated using a NanoDrop ND1000 spectrophotometer (Nano Drop Technologies, Inc.; Wilmington, DE, United States) and concentration was adjusted to 100-200 ng/µl for use in the PCR.

PCR amplifications were done with primers listed in Table 5-2 in 20 µl reactions using 1.5 U of Taq DNA polymerase, 0.2 mM of deoxynucleotide triphosphates (dNTPs), 10 mM Tris-HCl (pH 8.0), 50 mM KCl, 1.5 mM $MgCl_2$, 0.2 µM of each primer and 50-200 ng of the extracted genomic DNA. The thermal cycle program consisted of 10 min at 94°C and then 35 cycles of 1 min at 94°C (denaturation), 1 min at 57°C (primer annealing), 1 min at 72°C (polymerization) and 5 min at 72°C for a final elongation. Amplicons were resolved by 1% agarose gel electrophoresis (45 min at 110 V), stained with 0.01 µg/ml of ethidium bromide and visualized in an Alpha Imager HP system (San Jose, California, USA).

Table 5-2. 16S rDNA universal and bifidobacterial-specific primers

Primer ID	Sequence	Specificity/fragment size	Reference
E334-F	5'-ccagactcctacgggaggcag-3'	Universal, 16S rDNA, 746 bp	Rudi et al., 1997
E1080-R	5'-ttcacaacacgagctgacgacag-3'	Universal, 16S rDNA, 746 bp	This study
g-Bifid-F	5'-ctcctggaaacgggtgg-3'	Bifidobacteria, 16S rDNA 549-563 bp	Matsuki et al., 2002
g-Bifid-R	5'-ggtgttcttcccgatatctaca-3'	Bifidobacteria, 16S rDNA 549-563 bp	Matsuki et al., 2002

PCR amplicons were purified by Wizard SV Gel and PCR Clean-Up System (Promega; Madison, WI, USA) and both strands were Sanger sequenced at Génome Québec (Montréal, Québec, Canada). BLAST analysis was done against the 16S ribosomal RNA sequences (Bacteria and Archea) database at NCBI (National Center for Biotechnology Information) for confirmation of bacterial identification (Table 5-1).

5.3.4 Screening for antimicrobial activity

The bifidobacterial strains were tested for antimicrobial activity using spot-on-the lawn and well-diffusion assays. The spot-on-the lawn assay was executed by spotting 2 µl of cell suspension of a 'producer' strain (Table 5-1) on MRS-C agar (1.5%) plates with and without $NaHCO_3$ (2 g/l) and plates were incubated under anaerobic conditions at 37^{o}C for 16-24 hrs. The sodium bicarbonate was included to counteract the effect of the organic acids such as acetate and lactate produced by bifidobacterial strains (Touré et al., 2003). After incubation, the MRS-C agar plates with the producers were overlaid with 10 ml of 'indicator' bacteria suspended at 10^5 cells/ml in 50^{o}C LB + 0.8% agar or MRS + 0.8% agar. Plates were then incubated under aerobic conditions at 37^{o}C for 16 hours and inhibitory activity was identified by an inhibition (clear) zone around the producer spots.

For the well diffusion assay, producer strains were grown in MRS-C broth in anaerobic conditions until reaching the late logarithmic phase (about 16 hrs). After incubation, cultures were inactivated by a heat treatment at 80^{o}C for 10 min, and centrifuged at 5000 *g* for 10 min. The supernatant was recovered and adjusted to pH 5.0

using 5N NaOH or 5N HCl. The supernatants were concentrated 10x by evaporation in a Speed-Vac, filter-sterilized through 0.22 µm filter membranes and stored as Cell Free Supernatants (CFS) at 4^{o}C until use. The indicator strains were grown overnight at 37^{o}C in either LB or MRS (section 5.3.2) and resuspended in warm LB or MRS agar (0.8%) at a cell density of 10^5 cells/ml. Twenty-five ml of the inoculated agar suspension was poured into Petri dishes and let solidify prior to making 5 mm diameter wells in the agar medium with a cork-borer. One-hundred µl of CFS or the negative controls (25 mM lactic acid or 50 mM acetic acid adjusted to pH 5.0±0.02) was added to the wells and plates were incubated in aerobic conditions at 37^{o}C for 16-24 hrs. After incubation, inhibitory activity was identified by an inhibition (clear) zone around the wells.

5.3.5 Effect of different carbohydrates on the inhibitory activity of Bifidobacterial supernatant.

MRS broth and RCM broth were prepared in order to control the concentration and the type of carbohydrate used in the fermentation. MRS was prepared with 10 g/l peptone, 10 g/l beef extract, 5 g/l yeast extract, 2 g/l dipotassium hydrogen phosphate, 5 g/l sodium acetate, 2 g/l ammonium citrate, 0.2 g/l magnesium sulfate heptahydrate, 0.05 g/l manganous sulfate hydrate, 0.5 g/l L-cysteine hydrochloride and 1 ml/l Tween 80. RCM was prepared with 10 g/l peptone, 10 g/l beef extract, 3 g/l yeast extract, 5 g/l sodium chloride, 3 g/l sodium acetate and 0.5 g/l L-cysteine hydrochloride. Twenty g/l of each of the following carbohydrates was separately added to MRS and RCM: glucose, fructose,

galactose, lactose, raffinose and inulin. *Bifidobacterium breve* was inoculated in each of the modified versions of MRS-C and RCM and incubated under anaerobic conditions at 37^{o}C for 16 hrs at which time cell density and pH of each cell suspension were determined. To prepare CFS, bacterial cultures were inactivated at 80^{o}C for 10 min and centrifuged at 5000 *g* for 10 min. The CFS was recovered and divided into three parts and respectively adjusted to pH of 5.0 and 5.5 or 6.0, and each part was filter-sterilized with 0.22 µm filter membranes and stored at 4^{o}C until use. *E. coli* (K-12), the selected indicator bacterium, was exposed to the effect of the different CFS by using a microdilution method (NCCLS, 2012). In brief, 100 µl of a CFS was added to the first well and serially diluted 1:1 in LB broth in wells across the microtitration plate. A non-fermented supernatant supplemented with the corresponding carbohydrate (pH 5.0±0.02) was included as a negative control. A mixture of acetic (50 mM, pH 5.0) and lactic (25 mM, pH 5.0) acids was included as an additional control to assess the potential inhibitory effect of the organic acids that can be produced by *Bifidobacterium breve.* An overnight culture of *E. coli* (K-12) was diluted to adjust the cell density to 10^5 cells/ml and 50 µl of the cell suspension was added to each well. Microplates were incubated at 37^{o}C for 16-20 hrs and inhibitory effect was assessed based on optical density at 600 nm (OD_{600}). Percent inhibition was calculated by the formula: Inhibition % = 100-[(Abs_{CFS}-Abs_{blank})/(Abs_{NF-CFS}-Abs_{blank})]*100. Where Abs_{CFS} is the absorbance of the culture exposed to the cell free supernatant, Abs_{NF-CFS} is the absorbance observed in the bacterial culture when exposed to the non-fermented supernatant and Abs_{blank} is the absorbance of the blank (no cells) including the

corresponding dilution of the CFS. The antimicrobial assays were done at least in triplicate. One-way analysis of variance (ANOVA) with post-hoc Tukey's HSD (honest significant difference) tests were performed on arcsine-square-root transformed percent inhibition values to evaluate whether or not supplementing media (MRS or RCM) with different carbohydrates altered the antimicrobial activity of bifidobacterial fermented medium against *E. coli*.

To determine a suitable concentration to be used in the chemical-genetic profile, the minimum inhibitory concentrations (MIC_{90} and MIC_{50}) of the fermented supernatant against *E. coli* (indicator bacterium) were investigated using the microtitration method that was previously described. MIC_{90} was defined as the minimum concentration capable of causing at least 90% growth inhibition. MIC_{50} was defined as the minimum concentration capable of causing at least 50% growth inhibition. Percent growth inhibition was based on OD_{600} and calculated as previously described.

5.3.6 Inhibitory effect of bifidobacterial supernatant on food pathogens

The inhibitory effect of the MRS-Glucose, MRS-Lactose, RCM-Glucose and RCM-Lactose supernatants on food pathogen bacteria (Table 5-1) cultured in BHI broth at 37^{o}C were assessed by microdilution assays as previously described.

5.3.7 Large-scale screening (Keio deletion mutant set)

5.3.7.1 RCM-Lactose supernatant sub-inhibitory concentration determination for chemical-genetic profiling.

To investigate the mode of action of bifidobacterial-CFS (RCM-lactose), a chemical-genetic profile was done with the *E. coli* Keio set of deletion mutants. Prior to the large-scale screening, the *E. coli* K-12 MIC_{90} with CFS was determined to be between 20% and 25%. Next, *E. coli* colonies from two randomly chosen plates from the Keio set were transferred using a 384-floating replicator onto experimental and control plates. The experimental plates contained LB + 2.0% agar amended with 16, 18, 20, 22, 25, 30 and 35% of CFS and the control plate contained LB + 2.0% agar with an equivalent amount of non-fermented supernatant (pH 5.0±0.02). Inoculated plates were incubated at 32^{o}C for 16 hours and the colony sizes were visually examined. A CFS concentration that caused about 10-30% colony size reduction was selected as the appropriate sub-inhibitory concentration for experiments with the entire Keio set. Each batch of CFS was tested prior to large-scale assays to determine the appropriate sub-inhibitory concentration.

5.3.7.2 High throughput phenotypic screening/chemical-genetic profiling

The Keio deletion mutant collection containing about 3900 mutants distributed in 24 plates, was exposed to 19% (1st trial, 2 replicates) and 26% (2nd trial, 2 replicates) of the CFS of bifidobacterial fermented RCM-Lactose medium (pH 5.0 $\pm$ 0.02). Plates were prepared as before using LB agar (2.0 %) with the bifidobacterial fermented supernatant

or equivalent amount of non-fermented medium as a negative control. Deletion mutants were printed onto control and experimental plates with a 384-floating replicator. Plates were incubated at 32^{o}C for 16-24 hrs, digitally imaged, and pictures were analyzed by a growth detector from SGA tools (http://sgatools.ccbr.utoronto.ca/). Digital analysis was verified by visual examination of the plates. Percent inhibition was calculated based on colony size measurements of each mutant strain on control and experimental plates. The percent inhibition results obtained from the four replicas were averaged and are presented in Supplementary Table S5. Mutants that had mean inhibition values of 60-100% in RCM-Lactose fermented supernatant were selected as potential candidates to be further categorized into functional groups according to COG (Clusters of Orthologous Groups, http://www.ncbi.nlm.nih.gov/COG/; http://www.compsysbio.org/bacteriome/) to identify the major functional categories involved in high sensitivity to the bifidobacterial supernatant.

5.3 RESULTS AND DISCUSSION

5.3.1 Screening for antimicrobial activity

Potential antimicrobial activity by 'producer' strains was tested using selected 'indicator' strains with spot-on-lawn and well-diffusion assays (Table 5-3). Figure 5-1 shows an example of the inhibitory effect exerted by four Bifidobacterial strains and the decrease of this inhibitory effect when $NaHCO_3$ (2 g/l) is included in the medium. Figure 5-2 shows an example of a well-diffusion assay in which cell free fermented supernatant

produced by *B. breve* (41408) inhibits growth of *E. coli*. Generally, the spot-on-the lawn assay gave more pronounced inhibition zones than the well diffusion assays. This could reflect differences between the two assays. In the spot-on-lawn assay, production of inhibitory substances by producers may be elicited by the presence of a living indicator strain. In contrast, in the well-diffusion assay the antagonist activity was tested using fermented, cell-free medium that did not contain live competitor bacteria and may have a more limited concentration of 'induction' compounds. Nevertheless, results from the two antimicrobial assays were similar in that the producer strains *B. bifidum* (B-41410) and *B. breve* (B-41408) showed the greatest overall antagonist effect. In both assays, the most sensitive indicator strains were *E. coli* (W3110) and *B. cereus* (B-4288).

Table 5-3. Antagonist effect by producer strains on indicator strains using spot-on-the lawn (SOL) and well-diffusion (WDA) assays. Inhibition scores are based on diameter of inhibition zones given in mm ± standard error (SE). Inhibition zones were based on at least duplicate experiments.

	Indicator strains inhibition zone diameter (mm)							
	E. coli		***L. acidophilus***		***B. bifidum***		***B. cereus***	
Producer	SOL	WDA	SOL	WDA	SOL	WDA	SOL	WDA
B-41405	16±6.0	14.5±0.5	12.5±2.5	10±1.0	4±4.0	6±6.0	15.5±2.5	16.5±4.5
B-41410	43.5±1.5	18±3.0	14.5±0.5	13.5±1.5	3±3.0	6±6.0	45±3.0	13±2.0
B-41408	41±1.0	22±1.0	15±2.0	13±3.0	4±4.0	4±3.0	34.5±5.5	15.5±3.5
B-41661	22.5±2.5	0	6.5±3.2	0	0	0	29.5±5.5	10.5±0.5
B-1932	24±2.0	16±4.0	0	0	0	0	0	0
B-41522	22±2.0	18.5±1.5	0	0	0	0	16±1.0	13.5±1.5
B-4288	19.5±1.5	16.5±1.5	0	0	0	0	0	0

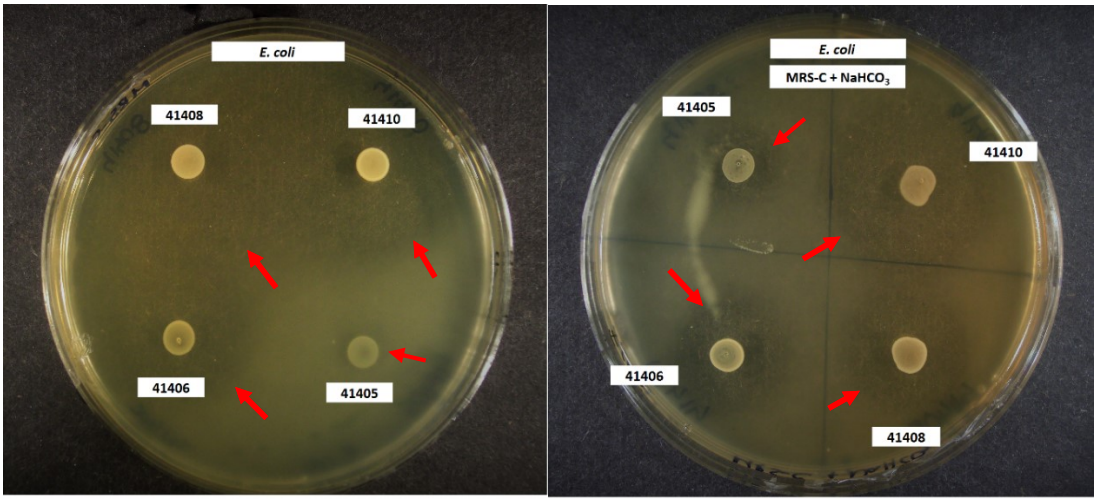

Figure 5-1. Inhibition of *E. coli* by four bifidobacterial strains in spot-on-the lawn assays. Plates contain MRS-C (left) and MRS-C + $NaHCO_3$ (right) media. Arrows indicate edge of zone of inhibition.

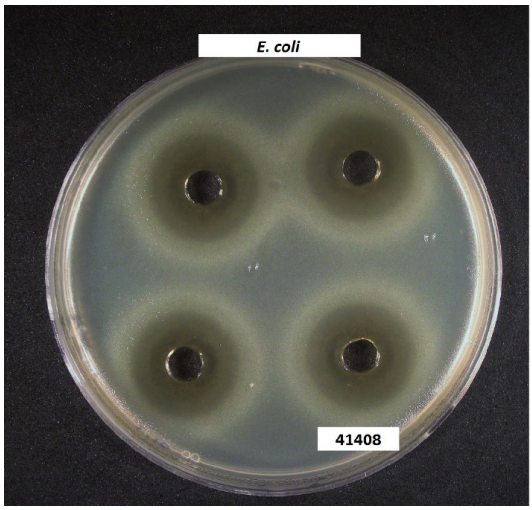

Figure 5-2. Inhibitory activity exerted by cell free fermented supernatant (pH 5.00±0.02) produced by *Bifidobacterium breve* (41408) on the indicator bacterium *E. coli.* Left panel shows the well diffusion assay inoculating the indicator bacterium in the LB agar.

The incorporation of the sodium hydrogen carbonate in the spot-on-lawn assays resulted overall in smaller zones of inhibition (Table 5-4). This indicates that part of the inhibitory activity exerted by producer strains is likely due to the production of organic

acids (Van der Meulen et al., 2006), which would be neutralized by $NaHCO_3$ in the medium. However, the inhibitory effects remained evident even in the presence of $NaHCO_3$ suggesting a mode of inhibition other than by production of acids. These results are in accordance with preliminary studies using TLC-bioautography with bifidobacterial fermented supernatant where it was observed that the inhibitory activity of the bifidobacterial fermented supernatant was due to the presence of a non-polar substance and not to lactic or acetic acids (data not shown). The purification and characterization of this non-polar inhibitor will require additional study.

In particular, *B. bifidum* (B-41410) and *B. breve* (B-41408) yielded pronounced inhibition of 'indicator' strains *E. coli* and *B. cereus* (but not *L. casei*) in the presence of $NaHCO_3$ (Table 5-5). The inhibitory effect of the MRS-CFS produced by B-41410 in presence of the neutralizing agent $NaHCO_3$ seems to be reduced by a greater degree than the inhibitory effect caused by B-41408. In addition, the bacteriocinogenic capabilities of a *B. bifidum* strain were previously studied by Yildrim and Johnson (1999), and attributed to a bacteriocin 'bifidocin B'. For these reasons, high activity and no previous characterization, I selected *B. breve* (B-41408) for further study.

Table 5-4. Antimicrobial activity by bifidobacterial species in the spot-on-the lawn assays with and without $NaHCO_3$ added to medium.

	Indicator strain inhibition zone diameter (mm)					
	E. coli		***B. cereus***		***L. casei***	
Producer Strain	MRS-C	MRS-C +$NaHCO_3$	MRS-C	MRS-C +$NaHCO_3$	MRS-C	MRS-C +$NaHCO_3$
B-41405	17.7±1.9	8±1	16±1.7	18±2.5	0	0
B-41406	31.3±4.7	22.7±2.3	24.7±2.7	22.3±1.4	11.3±1.0	0
B-41408	38±1.6	26.7±3.3	34.3±4.7	24.7±1.4	17±1.0	0
B-41410	43±1.5	23.3±6.5	45.3±2.4	30.7±2.7	28±1.5	0

5.4.2 Effect of different carbohydrates on the inhibitory activity exerted by the *B. breve* fermented supernatant

The effect of different carbon sources on inhibitory activity of the fermented supernatant by *B. breve* (B-41408) was investigated (Table 5-5). *B. breve* was grown in MRS-C or RCM supplemented separately with 3 different carbohydrates (glucose, fructose and lactose) which were selected based on preliminary studies. These preliminary studies showed that the inhibitory activity of the fermented broths against *E. coli* was not correlated with the growth rate of B-41408, nor with the acidification of the broth (results no shown). The preliminary study also showed that *E. coli* inhibition by the B-41408 broth depended on the sugar supplement used: in descending order, lactose, glucose, raffinose, fructose, galactose, and inulin. Note that the fermented supernatant pH was adjusted to 5.0±0.02 before being tested for inhibitory activity. Interestingly, visual observation after 48 hr incubation indicated that the inhibitory effect was

maintained with media supplemented with lactose and that media with other sugar supplements had a reduction in inhibition over time. These results indicated that the carbon source influences the production of inhibitory substance(s) and that optimizing bacterial growth rate does not necessarily increase production of inhibitory substances. Along these lines, Vamanu (2010) found that *Lactobacillus paracasei* grown in medium supplemented with raffinose produced the greatest amount of lactic acid, supplementing with lactulose resulted in the greatest growth rate, but bacteriocin production was greatest when inulin was used to supplement the medium. Other studies have demonstrated that the exposure of Bifidobacteria or lactic acid bacteria to different sources of carbon may modify the proportion of the end product formation (Van der Muelen et al., 2006; Amaretti et al., 2007; González-Rodríguez et al., 2013). Lactose, glucose and fructose were selected as candidate supplements for further study of inhibitor production and results are presented in Table 5-5.

Table 5-5. Effect of the fermentable carbohydrate and the medium composition on the antimicrobial activity by *B. breve* (B-41408) against *E. coli* strain W3110.

Supernatant	***Spnt. % [1]***	***Inhibition % ± SE [2]***	***ANOVA and Post-Hoc (HSD) analysis (MRS) [3]***	***ANOVA and Post-Hoc (HSD) analysis (RCM) [3]***
MRS-Glucose	12.5	88.54±4.72	ab	
RCM-Glucose	25.0	80.25±7.83		A
MRS-Fructose	12.5	76.13±6.09	a	
RCM-Fructose	25.0	95.53±2.71		A
MRS-Lactose	12.5	98.93±0.54	b	
RCM-Lactose	25.0	99.80±0.05		A

[1] Supernatant concentration in % (v/v) for inhibition assays (Supernatant pH adjusted to 5.0±0.2).

[2] Average % inhibition (± standard error) is based on at least 3 independent experiments.

[3] *Different letters indicate significant differences between arcsine-square-root transformed percent inhibition values, based on ANOVA with post-HOC HSD test*

Note that, in Table 5-5, data for inhibitory activity of the 25% MRS fermented supernatants are not available due to the inhibitory effect of the non-fermented supernatant (control) against the 'indicator' bacterium *E. coli.* This is probably due to relatively high concentrations of sodium acetate in MRS medium in comparison to RCM. Previous studies have demonstrated that sodium acetate has a buffering role in the medium but also exerts an inhibitory effect on *E. coli* and on some fungi, including species of *Fusarium, Aspergillus, and Penicillum* among others (Brul and Coote, 1999; Stiles et al., 2002; Oh et al., 2002). Therefore, when media containing sodium acetate are used in assays intended to screen for antimicrobials such as bacteriocins synthesized by lactic acid bacteria, this additional inhibitory effect provoked by the sodium acetate must be considered. The results shown in Table 5-5 are in accordance with the preliminary assays that indicated chemical composition of the medium can influence the production of inhibitory substances by the *B. breve* (B-41408). In particular, fermentation of MRS-lactose resulted in significantly greater inhibition than when MRS-fructose was used. A similar trend was observed in RCM media, with lactose supplementation yielding the highest inhibitory activity, although the differences were not significant. Further experiments were done in the following sections using *B. breve* (B-41408)-fermented lactose media, to investigate the inhibitor's efficacy against food pathogenic bacteria and mode of action.

5.4.3 Inhibitory effect of bifidobacterial supernatant on food pathogens

A microdilution format was used to investigate inhibition of foodborne pathogens by *B. breve* fermented MRS-Lactose and RCM-Lactose supernatants. Table 5-6 shows that all of the selected foodborne pathogens were sensitive to *B. breve* fermented supernatants. Similar to previous experiments with *E. coli*, in several cases, a lower concentration of the MRS-lactose fermented supernatant than RCM-lactose fermented supernatant was required to cause greater than 90% growth inhibition. This may be due to the inherent inhibition by MRS medium noted previously, or to other unknown factors. The most sensitive strains were *Salmonella enterica* ser. Typhimurium, *Salmonella enterica* ser. Enteritidis and *E. coli* (1285), three Gram-negative strains. Each of these three strains showed 91.62% or greater inhibition when the concentration of the RCM-Lactose CFS was 25% or lower. The *E. coli* (1285, a pathogenic isolate) sensitivity to the bifidobacterial supernatant was very similar to the sensitivity observed from *E. coli K-12* (Strain W3110) in the previous assay (Table 5-6). Additional studies, using serial dilutions with finer gradations are required to determine precise minimum inhibitory concentrations of the supernatant. However, more precise MIC assays would be more appropriate once pure inhibitor compound is isolated. In any case, pronounced inhibitory activity against Gram-negative bacteria examined in this study is encouraging since one of the challenges in antimicrobial discovery is to produce/discover inhibitory substances able to cross the outer membrane of these bacteria which serves as a protective barrier impeding the inhibitory substance reaching the intracellular target (Silver, 2011). In

general, the *B. breve* fermented supernatant appears to be an effective inhibitor of foodborne pathogens and its use in the food industry may be generally recognized as safe (GRAS), since *B. breve* is a well-known probiotic (Russell et al., 2011).

Several investigations have noted bifidobacterial species that produce effective, broad-spectrum antimicrobials. For example, Saleh and El-Sayed (2004) isolated the bacteriocin 'bifilact Bb-46' from *B. longum* Bb-46 which effectively inhibited growth of *Staphylococcus aureus, Salmonella enterica* ser. Typhimurium, *Bacillus cereus* and *E. coli*. Cheikhoyoussef and collaborators (2009a, 2010), isolated the bacteriocin 'bifidin I' that was effective against Lactic Acid Bacteria, *Staphylococcus*, *Bacillus, Streptoccocus, Salmonella, Shigella* and *E. coli.* Recently, Liu and colleagues (2015) purified bifidocin A produced by *B. animalis* BB04 showing a promising inhibitory activity to counteract *E. coli, Listeria monocytogenes, Staphyloccocus aureus* and some yeast. Lee and co-workers (2013) tested the anti-clostridium effect of some probiotics such as *B. breve* (BR3) and found that the fermented supernatant successfully decrease the *Clostridium difficile* growth rate. All the above provide evidence of the antimicrobial potential of bifidobacterial species and support the hypothesis that *B. breve* (B-41408) also produces a broad-spectrum antimicrobial substance.

Table 5-6. Effect of the fermentable carbohydrate and the medium composition on the antimicrobial activity of *B. breve* (B-41408) against foodborne pathogens.

Strain	Gram stain	MRS-Lact		RCM-Lact	
		Spnt. % [1]	***Inhibition %*** [2] ***± SE*** [3]	***Spnt. %***	***Inhibition % ± SE***
***Salmonella enterica* ser. Typhimurium**	Negative	25	99.97 ± 0.53	25	99.83 ± 0.41
***Salmonella enterica* ser. Enteritidis (PT13)**	Negative	25	99.98 ± 0.15	25	99.16 ± 0.68
***Salmonella enterica* ser. Heidelberg**	Negative	25	99.94 ± 0.03	50	99.43 ± 5.56
Escherichia coli (1285)	Negative	12.5	91.37 ± 1.33	25	96.86 ± 0.25
Listeria monocytogenes (005)	Positive	50	99.26 ± 1.10	50	91.62 ± 2.54
Listeria monocytogenes (017)	Positive	50	99.78 ± 2.22	50	96.21 ± 3.14
Enterococcus faecalis	Positive	50	99.48 ± 0.27	50	99.43 ± 0.06
Klebsiella pneumoniae	Negative	25	99.97 ± 0.02	50	99.83 ± 0.12
Staphylococcus aureus	Positive	25	99.96 ± 0.03	50	99.92 ± 0.08

[1] *Spnt. %* = Supernatant concentration in % (v/v)

[2] *Inhibition %* = 100-[(Abs_{CFS}-Abs_{blank})/($Abs_{NF\text{-}CFS}$-Abs_{blank})]*100. The values are averages based on at least triplicate experiments (Section 4.3.5).

[3] *SE* = Standard error calculated based on the standard deviation (SD) of at least a triplicate.

5.4.4 RCM-Lactose supernatant sub-inhibitory concentration determination for chemical-genetic profiling.

Because non-fermented MRS-based medium was shown to have inhibitory activity, RCM medium was selected to investigate mode of action of *B. breve* (B-41408) metabolites. To establish a suitable sub-inhibitory concentration for the large-scale screening, MICs for the RCM-lactose (pH 5.0±0.02) was determined using replicate experiments. Based on microdilution experiments, *E. coli* K-12 MICs were determined as $20\% < MIC_{90} < 25\%$ and $10\% < MIC_{50} \leq 15\%$. These MIC results were obtained in liquid medium and were taken into consideration to prepare the solid LB medium plates.

5.4.5 Identification of the *E. coli* deletion mutants most sensitive to bifidobacterial supernatant

RCM-Lact fermented supernatant produced by *B. breve* was used for chemical-genomic high-throughput screens. Concentrations of 19% and 28% (v/v, 1st and 2nd trial, respectively) of the *B. breve* fermented supernatant were used for the assays and 2 replica experiments were done in each trial. Supersensitive mutants were identified by a significant colony size reduction (≥60%, Supplementary Table S5). As shown in Figure 5-3, among the top 2.5% most inhibited deletion mutants, we distinguished 8 functional categories based on the COG (Clusters of Orthologous Groups of proteins, Tatusov et al., 2001; http://www.ncbi.nlm.nih.gov/COG/; http://www.compsysbio.org/bacteriome/).

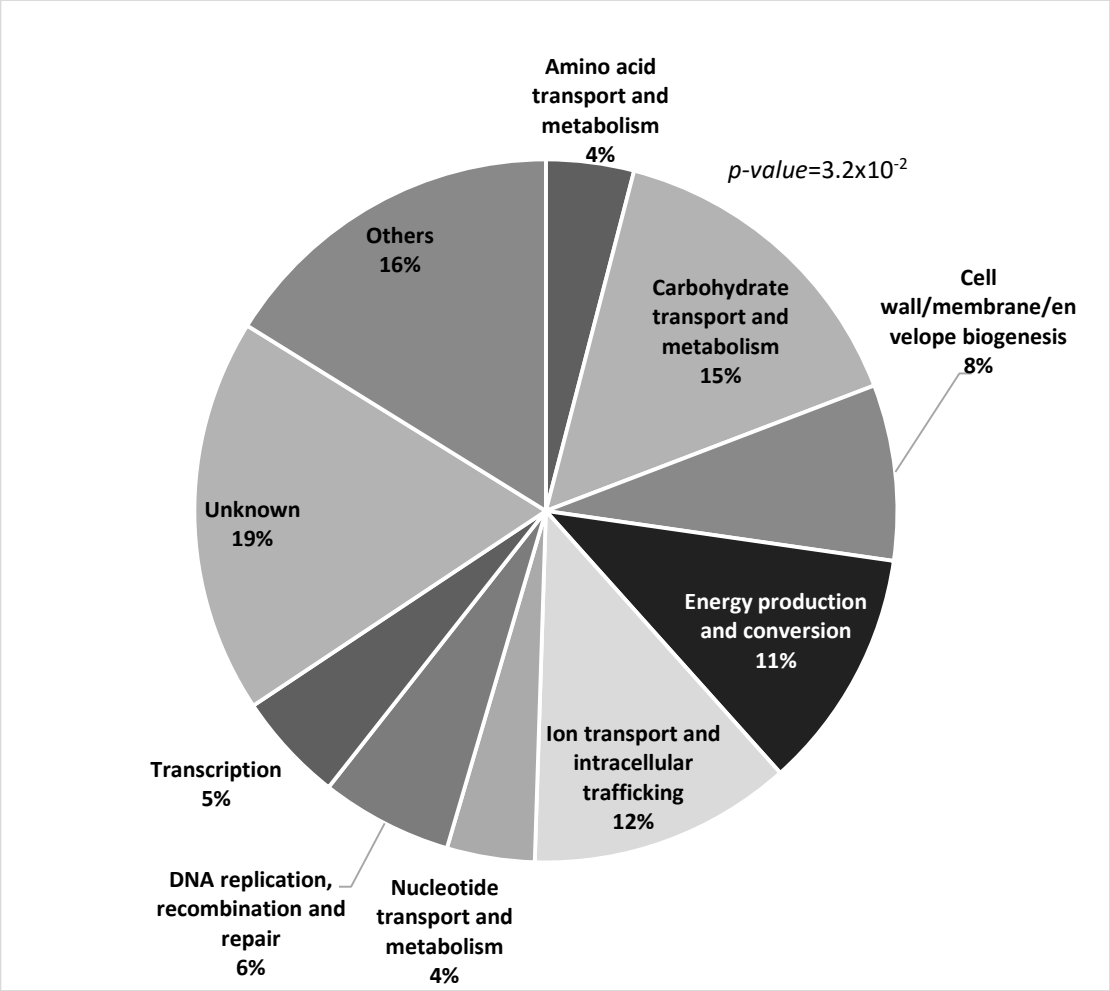

Figure 5-3. Functional distribution according to COG of genes deleted in 101 mutants that were most sensitive to RCM-lactose *B. breve* (B-41408) fermented supernatant. Major known function COG groups include carbohydrate transport and metabolism (15%), intracellular trafficking, secretion and vesicular transport (12%) and energy production and conversion (11%).

The major group of the supersensitive mutants is represented by strains containing deletions of genes involved in carbohydrate transport and metabolism (15%) such as *ΔbglX* (beta-D-glucoside glucohydrolase), *ΔmelA* (alpha-galactosidase, NAD(P)-binding), *ΔulaD* (3-keto-L-gulonate 6-phosphate decarboxylase) and *ΔulaE* (L-xylulose 5-phosphate 3-epimerase). To confirm the results obtained from our phenotypic large-scale

screening, secondary assays should be carried out. To investigate the effect of the secondary metabolite(s) contained in the fermented supernatant on carbohydrate metabolism and transport, a metabolic flux profiling based on the central carbon metabolism could be done using gas chromatography-mass spectrometry (GS-MS) (Fisher and Sauer, 2003) using ^{13}C-labelled glucose to track carbon incorporation through the carbon flux. Alternatively, a GC-MS or an HPLC (high pressure liquid chromatography) could be used to quantify intermediate and extracellular fermentation products to detect alterations in the carbohydrates metabolism.

The second largest group is represented by strains containing deletions of genes involved in intracellular trafficking, secretion and vesicular transport (12%) such as *ΔexbD* (membrane spanning protein)*, ΔtatC* (TatABCE protein translocation system subunit)*, ΔtolB* (TatABCE protein translocation system subunit) and *ΔpanF* (pantothenate:sodium symporter). This group, along with the cell wall/membrane/envelope biogenesis (8%) group that includes *tonB* (membrane spanning protein in TonB-ExbB-ExbD complex) and *ypjA* (adhesin-like autotransporter), suggests that *B. breve* supernatant affects membrane functions. Bacteriocins classes I and II, such as sakacin and nisin, both disrupt cell membrane (Chapter 4, Cotter et al., 2005). Although the active substance in *B. breve* was not identified in this study, the membrane-associated factors category revealed by our phenotypic screening, may indicate a potential cellular target that is common to these bacteriocin-like substances. However, further studies are required to determine the type of metabolite(s) produced by *B. breve* that are responsible for the inhibition *of E.* coli. This

study encourages us to isolate and identify the metabolites, and to do follow up experiments to corroborate the effect of the active substance(s) on the cell membrane structure/function. To confirm that fermented *bacterial B. breve* (B-41408) supernatant affects intracellular trafficking, secretion and vesicular transport, detection of cell membrane depolarization may be assayed by carrying out a flow cytometry with $DiSBAC_2(3)$ [Bis-(1,3-Diethylthiobarbituric Acid)Trimethine Oxonol], a dye that penetrates the cells only when a membrane depolarization has occurred (Chapter 3).

The third largest group of supersensitive mutants is represented by deletion strains lacking genes involved in energy production and conversion (10%), such as *cybB* (cytochrome b561), *cydB* (cytochrome d terminal oxidase, subunit II) and *nuoC* (NADH:ubiquinone oxidoreductase). This functional category and the major category (carbohydrate metabolism and transport) are correlated since carbohydrates are an important part of energy production and conversion (cellular respiration, fermentation, Krebs and glyoxylate cycles, etc.) Therefore, affecting carbohydrate metabolism may alter other metabolic pathways through an indirect interaction.

Clearly, the bifidobacterial metabolite(s) produced through fermentation has potential antimicrobial activity. Further investigations are required to identify the inhibitory substance and corroborate the potential molecular targets suggested by the results of our large-scale phenotypic screen using the crude CFS.

Chapter 6

Summary and General Conclusions

6.1 SUMMARY OF FINDINGS

The objective of this thesis was to investigate the modes of inhibitory activity of a variety of chemical species using a functional genomic approach. Mechanistic studies to confirm the cellular/pathway targets elucidated by the large-scale phenotypic screens were then performed. The findings of each chapter are summarized in the following sections and in the table 6-1.

In Chapter 2, the antifungal activity of chitosan, a natural by-product of animal or fungal origin, was elucidated using the yeast gene deletion mutant set through a high-throughput phenotypic screening. Chitosan interferes primarily with protein synthesis in addition to other processes including membrane/cell wall function and cellular trafficking and secretion. The later antifungal mode of action for chitosan, perturbation of membrane/cell wall function, was previously proposed and supported in our studies. Chitosan's putative effect on protein synthesis has not been reported before. Chapter 3 focused on investigating the cytotoxic effect of engineered zinc oxide and silver nanoparticles on *S. cerevisiae*. ZnONPs exert an antifungal effect by depolarizing and disrupting cell membrane, and altering cell wall. AgNPs on the other hand, exert an inhibitory effect by influencing transcription, cellular respiration and endocytosis. In the case of AgNPs, it can be observed that cellular respiration and endocytosis are not usually considered as typical targets for antibiotics. In Chapter 4, the mode of action of nisin, a

polycyclic antimicrobial peptide of bacterial origin, was explored in a Gram-negative bacterium, *E. coli*. Nisin is well known to be active on Gram-positive bacteria. By using citric acid as a chelator its inhibitory capability on *E. coli* was enabled. Our high-throughput phenotypic screening of nisin revealed that it mainly targets the cell wall, cell membrane and envelope biogenesis, confirming its well-known mode of action in Gram-positive bacteria. However, we also detected a second, previously unrecognized mode of activity, whereby nisin interferes with DNA replication processes. Nisin's effect on DNA replication was confirmed with secondary assays that measured plasmid replication and cellular genomic DNA content. To gain insights on putative inhibition of DNA synthesis, ciprofloxacin-resistant mutants were exposed to nisin and results showed that the majority of the mutants were sensitive to nisin, indicating that the bacteriocin may be used to counteract bacterial resistance to ciprofloxacin. Nisin should be considered as a multi-targeted antimicrobial compound. Finally, in Chapter 5, the potential mode of action of the fermented supernatant produced by the probiotic *Bifidobacterium breve* was investigated using the *E. coli gene* deletion mutant set. The results of our phenotypic screening using the Keio set to test the raw supernatant produced by *B. breve*, revealed a very different pattern from that of nisin. With *B. breve* supernatant, the chemical-genetic profile analysis revealed that secondary metabolite(s) produced by this probiotic might exert their antimicrobial effects by interfering with the carbohydrate metabolism, intracellular trafficking, secretion and vesicular transport. Further studies are suggested to identify the antimicrobial substances and their mode(s) of action.

Table 6-1. Summary of findings

Chemical	Chitosan (Antifungal)	ZnONPs (Antifungal)	AgNPs (Antifungal)	Nisin (Antibacterial)	Bacterial spnt. (Antibacterial)
Pathway/process target					
Cell membrane	Confirmed	Confirmed		Confirmed	
Cell wall		Confirmed			
Protein synthesis	Confirmed				
Transcription			Confirmed		
Ion homeostasis		Confirmed			
Endocytosis			Confirmed		
DNA replication				Confirmed	
Cellular respiration			Confirmed		
Carbohydrate metabolism					To be confirmed
Intracellular trafficking and transport					To be confirmed

6.2 CONTRIBUTION TO SCIENTIFIC KNOWLEDGE

The major contributions of this thesis are in filling in knowledge gaps on antimicrobial discovery and the mode of activity of antimicrobial compounds. We demonstrated that chitosan, ZnONPs, AgNPs, nisin and the bifidobacterial supernatant, chemicals of different origin (natural, engineered), are all, apparently, able to exert antimicrobial activities in distinct and in multi-targeted ways – a desirable feature for the next generation of antimicrobials.

In addition to providing insights into the mode of action of several inhibitory substances, this study provides additional evidence for the usefulness of large-scale genomics screening to dissect modes of activity. It demonstrates that chemical-genetic profiling can be a suitable approach to examine cytotoxic mode of action exhibited by a variety of inhibitory substances, from nanoparticles to crude extracts. The speed and ease of use coupled with relatively simple data analysis makes chemical-genetic analysis using GDA an ideal tool for the preliminary investigation of modes of activity.

6.3 FUTURE DIRECTIONS

A possible future direction is to study the effect of target compounds using gene overexpression libraries such as the one in yeast (Li et al., 2011). The use of such libraries can provide complementary information about the way in which a compound affects the biology of a cell. Similarly, development and use of human gene knockout libraries could provide important information about the toxicity of target compounds in human. Since in general, humans are of primary interest as the host for microbial infections, it would be very interesting to compare and contrast the toxicity of antimicrobials in this organism relative to yeast, for example. Other approach to investigate the toxicity of antimicrobials on eukaryotic organisms including humans, is the comparative genomics extrapolating the information acquired through functional genomics in an eukaryotic model such as yeast to analogous and orthologus genes in humans.

In addition, for the uncharacterized inhibitor in *B. breve* supernatant that was identified in this thesis, I propose follow up bioassay-guided fractionation of the crude fermented supernatant to isolate the inhibitory compound in its pure form. Preparative HPLC would appropriately separate the active fraction(s), and sub-fractions can then be tested for antimicrobial activity. Active sub-fractions may be analyzed by UPLC-Qtof-MS/MS (Ultra-performance liquid chromatography coupled to a hybrid quadrupole orthogonal time of flight (Q-Tof) mass spectrometer) to acquire tentative chemical structure of the compound. Structure identification can be confirmed via NMR (Nuclear magnetic resonance) spectroscopy. Once the active component(s) is isolated, a GDA screen analysis can be used to study the mode of activity of these compounds and to compare the effects of the pure compound with crude extracts studies in this thesis.

6.4 CONCLUDING REMARKS

Antimicrobial resistance is an inevitable consequence of antimicrobial use that has been exacerbated by inappropriate use of antibiotics. As a consequence, the emergence of 'superbugs' and untreatable life-threatening infections is undeniable. To address this problem, antimicrobial discovery should continue despite the fact that the pharmaceutical industry has shifted interest to the development of other drug types such as anti-cancer, anti-HIV, anti-inflammatory, painkillers, etc. Some of the reasons for this move away from antimicrobial discovery are high costs and lack of profitability, lengthy

investment time to bring a sole drug from the bench to product launch, and the lack of substantial success (Spellberg et al., 2003; Hughes and Karlén, 2014).

Nevertheless, the discovery of antimicrobials with new molecular targets is becoming critical to stem the rapid increase of the antimicrobial resistance. Natural products produced by plants, algae, fungi or bacteria, remain excellent resources of new antimicrobial substances. Coupled with synthetic chemistry and nanochemistry, these new sources provide a sub-exploited scaffold of chemical species that may be suitable for antimicrobial discovery.

To reduce the reoccurrence of resistance, the discovery of new antimicrobial substances that act on multiple cellular targets should be emphasized. However, unveiling drug targets is still a challenging task for the pharmaceutical industry. In this context, functional genomics methods have provided excellent alternatives to tackle this issue. The availability of deletion sets for model organisms such as *S*. *cerevisiae, E. coli* and *B. subtilis* provide outstanding resources to identify antimicrobial cellular/pathway targets *in vivo*. Through functional genomics, clues regarding the mode of activity and the potential drug resistance mechanisms can be studied. In addition, the use of *in vivo* assays overcomes some of the encountered problems in the target-based approach including inability of the compound to reach the intended cellular target, potential off target side effects, and underestimation of effective compound concentration (Harvey et al., 2015). In addition, with the availability of gene deletion and overexpression libraries, it is possible to identify drug targets and potential drug resistance mechanisms.

Regardless of the effort that the pharmaceutical industry and the scientific community has put into the discovery and development of new antimicrobials, no significant gains have been made in recent years. The finding of new classes of antimicrobials has been almost fruitless. After the "Golden Age" (1940-1970) of the antimicrobial discovery stage, just two classes of "first-in-class" antimicrobials (those that work against new targets) have been discovered, linezolid and daptomycin (Swinney and Anthony, 2011; Roemer and Boone, 2013). To overcome some of the existing gaps in the field antimicrobial discovery, one of the directions that the field has taken is to continue expanding chemical libraries that can target different cellular sites. To date, most discovered antimicrobials have targeted a set of biological processes that include nucleic acids synthesis, protein synthesis, cell wall synthesis, cell membrane structure and folate metabolism. Some examples of the new targets are peptidoglycan biosynthesis, mevalonate-independent pathway, wall teichoic acid, folate biosynthesis, fatty acid biosynthesis, protein secretion systems, peptide deformylase (Brown and Wright, 2005), and virulence factors (Clatworthy et al., 2007). Another way to expand potential drug targets is to explore interruption of important protein-protein interactions where small molecules may act as protein-protein interaction inhibitors (Harvey et al., 2015). Acquiring more knowledge and understanding of the antimicrobial resistance mechanisms will provide significant knowledge to enhance the development of more effective antibiotics.

An underexploited strategy for the antimicrobial discovery, is exploring the study of synergistic agents such as cell envelope permeabilizers, β-lactamase inhibitors, efflux pump inhibitors, etc. Functional genomics is a great source to screen chemical system with potential synergistic or antagonistic effects. Besides the chemical-genetic interaction, the investigation of genetic-genetic interaction (double mutant phenotype) may be very useful in the study of synergistic effect in a biological system (Alamgir et al., 2008; Alamgir et al., 2010; Roemer and Boone, 2013). Hoon and collaborators (2008) have demonstrated that using haplo-insufficiency profiling (HIP), homozygous profiling (HOP) and multi-copy suppression profiling (MSP) strategies as an integrative platform for the antimicrobial target discovery, allows a more precise and accurate target prediction (Hoon et al., 2008). The inclusion of such combined strategies to discover antimicrobial targets may be a suitable future direction.

A problem encountered when employing GDAs to investigate drug targets is the number of uncharacterized gene products in genomes. Almost one third of the genes in a given microbial genome encode for 'biochemically uncharacterized' proteins (Brown and Wright, 2005). In this context, systems molecular biology is continuously investigating the novel functions of genes (Samanfar et al., 2013; Omidi et al., 2014) and characterizing orphan genes (Samanfar et al., 2014; Jessulat et al., 2015). Another gap of knowledge in this area stems from transforming the information gathered from the model organisms to other organisms of interest. For example, the antibiotics ampicillin and chloramphenicol that work efficiently against *E. coli* are simply useless against

Agrobacterium tumefaciens (Golshani et al., 2002). Absence of essential genes in the haploid GDA collections constitute another challenge. To this end a series of conditionally knocked down essential genes has been generated in *S. cerevisiae* (Yu et al., 2006). The conditional growth requirement for this essential gene collection, however, complicates analysis of the data generated by this library.

The world-wide antimicrobial resistance problem still requires solutions. Functional genomics supports antimicrobial discovery by improving knowledge on gene function, microbial physiology, metabolism and virulence; and more importantly provides relevant information for the target discovery for antimicrobials and antimicrobial resistance as demonstrated in this thesis. The studies realized in this thesis also demonstrate that chemical-genetic profiling, a functional genomics tool, is a suitable approach to examine cytotoxic mode of action of wide array of inhibitory substances.

Appendices

Supplementary Table 1 (S1): Highly sensitive yeast deletion mutants to chitosan.

GENE	*GENE FUNCTION*	*GDA % colony size reduction*
A. Amino acid metabolism and transport and Translation		
MRPL28	Mitochondrial ribosomal protein of the large subunit	97.20
RPL13B	Ribosomal protein L13 (rat L13), nearly identical to Rpl13Bp	88.15
MUP3	Low affinity methionine amino acid permease	86.07
PRO2	Gamma-glutamyl phosphate reductase (phosphoglutamate dehydrogenase), proline biosynthetic enzyme	82.10
RPS17A	Ribosomal protein S17 (rp51; rat S17), nearly identical to Rps17Bp	80.42
RPL2B	Ribosomal protein L2 (yeast L5; YL6; rp8; E. coli L2; tobacco L2; rat L8)	79.88
RPS23A	Ribosomal protein S23 (yeast S28; rp37; YS14; E. coli S12; rat S23), identical to Rps23Bp	79.76
CYS3	Cystathionine gamma-lyase, generates cysteine from cystathionine	76.54
ALD3	Cytoplasmic, stress inducible aldehyde dehydrogenase, probable isoform of Ald2p	76.29
RPL20B	Ribosomal protein L20, nearly identical to Rpl20Bp	75.40
RPS18B	Ribosomal protein S18 (E. coli S13; rat S18), identical to Rps18Ap	75.06
RPL15B	Ribosomal protein L15 (yeast L13; YL10; rp15R; rat L15), nearly identical to Rpl15Ap	74.23
RPL20A	Ribosomal protein L20, nearly identical to Rpl20Bp	73.21
RPS4B	Ribosomal protein S4 (yeast S7; YS6; rp5; rat and human S4), identical to Rps4Ap	73.21
RPL13A	Ribosomal protein L13 (rat L13), nearly identical to Rpl13Bp	72.38
RPL43B	Ribosomal protein L43B (human L37A), identical to Rpl43Ap	70.30
YOL027C	Mitochondrial protein, forms a complex with Mba1p to facilitate recruitment of mRNA-specific translational activators to ribosomes	68.99
SAM1	S-adenosylmethionine synthetase 1	68.21
RPS18A	Ribosomal protein S18 (E. coli S13; rat S18), identical to Rps18Bp	66.85
RPS16A	Ribosomal protein S16 (rp61R; rat S16), identical to Rps16Bp	66.67
RPS10B	Ribosomal protein S10 (rat S10), nearly identical to Rps10Ap	64.70
HIS6	Phosphoribosyl imidazolecarboxamide isomerase	64.64
RPS24B	Ribosomal protein S24 (rat S24), identical to Rps24Ap	60.95
AGP3	Amino acid permease for serine, aspartate and glutamate; shows similarity to Gap1p and other amino acid permeases	58.63
RPS30A	Ribosomal protein S30A (mammalian S30), identical to Rps30Bp	56.96
RPS19A	Ribosomal protein S19 (rp55; YS16A; rat S19), nearly identical to Rps19Bp	50.15
B. Cell cycle and DNA processing		

Cell division/cell cycle control and mitosis/chromatine/DNA replication, recombination and repair		
YBR267W	Cytoplasmic pre-60S factor; required for the correct recycling of shuttling factors Alb1, Arx1 and Tif6 at the end of the ribosomal large subunit biogenesis; involved in bud growth in the mitotic signaling network	98.81
YKL037W	Protein of unknown function	96.19
SCP160	Protein involved in control of mitotic chromosome transmission, contains 14 KH domains which are found in RNA-binding proteins such as Mer1p and mouse hnRNP X	84.05
SNF2	Component of SWI-SNF global transcription activator complex, acts to assist gene-specific activators through chromatin remodeling	82.37
YOR197W	Ca2+-activated cysteine protease,contributes to clearance of insoluble protein aggregates during normal growth	82.08
CLB6	B-type cyclin appearing late in G1, involved in initiation of DNA synthesis	82.02
ADE3	C1-tetrahydrofolate synthase (trifunctional enzyme), cytoplasmic	80.91
PMS1	Protein required for mismatch repair, homologous to E. coli MutL	79.58
RPO41	RNA polymerase, mitochondrial	79.23
YBL006C	Component of the RSC chromatin remodeling complex; interacts with Rsc3p, Rsc30p, Npl6p, and Htl1p to form a module important for a broad range of RSC functions	77.00
CCR4	Component of the CCR4 transcriptional complex; has positive and negative effects on transcription	74.52
SIN3	Component of histone deacetylase B and transcriptional regulator of RNA polymerase II, has negative and positive effects on gene expression	73.15
SRL3	Cytoplasmic protein that, when overexpressed, suppresses the lethality of a rad53 null mutation; potential Cdc28p substrate	68.63
YNG1	Component of histone acetyltransferase complex, has similarity to human retinoblastoma binding protein 2	66.67
RAD55	Component of recombinosome complex involved in meiotic recombination and recombinational repair; with Rad57p promotes DNA strand exchange by Rad51p recombinase	66.49
BUD25	Protein involved in bipolar budding	63.45
FIS1	Protein involved in mitochondrial division	61.49
YOR295W	Subunit of UAF (upstream activation factor), which is an RNA polymerase I specific transcription stimulatory factor	57.02
CCE1	Cruciform cutting endonuclease	48.93
C. Transport and secretion		
YPT32	GTP-binding protein required in the secretory pathway at the stage of formation of trans-Golgi vesicles, member of the rab family in the ras superfamily	84.82
SRP40	Nucleolar protein, suppressor of rpc40 and rpb10 mutations	82.38
LTV1	Protein required for viability at low temperature	82.26
NHX1	Na+/H+ antiporter required for endosomal protein trafficking	74.94
RSN1	Possible membrane transporter involved in tunicamycin sensitivity	74.70
FYV5	Protein involved in regulation of the mating pathway; binds with Matalpha2p to promoters of haploid-specific genes	71.56

YMR166C	Member of the mitochondrial carrier (MCF) protein family of membrane transporters	71.43
VID22	Plasma membrane associated protein required for targeting of fructose-1,6-bisphosphatase to Vid vesicles, has weak similarity to Von Willebrand factor	61.31
APL4	Gamma-adaptin, large subunit of the clathrin-associated protein (AP) complex	56.49
FAB1	Phosphatidylinositol-3-phosphate 5-kinase involved in orientation or separation of mitotic chromosomes	47.32
ESBP6	Protein with similarity to mammalian monocarboxylate transporters MCT1 and MCT2, member of the monocarboxylate porter (MCP) family of the major facilitator superfamily (MFS)	44.94
D. Post-translational modification, protein turnover, chaperon		
STP22	Protein required for vacuolar targeting of temperature-sensitive plasma membrane proteins such as Ste2p and Can1p	77.86
SNF8	Protein involved in glucose derepression	75.30
VPS25	Protein required for normal mating efficiency, pseudohyphal growth, and resistance to NaCL, KCl, and H2O2	75.21
LHS1	Hsp70 superfamily member required for efficient translocation of protein precursors across the ER membrane	70.12
YNL080C	Protein involved in N-glycosylation; deletion mutation confers sensitivity to exidative stress and shows synthetic lethality with mutations in the spindle checkpoint genes BUB3 and MAD1	66.96
RIM13	Sporulation protein involved in proteolytic processing of Rim101p	66.01
OST6	Oligosaccharyltransferase subunit of 37 kDa	61.67
YDR533C	Possible chaperone and cysteine protease with similarity to E. coli Hsp31	61.55
PNG1	Conserved peptide N-glycanase required for deglycosylation of misfolded glycoproteins during proteasome-dependent degradation	60.36
APG12	Protein conjugated to Apg5p, involved in autophagy and cytoplasm-to-vacuole protein targeting pathway	56.85
UBA3	Rub1-activating enzyme, similar to ubiquitin-activating E1-like proteins	50.12
E. Cell wall/cell membrane biogenesis		
ERG5	Cytochrome P450	78.72
LAS21	Protein required for addition of a side chain to the glycosylphospatidylinositol (GPI) core structure	78.04
SKN1	Glucan synthase subunit involved in synthesis of beta-1,6-glucan	77.86
IPT1	Inositolphosphotransferase 1, required for synthesis of mannosyl diphosphorylinositol ceramide (M(IP)2C) the most abundant and complex sphingolipid	77.50
FKS1	Component of beta-1,3-glucan synthase, probably functions as an alternate subunit with Gsc2p with which it has strong similarity	62.62
YPK1	Serine/threonine protein kinase with similarity to protein kinase C, possibly involved in a sphingolipid-mediated signaling pathway	62.26
SUR1	Protein required for the synthesis of mannosylated sphingolipids	61.01
LCB3	Sphingoid base-phosphate phosphatase, putative regulator of sphingolipid metabolism and stress response	59.58
ERG3	C-5 sterol desaturase, an iron, non-heme, oxygen-requiring enzyme of the ergosterol biosynthesis pathway	57.26

F.Transcription		
SWI6	Transcription factor that participates in the SBF complex (Swi4p-Swi6p) for regulation at the cell cycle box (CCB) and in the MBF complex (Mbp1p-Swi6p) for regulation at the Mlu1 cell cycle box (MCB)	74.82
SRB9	Component of RNA polymerase II holoenzyme and Kornberg's mediator (SRB) subcomplex	72.38
ARC1	Cofactor for methionyl- and glutamyl-tRNA synthetases and G4 quadruplex nucleic acid binding protein	68.69
YPL101W	Component of NuA3 histone acetyltransferase complex	58.27
MFT1	Targeting factor for mitochondrial precursor proteins, member of a family of transmembrane transition metal transporters	55.24
CAF4	WD40 repeat-containing protein associated with the CCR4-NOT complex, interacts in a Ccr4p-dependent manner with Ssn2p; also interacts with Fis1p, Mdv1p and Dnm1p and plays a role in mitochondrial fission	54.11
LEU3	Transcription factor regulating genes of branched chain amino acid biosynthesis pathways, acts as both a repressor and an inducer	53.75
G. RNA processing and modification		
NCL1	Methyltransferase that methylates cytidine to 5-methyl-cytidine (m5C) at several positions in different tRNAs, has similarity to human proliferating cell nucleolar antigen (p120), a proliferation antigen of human tumors	90.54
NSR1	Nucleolar protein involved in processing 20S to 18S rRNA, has 2 RNA recognition (RRM) domains and is member of GAR (glycine/arginine-rich repeats) family of proteins	90.24
FYV7	Essential protein required for maturation of 18S rRNA;	75.89
RNH1	Ribonuclease H, endonuclease that degrades RNA in RNA-DNA hybrids	68.99
PRS3	Phosphoribosylpyrophosphate synthetase (ribose-phosphate pyrophosphokinase II); component of yeast 20S proteasome, with a role in cell cycle regulation	68.79
BUD23	Protein with similarity to rat methylglycine transferase	57.61
H. Unknown function		
YDR525W	Protein of unknown function, has similarity to Ydr525W-Ap and Ydl123p	85.48
YDR442W	Protein of unknown function	82.95
YHR126C	Protein with similarity to members of the Pir1p/Hsp150p/Pir3p family	81.31
KRE24	Protein of unknown function	75.71
YLR454W	Protein of unknown function	74.82
YLR322W	Protein of unknown function	73.57
FYV11	Protein of unknown function	70.24
YBL094C	Protein with weak similarity to *Neurospora crassa* chitin synthase, may not be an expressed ORF	68.99
YDR455C	Protein of unknown function	66.61
YFL015C	Protein of unknown function	65.65
YLL020C	Protein of unknown function	62.38
TOS5	Protein of unknown function	59.35

YLR374C	Protein of unknown function	58.63
YML095C-A	Protein of unknown function, questionable ORF	55.29
YHR140W	Protein of unknown function, has 6 potential transmembrane segments	38.39
I. Others		
FLO1	Flocculin, cell wall protein involved in flocculation, member of the Flo1p family of flocculation proteins	86.13
POS5	Protein involved in sensitivity to peroxide, has similarity to Utr1p and Yel041p	59.52
BIO2	Biotin synthetase, catalyzes insertion of a sulfur atom between two carbon atoms of dethiobiotin in the last step of the biotin synthesis pathway	51.46

Supplementary Table 2 (S2): Highly sensitive yeast deletion mutants to ZnONPs.

Gene name	Function/Description	% Colony size reduction
A. Transmembrane and membrane transport		
PKR1	V-ATPase assembly factor, functions with other V-ATPase assembly factors in the ER	80.70
FEN2	Plasma membrane H+-pantothenate symporter	79.30
GUP1	Plasma membrane protein involved in remodeling GPI anchors	81.20
ERG2	C-8 sterol isomerase, catalyzes isomerization at an intermediate step in ergosterol biosynthesis	78.60
BUD18/ERG28	Endoplasmic reticulum membrane protein, may facilitate protein-protein interactions between the Erg26p dehydrogenase and the Erg27p 3-ketoreductase	83.40
ARG82	Inositol polyphosphate multikinase (IPMK), also has diphosphoinositol polyphosphate synthase activity	85.20
ERD1	Predicted membrane protein required for the retention of lumenal endoplasmic reticulum proteins	88.10
YLR386W/VAC14	Involved in synthesis of phosphatidylinositol 3,5-bisphosphate, in control of trafficking of some proteins to the vacuole lumen	69.80
YBR246W/RRT2	Involved in endosomal recycling; forms complex with Rtt10p that functions in retromer-mediated pathway for recycling internalized cell-surface proteins	86.40
VPS65	Dubious open reading frame, unlikely to encode a protein; not conserved in closely related *Saccharomyces* species	77.10
CCZ1	Protein involved in vacuolar assembly, essential for autophagy and the cytoplasm-to-vacuole pathway	80.10
B. Ion homeostasis and transport		
CCC2	Cu(+2)-transporting P-type ATPase, required for export of copper from the cytosol into an extracytosolic compartment	74.20
FTR1	High affinity iron permease involved in the transport of iron across the plasma membrane	79.50
GEF1	Voltage-gated chloride channel localized to the golgi, the endosomal system, and plasma membrane, and involved in cation homeostasis	84.60
NHA1	Na+/H+ antiporter involved in sodium and potassium efflux through the plasma membrane	72.90
SPF1	P-type ATPase, ion transporter of the ER membrane involved in ER function and Ca2+ homeostasis	74.20
VPH1	Subunit a of vacuolar-ATPase V0 domain, one of two isoforms (Vph1p and Stv1p)	91.50
AGP3	Low-affinity amino acid permease, may act to supply the cell with amino acids as nitrogen source in nitrogen-poor conditions	100

YMR166C	Predicted transporter of the mitochondrial inner membrane	100
FYV5	Protein involved in regulation of the mating pathway; binds with Matalpha2p to promoters of haploid-specific genes	77.10
SOD1	Cytosolic copper-zinc superoxide dismutase	82.50
C. Transcription and RNA processing		
NAM8	RNA binding protein, component of the U1 snRNP protein	63.20
MGA2	ER membrane protein involved in regulation of OLE1 transcription, acts with homolog Spt23p	72.50
PHO2	Homeobox transcription factor; regulatory targets include genes involved in phosphate metabolism	71.90
PHO4	Basic helix-loop-helix (bHLH) transcription factor of the myc-family; activates transcription cooperatively with Pho2p in response to phosphate limitation	66.30
POP2	RNase of the DEDD superfamily, subunit of the Ccr4-Not complex that mediates 3' to 5' mRNA deadenylation	73.20
DBR1	RNA lariat debranching enzyme, involved in intron turnover; required for efficient Ty1 transposition	55.20
D. Cell wall organization or biogenesis		
DFG5	Putative mannosidase, essential glycosylphosphatidylinositol (GPI)-anchored membrane protein required for cell wall biogenesis in bud formation	90.60
BCK1	Mitogen-activated protein (MAP) kinase kinase kinase acting in the protein kinase C signaling pathway, which controls cell integrity	96.90
HOC1	Alpha-1,6-mannosyltransferase involved in cell wall mannan biosynthesis	88.20
KRE6	Type II integral membrane protein required for beta-1,6 glucan biosynthesis	81.90
ROM2	GDP/GTP exchange factor (GEF) for Rho1p and Rho2p	89.50
SLT2	Serine/threonine MAP kinase; involved in regulating maintenance of cell wall integrity	94.70
YLL005C/SPO75	Meiosis-specific protein of unknown function; required for spore wall formation during sporulation	79.10
E. Cell cycle regulation		
PPH3	Catalytic subunit of protein phosphatase PP4 complex; regulates recovery from the DNA damage checkpoint and also the gene	63.50
SPC72	Component of the cytoplasmic Tub4p (gamma-tubulin) complex, binds spindle pole bodies and links them to microtubules	78.90
PHO81	Cyclin-dependent kinase (CDK) inhibitor, regulates Pho80p-Pho85p and Pcl7p-Pho85p cyclin-CDK complexes in response to phosphate levels	85.10
SCP160	Essential RNA-binding G protein effector of mating response pathway, mainly associated with nuclear envelope and ER,	73.90
URM1	Ubiquitin-like protein involved in thiolation of cytoplasmic tRNAs; receives sulfur from the E1-like enzyme Uba4p and transfers it to tRNA	52.30
G. DNA recombination/repair		
RNR3	Minor isoform of the large subunit of ribonucleotide-diphosphate reductase; regulated by DNA replication and DNA damage checkpoint pathways	80.20

SML1	Ribonucleotide reductase inhibitor involved in regulating dNTP production; regulated by Mec1p and Rad53p during DNA damage and S phase	71.20
BUD32	Protein kinase, component of the EKC/KEOPS complex required for t6A tRNA modification and may have roles in telomere maintenance and transcription	70.10
MET18	DNA repair and TFIIH regulator, required for both nucleotide excision repair (NER) and RNA polymerase II (RNAP II) transcription; involved in telomere maintenance	77.30
YDR433W (KRE22)	Response to DNA damage	52.50
H. Signaling		
YHL023C/NPR3	ubunit of SEACIT, a subcomplex of the SEA complex that acts as a GTPase-activating protein (GAP) to negatively regulates signaling	75.50
DUN1	Cell-cycle checkpoint serine-threonine kinase required for DNA damage-induced transcription of certain target genes	55.30
RAM1	Beta subunit of the CAAX farnesyltransferase (FTase) that prenylates the a-factor mating pheromone and Ras proteins	71.90
CLA4	Cdc42p-activated signal transducing kinase of the PAK family, along with Ste20p and Skm1p; involved in septin ring assembly, vacuole inheritance, cytokinesis, sterol uptake regulation	80.40
I. Others		
YPR100W/MPRL51	Mitochondrial ribosomal protein of the large subunit	81.20
HOM6	Homoserine dehydrogenase (L-homoserine:NADP oxidoreductase), enzyme has nucleotide-binding, dimerization and catalytic regions	62.40
ILV1	Threonine deaminase, catalyzes the first step in isoleucine biosynthesis; expression is under general amino acid control	71.30
PRO2	Gamma-glutamyl phosphate reductase, catalyzes the second step in proline biosynthesis	61.50
J. Unknown function		
MTC7 (YEL033W)	Unknown function	51.30
YIL014C-A (YIL015C-A)	Unknown function	72.50
YML020W	Unknown function	61.60
YNR073C	Unknown function	62.30
YOR291W	Unknown function	69.80
YLR412W	Unknown function	71.60

Supplementary Table 3 (S3): Highly sensitive yeast deletion mutants to AgNPs.

Gene name	Function/Description	% Colony size reduction
A. Transcription and RNA processing		
GAL80	Transcriptional regulator involved in the repression of GAL genes in the absence of galactose	76.70
HMO1	Chromatin associated high mobility group (HMG) family member involved in genome maintenance;	73.50
HOS1	Class I histone deacetylase (HDAC) family member that deacetylates Smc3p on lysine residues at anaphase onset	63.50
NUT1	Component of the RNA polymerase II mediator complex	58.90
RLR1/THO2	Subunit of the THO complex, which is required for efficient transcription elongation and involved in transcriptional elongation-associated recombination	72.70
SPT4	Protein involved in the regulating Pol I and Pol II transcription, pre-mRNA processing	70.20
SSN3	Cyclin-dependent protein kinase, component of RNA polymerase II holoenzyme; involved in phosphorylation of the RNA polymerase II	60.80
STP2	Response to signals from the SPS sensor system for external amino acids;	100.00
SWI4	DNA binding component of the SBF complex (Swi4p-Swi6p), a transcriptional activator	100.00
TEC1	Transcription factor targeting filamentation genes and Ty1 expressio	73.00
THP2	Subunit of the THO complex, which connects transcription elongation and mitotic recombinatio	58.2
PTC1/YDL006W	Type 2C protein phosphatase (PP2C); dephosphorylates Hog1p, inactivating osmosensing MAPK cascade; involved in Fus3p activation during pheromone response	79.20
YJR084W	Protein that forms a complex with Thp3p; may have a role in transcription elongation and/or mRNA splicing	86.10
CTK1	Catalytic (alpha) subunit of C-terminal domain kinase I (CTDK-I); phosphorylates both RNA pol II subunit Rpo21p	73.40
LOS1	Nuclear pore protein involved in nuclear export of pre-tRNA and in re-export of mature tRNAs	65.50
B. Cellular respiration and mitochondrion organization		
IDH1	Subunit of mitochondrial NAD(+)-dependent isocitrate dehydrogenase,	77.20
SOD1	Cytosolic copper-zinc superoxide dismutase; some mutations are analogous to those that cause ALS	79.90
ETR1/YBR026C	2-enoyl thioester reductase, member of the medium chain dehydrogenase/reductase family;	74.50
AAC3/ YBR085W	Mitochondrial inner membrane ADP/ATP translocator, exchanges cytosolic ADP for mitochondrially synthesized ATP	68.80
GDS1	Protein required for growth on glycerol, encountered in mitochondria	65.50
KGD1/YIL125W	Subunit of the mitochondrial alpha-ketoglutarate dehydrogenase complex; catalyzes a key step in the tricarboxylic acid (TCA) cycle,	96.80
AAC1 YMR056C	Mitochondrial inner membrane ADP/ATP translocator, exchanges cytosolic ADP for mitochondrially synthesized ATP; phosphorylated	70.70

COQ10/YOL008W	Coenzyme Q (ubiquinone) binding protein	65.70
PDA1	E1 alpha subunit of the pyruvate dehydrogenase (PDH) complex	70.40
INA22/YIR024C	non-tagged protein is detected in highly purified mitochondria in high-throughput	55.00
PCP1/YGR101W	Mitochondrial serine protease; required for the processing of various mitochondrial proteins and maintenance of mitochondrial DNA	61.90
AIM17/YHL021C	protein is detected in highly purified mitochondria in high-throughput studies	78.00
YPR097W	Protein that contains a Phox homology (PX) domain and binds phosphoinositide	89.10
YLH47/YPR125W	Mitochondrial inner membrane protein exposed to the mitochondrial matrix	76.50
ILM1/YJR118C	Protein involved in mitochondrial DNA maintenance;	61.90
C. Endocytosis and vesicular transport		
YPK9/YOR291W	Vacuolar protein with a possible role in sequestering heavy metals	83.70
PTK2	Putative serine/threonine protein kinase involved in regulation of ion transport across plasma membrane	96.50
INP52/YNL106C	Polyphosphatidylinositol phosphatase, dephosphorylates a number of phosphatidylinositols (PIs) to PI; involved in endocytosis	78.00
SLA1	endocytosis; found in the nucleus and cell cortex; has 3 SH3	58.00
LAA1/ YJL207C	Golgi apparatus; involved in TGN-endosome transport; physically interacts with AP-1;	86.60
ENT3	Protein containing an N-terminal epsin-like domain involved in clathrin recruitment and traffic between the Golgi and endosomes	56.20
APM4	Mu2-like subunit of the clathrin associated protein complex (AP-2); involved in vesicle transport	86.00
UBP3	Ubiquitin-specific protease involved in transport and osmotic response; co-regulates anterograde and retrograde transport between the ER and Golgi;	100.00
APL2	Beta-adaptin, large subunit of the clathrin-associated protein (AP-1) complex; binds clathrin	78.50
SLM4/YBR077C	Component of the EGO complex, which is involved in the regulation of microautophagy	91.00
SPF1/YEL031W	P-type ATPase, ion transporter of the ER membrane involved in ER function and Ca2+ homeostasis	93.90
YPK1	Receptor-mediated endocytosis and sphingolipid-mediated and cell integrity signaling pathways	67.50
APL1	Beta-adaptin, large subunit of the clathrin associated protein complex (AP-2); involved in vesicle mediated transport	61.80
D. Translationand protein processing		
UBA3	Protein that acts together with Ula1p to activate Rub1p before its conjugation to proteins	94.30
ICP55/YER078C	Mitochondrial aminopeptidase; cleaves the N termini of at least 38 imported proteins after cleavage by the mitochondrial processing peptidase	66.00
DDI1	DNA damage-inducible v-SNARE binding protein with a role in suppression of protein secretion	78.00

MCA1/YOR197W	Ca^{2+}-dependent cysteine protease; may cleave specific substrates during the stress response	56.80
RAM1	Beta subunit of the CAAX farnesyltransferase (FTase) that prenylates the a-factor mating pheromone and Ras proteins	74.70
MRPL51/YPR100W	Mitochondrial ribosomal protein of the large subunit	84.60
MPRL28/YDR462W	Mitochondrial ribosomal protein of the large subunit	72.90
RPL8B	Ribosomal protein L4 of the large (60S) ribosomal subunit	94.40
RPL29	Protein component of the large (60S) ribosomal subunit, has similarity to rat L29 ribosomal protein	50.00
GAL83/YER027C	One of three possible beta-subunits of the Snf1 kinase complex; allows nuclear localization of the Snf1 kinase complex	50.00
TOS3	Protein kinase, related to and functionally redundant with Elm1p and Sak1p for the phosphorylation and activation of Snf1p	76.20
E. Regulation of cell cycle		
SEM1	Component of the lid subcomplex of the regulatory subunit of the 26S proteasome; involved in mRNA export	77.20
CIK1	Kinesin-associated protein required for both karyogamy and mitotic spindle organization	52.80
BUB1/YGR188C	Protein kinase involved in the cell cycle checkpoint into anaphase	50.00
AOR1	Component of the SWR1 complex; complex exchanges histone variant H2AZ (Htz1p) for chromatin-bound histone H2A	43.40
RTS1/YOR014W	B-type regulatory subunit of protein phosphatase 2A (PP2A)	50.00
OPY2/YPR075C	Integral membrane protein that acts as a membrane anchor for Ste50p; involved in the signaling branch of the high-osmolarity glycerol (HOG) pathway and as a regulator of the filamentous growth pathway	71.30
CTF8	Subunit of a complex with Ctf18p that shares some subunits with Replication Factor C and is required for sister chromatid cohesion	60.40
BEM2	Rho GTPase activating protein (RhoGAP) involved in the control of cytoskeleton organization and cellular morphogenesis	66.30
F. DNA damage and stress response		
GPX2	Phospholipid hydroperoxide glutathione peroxidase induced by glucose starvation that protects cells from phospholipid hydroperoxides and nonphospholipid peroxides during oxidative stress	82.60
BEM1	Protein containing SH3-domains, involved in establishing cell polarity and morphogenesi	66.30
TPS1	Synthase subunit of trehalose-6-phosphate synthase/phosphatase complex	83.30
IRC21/YMR073C	Protein involved in resistance to carboplatin and cisplatin	88.90
ECM4/YKR076W	Omega class glutathione transferase; not essential	81.10
MET18	DNA repair and TFIIH regulator, required for both nucleotide excision repair (NER) and RNA polymerase II (RNAP II) transcription	78.70
SLX4	Endonuclease involved in processing DNA during recombination and repair	70.50
ARP8	Nuclear actin-related protein involved in chromatin remodeling	50.00

VID31/DEF1	RNAPII degradation factor; forms a complex with Rad26p in chromatin, enables ubiquitination and proteolysis of RNAPII	78.70
MRC1/YCL061C	S-phase checkpoint protein required for DNA replication	41.60
GRX4/YER174C	Hydroperoxide and superoxide-radical responsive glutathione-dependent oxidoreductase	64.20
DOT1/YDR440W	Nucleosomal histone H3-Lys79 methylase; methylation is required for telomeric silencing	71.30
G. Metabolic processes		
ARO1	Pentafunctional arom protein, catalyzes steps 2 through 6 in the biosynthesis of chorismate	98.10
ARO2	Bifunctional chorismate synthase and flavin reductase	50.00
ARO7	Chorismate mutase, catalyzes the conversion of chorismate to prephenate	44.80
URA2	Bifunctional carbamoylphosphate synthetase, biosynthesis of pyrimidines	72.50
LPD1/YFL018C	Dihydrolipoamide dehydrogenase, the lipoamide dehydrogenase component (E3) of the pyruvate dehydrogenase	48.80
DIE2	Dolichyl-phosphoglucose-dependent alpha-1,2 glucosyltransferase of the ER	57.60
RBK1	Putative ribokinase	50.90
LIP5	Protein involved in biosynthesis of the coenzyme lipoic acid, has similarity to *E. coli* lipoic acid synthase	47.10
OPI3	Phospholipid methyltransferase (methylene-fatty-acyl-phospholipid synthase)	98.90
TES1	Peroxisomal acyl-CoA thioesterase likely to be involved in fatty acid oxidation rather than fatty acid synthesis	68.80
H. Others		
EIS1/YMR031C	Component of the eisosome that is required for proper eisosome assembly	80.40
HOC1	Alpha-1,6-mannosyltransferase involved in cell wall mannan biosynthesis	54.50
ECM23/SRD2	Non-essential protein of unconfirmed function; affects pre-rRNA processing	81.20
SMI1/YGR229C	Protein involved in the regulation of cell wall synthesis	57.50
CHS3	Chitin synthase III, catalyzes the transfer of N-acetylglucosamine (GlcNAc) to chitin	72.50
ECM4/YKR076W	Omega class glutathione transferase	62.10
TIP1	Major cell wall mannoprotein with possible lipase activity	63.80
MOG1	Conserved nuclear protein that interacts with GTP-Gsp1p, which is a Ran homolog of the Ras GTPase family	63.00
KIN82	Putative serine/threonine protein kinase implicated in the regulation of phospholipid asymmetry	79.20
I. Unkown process/function		
DSF2/YBR007C	Unknown function	72.90
YCR100C	Unknown function	42.90
JIP4/YDR475C	Unknown function	33.50

Supplementary Table 4 (S4): Highly sensitive E. coli deletion mutants to nisin-CA.

Gene name	Function/Description	Colony size reduction %
	A. Cell wall/membrane/envelope biogenesis	
amiA	N-acetylmuramoyl-l-alanine amidase I	100
rffC	TDP-fucosamine acetyltransferase; needed for ECA (enterobacterial common antigen) synthesis	100
hlpA	periplasmic chaperone	100
rffT	TDP-Fuc4NAc:lipidIIFuc4NAc transferase	100
tolC	Outer membrane factor (OMF) of tripartite efflux pumps; channel-tunnel spanning the outer membrane and periplasm; homotrimeric; ColE1 tolerance	93.40
amiC	N-acetylmuramoyl-L-alanine amidase	89.00
rffH	glucose-1-phosphate thymidylyltransferase	87.30
rffA	TDP-4-oxo-6-deoxy-D-glucose transaminase	74.50
rfaD	ADP-L-glycero-D-manno-heptose-6-epimerase; heat-inducible, LPS; allows high-temperature growth	69.00
rfaC	ADP-heptose:LPS heptosyl transferase I	62.30
spr	mutational suppressor of prc thermosensitivity, outer membrane lipoprotein	61.20
	B. Cell cycle, DNA replication, recombination and repair	
envC	activator of AmiB,C murein hydrolases, septal ring factor	98.70
parC	DNA topoisomerase IV, subunit A	98.40
damX	Cell division protein, binds septal ring	93.80
dnaQ	DNA polymerase III epsilon subunit	81.40
yraN	conserved protein, UPF0102 family	81.30
tatD	quality control of Tat-exported FeS proteins; Mg-dependent cytoplasmic DNase	77.40
gidA	5-methylaminomethyl-2-thiouridine modification at tRNA U34	76.20
intB	Pseudogene reconstruction, P4-like integrase	68.20
dnaG	DNA primase	64.70
	C. Carbohydrate transport and metabolism	
rffE	UDP-N-acetyl glucosamine-2-epimerase	85.90
fsaA	Fructose-6-phosphate aldolase A	78.20
yciM	TPR-repeats-containing protein, function unknown	75.10
ycjR	sugar isomerase homolog	72.90
ycdR	biofilm adhesin polysaccharide PGA export lipoprotein with a polysaccharide deacetylase activity needed for export	71.40
fruB	fused fructose-specific PTS enzymes: IIAcomponent/HPr component	66.20
yphD	predicted sugar transporter subunit: membrane component of ABC superfamily	61.40

rfaP	Lipopolysaccharide kinase; LPS core biosynthesis; phosphorylation of core	61.30
D. Aminoacids and protein synthesis, protein processing		
tatB	TatABCE protein translocation system subunit	95.60
rsgA	Ribosome-stimulated GTPase, 30S subunit assemby	93.60
ppiB	Periplasmic peptidylprolyl-cis-trans-isomerase B, rotamase	84.70
tatA	TatABCE protein translocation system subunit	83.60
yhbC	ribosome maturation factor for 30S subunits	75.30
smpA	Lipoprotein stabilizer of BamABCDE OM biogenesis complex	71.80
ybaS	Glutaminase, l-glutamine catabolism	68.10
dsbG	Thiol:disulfide interchange protein, periplasmic; molecular chaperone; multicopy resistance to DTT	63.80
E. Ion transport and intracellular trafficking		
tolR	membrane spanning protein in TolA-TolQ-TolR complex	100.0
tolB	periplasmic protein	99.20
tatC	TatABCE protein translocation system subunit	98.30
trkA	NAD-binding component of TrK potassium transporter	67.10
modE	DNA-binding transcriptional repressor for the molybdenum transport operon modABC	64.90
F. General function prediction only		
tehB	Tellurite, selenium resistance protein, probable methyltransferase; confers multidrug resistance in multicopy	84.80
ybhL	inner membrane protein, UPF0005 family	78.40
yhbG	lipopolysaccharide export ABC transporter ATP-binding protein of the LptBFGC export complex	73.50
mviM	predicted oxidoreductase with NAD(P)-binding Rossmann-fold domain	70.30
yceG	predicted aminodeoxychorismate lyase, Septation protein	60.60
G. Lipid transport and metabolism		
ybgC	Acyl-CoA thioesterase, involved in phospholipid metabolism; binds ACP; acyl-ACP could be native substrate	89.3
plsX	probable phosphate acyltransferase	83.3
fabF	3-oxoacyl-[acyl-carrier-protein] synthase II	63.9
H. Others		
yiaK	L-dehydroascorbate (2,3-diketo-L-gulonate) reductase, NADH-dependent	87.0
rsxB	electron transport complex protein, iron-sulfur protein, required for the reduction of SoxR	75.30
yhbC	ribosome maturation factor for 30S subunits	74.70
dinF	DNA-damage-inducible SOS response protein	71.40
smpA	Lipoprotein stabilizer of BamABCDE OM biogenesis complex	70.80
I. Unknown function		
ychJ	UPF0225 family proten, function unknown	89.30
yjcF	Pentapeptide repeat protein	81.40
ymgD	predicted protein	78.90
yoaD	Predicted cyclic-di-GMP phosphodiesterase	76.90
ygaC	Function unknown; Fur regulon	76.80

ydcX	conserved protein, DUF2566 family	75.80
yidQ	conserved outer membrane protein	72.00
ybgO	predicted fimbrial-like adhesin protein	71.40
ycfQ	predicted DNA-binding transcriptional regulator	70.90
ybaY	outer membrane lipoprotein	68.40
yqiJ	Inner membrane protein, DUF1449 family	67.10
ylcG	expressed protein, DLP12 prophage	63.50

Supplementary Table 5 (S5): Highly sensitive E. coli deletion mutants to bifidobacterial fermented supernatant

Gene name	Function/description	% Colony size reduction
A. Carbohydrate transport and metabolism		
bglX	beta-D-glucoside glucohydrolase, periplasmic	68.90
hyi	hydroxypyruvate isomerase	68.10
idnK	D-gluconate kinase, thermosensitive	71.40
melA	alpha-galactosidase, NAD(P)-binding	80.10
nagZ	beta N-acetyl-glucosaminidase	74.40
ulaD	3-keto-L-gulonate 6-phosphate decarboxylase	70.50
ulaE	L-xylulose 5-phosphate 3-epimerase	82.50
yciM	conserved protein	71.20
yicM	predicted transporter	68.10
yihQ	alpha-glucosidase	79.20
galE	UDP-galactose-4-epimerase	82.40
yihR	predicted aldose-1-epimerase	71.50
yicL	predicted inner membrane protein	77.30
hsrA	predicted multidrug or homocysteine efflux system	84.80
setC	predicted sugar efflux system	70.50
B. Ion transporta and intracellular trafficking		
amtB	ammonium transporter	74.70
cyaY	frataxin, iron-binding and oxidizing protein	81.30
fepG	iron-enterobactin transporter subunit; membrane component of ABC superfamily	71.60
fur	DNA-binding transcriptional dual regulator of siderophore biosynthesis and transport	85.00
yrbG	predicted calcium/sodium:proton antiporter	71.40
exbD	membrane spanning protein in TonB-ExbB-ExbD complex	66.80
tatC	TatABCE protein translocation system subunit	74.40
tolB	TatABCE protein translocation system subunit	92.70
tolR	membrane spanning protein in TolA-TolQ-TolR complex	86.50
panF	pantothenate:sodium symporter	65.60
tesB	acyl-CoA thioesterase II	73.70
yciK	predicted oxoacyl-(acyl carrier protein) reductase, EmrKY-TolC system	86.30
C. Energy production and conversion		
cybB	cytochrome b561	89.40
cydB	cytochrome d terminal oxidase, subunit II	89.60
fixC	predicted oxidoreductase with FAD/NAD(P)-binding domain	84.00
hybO	hydrogenase 2, small subunit	71.10

narJ	molybdenum-cofactor-assembly chaperone subunit (delta subunit) of nitrate reductase 1	81.50
nuoC	NADH:ubiquinone oxidoreductase, chain C,D	73.40
rsxD	predicted inner membrane oxidoreductase	81.70
torY	TMAO reductase III (TorYZ), cytochrome c-type subunit	77.30
ynfE	oxidoreductase subunit	66.60
hcaD	phenylpropionate dioxygenase, ferredoxin reductase subunit	68.60
hyfJ	predicted processing element hydrogenase 4	70.00
D. Cell wall/membrane/envelope biogenesis		
galU	glucose-1-phosphate uridylyltransferase	91.40
rfaE	fused heptose 7-phosphate kinase; heptose 1-phosphate adenyltransferase	96.50
rhsE	rhsE element core protein RshE	81.00
tonB	membrane spanning protein in TonB-ExbB-ExbD complex	89.80
dcrB	periplasmic protein	95.40
ytfG	NAD(P)H:quinone oxidoreductase	75.00
ypjA	adhesin-like autotransporter	63.30
ytfL	predicted inner membrane protein	81.70
E. DNA replication, recombination and repair		
intR	Rac prophage; integrase	78.40
mutH	methyl-directed mismatch repair protein	69.20
sbcD	exonuclease, dsDNA, ATP-dependent	87.00
seqA	regulatory protein for replication initiation	76.40
uvrB	excinulease of nucleotide excision repair, DNA damage recognition component	68.70
xerD	site-specific tyrosine recombinase	89.30
F. Transcription		
ydcQ	predicted DNA-binding transcriptional regulator	95.20
rpoS	RNA polymerase, sigma S (sigma 38) factor	93.20
ytfA	predicted transcriptional regulator	65.80
yfeD	predicted DNA-binding transcriptional regulator	74.90
fhlA	DNA-binding transcriptional activator	76.60
G. Amino acid transport and metabolism		
gmhB	D,D-heptose 1,7-bisphosphate phosphatase	79.30
metL	fused aspartokinase II; homoserine dehydrogenase II	59.50
potD	polyamine transporter subunit; periplasmic-binding component of ABC superfamily	83.30
carB	carbamoyl-phosphate synthase large subunit	82.60
H. Nucleotide transport and metabolism		
yhcM	conserved protein with nucleoside triphosphate hydrolase domain	77.00
guaB	IMP dehydrogenase	82.20
rihA	ribonucleoside hydrolase 1	82.60
tdk	thymidine kinase/deoxyuridine kinase	82.30

I. Others		
gidA	glucose-inhibited cell-division protein	76.10
envC	protease with a role in cell division	79.90
flgF	flagellar component of cell-proximal portion of basal-body rod	84.20
mdlA	fused predicted multidrug transporter subunits of ABC superfamily: ATP-binding components	76.30
kdsC	3-deoxy-D-manno-octulosonate 8-phosphate phosphatase	82.80
nlpI	conserved protein	73.10
rssA	conserved protein	77.10
tam	trans-aconitate methyltransferase	81.40
wzxC	colanic acid exporter	66.30
yjgX	KpLE2 phage-like element; predicted protein, middle fragment (pseudogene)	78.60
yrbD	predicted ABC-type organic solvent transporter	73.30
yrbE	predicted toluene transporter subunit: membrane component of ABC superfamily	89.50
yrbF	predicted toluene transporter subunit: ATP-binding component of ABC superfamily	90.50
apaH	diadenosine tetraphosphatase	98.30
yddV	predicted diguanylate cyclase	89.20
glnE	fused deadenylyltransferase; adenylyltransferase for glutamine synthetase	70.60
rbfA	30s ribosome binding factor	61.00
rpmG	50S ribosomal subunit protein L33	76.30
J. Unknown		
slyX	conserved protein	79.30
yqfB	conserved protein	72.90
gntY	predicted gluconate transport associated protein	66.70
racC	Rac prophage; predicted protein	62.70
yccE	predicted protein	71.10
ydcO	predicted benzoate transporter	76.30
yfbO	predicted protein	73.40
yfjS	CP4-57 prophage; predicted protein	62.40
yicH	conserved protein	70.30
yjiS	conserved protein	71.70
ymdE	predicted protein (pseudogene)	78.80
yneI	predicted aldehyde dehydrogenase	66.60
yohO	predicted protein	83.50
ypjB	predicted protein	64.40
yqgE	predicted protein	70.20
ytfK	conserved protein	70.30

References

Adams, P. G., Lamoureux, L., Swingle, K. L., Mukundan, H., and Montaño, G. A. 2014. Lipopolysaccharide-Induced Dynamic Lipid Membrane Reorganization: Tubules, Perforations, and Stacks. Biophysical Journal, 106(11): 2395–2407

Alakomi, H. L., Skyttä, E., Saarela, M., Mattila-Sandholm, T., Latva-Kala, K., Helander, I.M. 2000. Lactic acid permeabilizes gram-negative bacteria by disrupting the outer membrane. Applied and Environmental Microbiology, 66(5): 2001-5

Alamgir, M. D., Erukova, V., Jessulat, M., Azizi, A., and Golshani, A. 2010. Chemical-genetic profile analysis of five inhibitory compounds in yeast. BMC Chemical Biology, 10, 1-15

Alamgir, M., Eroukova, V., Jessulat, M., Xu, J., and Golshani, A., 2008. Chemical-genetic profile analysis in yeast suggests that a previously uncharacterized open reading frame, YBR261C, affects protein synthesis. BMC Genomics 9: 583, 1-13.

Alekshun, M. N., Kim, Y. S., and Levy, S. B. 2000. Mutational analysis of MarR, the negative regulator of marRAB expression in *Escherichia coli*, suggests the presence of two regions required for DNA binding. Molecular Microbiology, 35(6), 1394±1404

Allan, C. R., and Hadwiger, L. A., 1979. The fungicidal effect of chitosan on fungi of varying cell wall composition. Experimental Mycology 3, 285-287.

Amsterdam D. 1996. Susceptibility testing of antimicrobials in liquid media*. in* Antibiotics in laboratory medicine*, Ed.* Lorian V. *(*Williams & Wilkins*,* Baltimore, Md*),* 4th ed. *pp* 52–11

Anand, S.K., Srinivasan, R.A., Rao, L.K. 1985. Antibacterial activity associated with *Bifidobacterium bifidum-II*. Cult Dairy Production Journal, 2 :21–23

Anderson, J.B. 2005. Evolution of antifungal-drug resistance: mechanisms and pathogen fitness. Nature Reviews Microbiology 3, 547-556

AshRani, P.V., Low Kah Mun, G., Hande, M.P., and Valiyaveettil, S. 2009. Citotoxicity and genotoxocity of silver nanoparticles in human cells. American Chemical Society Nano (2): 279-290.

Baba, T., Ara, T., Hasegawa, M., Takai, Y., Okumura, Y., Baba, M., Datsenko, K. A., Tomita, M., Wanner, B. L., and Mori, H. 2006. Construction of *Escherichia coli* K-12 in-frame, single-gene knockout mutants: the Keio collection. Molecular Systems Biology, 1-11.

Babu, M., Musso, G., Díaz-Mejía, J. J., Butland, G., Grenblatt, J. F., and Emili, A.
2009. Systems-level approaches for identifying and analyzing genetic interaction networks in *Escherichia coli* and extensions to other prokaryotes. Molecular Systems Biology, 5: 1439–1455

Babu, M., Díaz-Mejía, J. J., Vlasblom, J., Gagarinova, A., Phanse, S., Graham, C., Youasif, F., Ding, H., Xiong, X., Nazarians-Armavil, A., Alamgir, Md., Ali, M., Pogotuse, O., Pe'er, A., Arnold, R., Michaut, M., Parkinson, J., Golshani, A., Whitfield, C., Wodak, S. J., Moreno-Hagelsieb, G., Greenblatt, J. F., Emili, A. 2011. Genetic Interaction Maps in *Escherichia coli* Reveal Functional Crosstalk among Cell Envelope Biogenesis Pathways. PLoS Genetics, 7(11), e1002377.

Bandow, J. E., Brötz, H., Ole Leichert, L. I., Labischinski, H., and Hecker, M. 2003. Proteomic Approach to Understanding Antibiotic Action. Antimicrobial Agents Chemotherapy, 47(3): 948-955.

Bansal, S., and V. Tandon. 2011. Contribution of mutations in DNA gyrase and topoisomerase IV genes to ciprofloxacin resistance in Escherichia coli clinical isolates. International Journal of Antimicrobial Agents, 37: 253-5

Barnard, F. M., & Maxwell, A. (2001). Interaction between DNA Gyrase and Quinolones: Effects of Alanine Mutations at GyrA Subunit Residues Ser83 and Asp87. Antimicrobial Agents and Chemotherapy, 45(7), 1994–2000.

Bauer, R. and Dicks, L. M. T. 2005. Mode of action of lipid II-targeting lantibiotics. International Journal of Food Microbiology, 101(2): 201-216

Berardis, B., Civitelli, G., Condello, M., Lista, P., Pozzi, R., Arancia, G., Meschini, S. 2010. Exposure to ZnO nanoparticles induces oxidative stress and cytotoxicity in human colon carcinoma cells. Toxicology and Applied Pharmacology 246, 116-127

Berridge, M. V., Herst, P. M., Tan, A. S. 2005. Tetrazolium dyes as tools in cell biology: new insights into their cellular reduction. Biotechnology Annual Review, 11:127-52.

Berridge, M., and Tan, A. S. 1993. Characterization of the cellular reduction of 3-(4,5-dimethylthiazol-2-yl)-2,5-diphenyltetrazolium bromide (MTT): subcellular localization, susbtrate dependence and involvement of mitochondrial electron transport in MTT reduction. Archives of Biochemistry and Biophysics, 303(2): 474-482

Bevilacqua, L., Ovidi, M., Di Mattia, E., Trovatelli, L. D., Canganella, F. 2003. Screening of *Bifidobacterium* strains isolated from human faeces for antagonistic activities against potentially bacterial pathogens. Microbiology Research, 158: 179–185

Bonte, F., and Juliano, R. L. 1986. Interaction of liposomes with serum proteins. Chemistry and Physics of lipids; 40(2); 359-372

Boziaris, I. S., Adams, M. R. 1999. Effect of chelators and nisin produced in situ on inhibition and inactivation of Gram-negative. International Journal of Food Microbiology, 53: 105–113

Bowler, M. W., Montgomery, M. G., Leslie, A. G. W., and Walker, J. 2006. How azide inhibits ATP hydrolysis bythe F-ATPases. Proceedings of the National Academy of Sciences of the United States of America; 103(23); 8646-8649.

Brochado, A., and Typas, A. 2013. High-throughput approaches to understanding gene function and mapping network architecture in bacteria. Current Opinion in Microbiology, 16(2): Pages 199–206

Brooks, B. C., and Brooks, A. E. 2014. Therapeutic strategies to combat antimicrobial resistance. Advanced Drug Delivery Reviews, 78: 14-27.

Brown, T.A. Genomes. 2nd edition. Oxford: Wiley-Liss; 2002. Chapter 13, Genome Replication. Available from: http://www.ncbi.nlm.nih.gov/books/NBK21113/

Brown, E. and Wright, G. 2005. New targets and screening approaches in antimicrobial drug discovery. Chemical Reviews, 105(2), 759-774.

Brul, S., and Coote, P. 1999. Mode of action and microbial resistance mechanisms; Review: Preservative agents in foods. International Journal of Food Microbiology, 50: 1–17

Camps, M., Naukkarinen, J., Johnson, B. P., and Loeb, L. A. 2003. Targeted gene evolution in *Escherichia coli* using a highly error-prone DNA polymerase I. Proceedings of the National Academy of Sciences, 100(17): 9727–9732

Castillo, F. A. Castillo Martinez, Balciunas, E. M., Converti, A., Cotter, P. C., Pinheiro de Souza Oliveira, R. 2013. Bacteriocin production by *Bifidobacterium* spp. A review. Biotechnology Advances 31(4): 482–488

Chai, C., Lee, K-S., Oh, S-W. 2015. Synergistic inhibition of Clostridium difficile with nisin-lysozyme combination treatment. Anaerobe, 34: 24-26

Cheetham, J. J., Murray, J., Ruhkalova, M., Cuccia, L., McAloney, R., Ingold, K. U., Johnston, L. J. 2003. Interaction of synapsin I with membranes. Biochemical and Biophysical Research Communications 309, 823-829.

Cheigh, C-I., Pyun, Y-R. 2005. Nisin, Biosynthesis and its properties. Biotechnology Letters, 27(21): 1641-1648.

Cheikhyoussei, A., Pogori, N., Chen, H., Fengwei, T., Chen, W., Tang, J., and Zhang, H., 2009. Antimicrobial activity and partial characterization of bacteriocin-like inhibitory substances (BLIS) produced by *Bifidobacterium infantis* BCRC 14602. Food Control, 20: 553 -559

Chen, C. Y., Nace, G. W., and Irwin, P. L., 2003. A 6x6 drop plate method for simultaneous colony counting MPN enumeration of *Campylobacter jejuni, Listeria monocytogenes* and *Escherichia coli*. Journal of Microbiology Methods 55, 475-479.

Chen, Y.C., Li, C.L., Hsiao, Y. Y., Duh, Y., Yuan, H.S. 2014. Structure and function of TatD exonuclease in DNA repair. Nucleic Acids Research, 42(16): 10776-85. doi: 10.1093/nar/gku732.

Chirkov, S. N., 2002. The antiviral activity of chitosan (Review). Applied Biochemistry and Microbiology 38, 1-8.

Chollet, R., Chevalier, J., Bryskier, A., & Pagès, J.-M. 2004. The AcrAB-TolC Pump Is Involved in Macrolide Resistance but Not in Telithromycin Efflux in*Enterobacter aerogenes* and *Escherichia coli*. *Antimicrobial Agents and Chemotherapy*, *48*(9), 3621–3624.

Christ, K., Wiedemann, I., Bakowsky, U., Sahi, H-G., Bendas, G. 2007. The role of lipid II in membrane binding of and pore formation by nisin analyzed by two combined biosensor techniques. Biochimica et Biophysica Acta (BBA) - Biomembranes, 1768(3): 694-704

Clarkson, T. W. 1993. Molecular ionic mimicry of toxic metals. Annual Review of Pharmacology and Toxicology, 33: 545-571

Cleveland, J., Monteville, T. J., Nes, I. F., Chikindas, M. L. 2001. Bacteriocins: safe, natural antimicrobials for food preservation. International Journal of Food Microbiology, 71(1): 1-20

CLSI. 2012. Methods for Dilution Antimicrobial Susceptibility Test for Bacteria that Grow Aerobically. Approved Standard –Ninth Edition M07 – A09, In: NCCLS, 2012.

Cohen, E., 1987, Chitin biochemistry: synthesis and inhibition. Annual Review of Entomology 32, 71-92.

Coma, V., Sebti, I., Pardon, P., Deschamps, A., Pichavant, F. H. 2001. Antimicrobial Edible Packaging Based on Cellulosic Ethers, Fatty Acids, and Nisin Incorporation To Inhibit *Listeria innocua* and *Staphylococcus aureus.* Journal of Food Protection, 4: 470-475(6)

Costa, C. S., Vieira Ronconi, J. V., Felipe Daufenback, J., Gonçalves, C. L., Rezin, G. T., Streck E. L., da Silva Paula, M. M. 2010. *In vitro* effects of silver nanoparticles on the mitochondrial respiratory chain
Molecular and Cellular Biochemistry, 342: 51–56

Costa, E. M., Silva, S., Pina, C., Tavaria, F.K., Pintado, M. M., 2012. Evaluation and insights into chitosan antimicrobial activity against anaerobic oral pathogens. Anaerobe 18, 305-309.

Cotter, P. D., Hill, C., and Ross, P. 2005. Bacteriocins: developing innate immunity for food. Nature Reviews Microbiology, 3(10):777-88.

Cruz, I., Cheetham, J. J., Arnason, J.T., Yack, J.E., and Smith, M.L. 2014. Alkamides from Echinacea disrupts the fungal cell wall-membrane complex. Phytomedicine 21: 435–442

Dahiya, S., Kapil, A., Lodha, R., Kumar, R., Kumar, B., Sood, S., and Kabra, S. K. 2014. Induction of resistant mutants of Salmonella enterica serotype Typhi under ciprofloxacin selective pressure. Indian Journal of Medical Research 139(5): 746-753

Darzynkiewicz, Z., Halicka, H. D., & Zhao, H. 2010. Analysis of Cellular DNA Content by Flow and Laser Scanning Cytometry. Advances in Experimental Medicine and Biology, 676: 137–147

De Berardis, B., Civitelli, G., Condello, M., Lista, P., Pozzi, R., Arancia, G., Meschini, S. 2010. Exposure to ZnO nanoparticles induces oxidative stress and cytotoxicity in human colon carcinoma cells. Toxicology and Applied Pharmacology, 246(3): 116–127

Debabrata, D., Giassudin, A. 2013. Cellular responses of *Saccharomyces cerevisiae* to silver nanoparticles. Research Journal of Biotechnology, 8: 72-77

Delves-Broughton, J., Blackburn, P., Evans, R., Hugenholtz, J. 1996. Applications of the bacteriocin, nisin. Antonie van Leeuwenhoek, 69(2): 193-202

Dettmer, J., Hong-Hermesdorf, A., Sterhof, Y-D., and Shumacher, K. 2006. Vacuolar H^+ -ATPase activity is required for endocytic and secretory trafficking in *Arabidopsis*. The Plant Cell; 18: 715-730

Donald, R. G. K., Skwish, S., Forsyth, R. A., Anderson, J. W., Zhong, T., Burns, C., Lee, S., Meng, X., LoCastro, L., Jarantow, L. W., Martin, J., Lee, S. H., Taylor, I., Robbins, D., Malone, C., Wang, L., Zamudio, C. S., Youngman, P. J., Phillips, J.W. 2009. A *Staphylococcus aureus* Fitness Test Platform for Mechanism-Based Profiling of Antibacterial Compounds. Chemistry & Biology, 16(8): 826-836

Du, D., Wang, Z., James, N. R., Voss, J. E., Klimont, E., Ohene-Agyei, T., Venter, H., Chiu, W., and Luisi, B. F. 2014. Structure of the AcrAB-TolC multidrug efflux pump. Nature, 509(7501), 512–515.

Dulic, V., Egeron, M., Elguindi, I., Raths, S., Singer, B., Riezman, H. 1991. Yeast endocytosis assays. Methods Enzymology, 194: 697-710

Espitia, P. J. P., Soares, N. d. F. F., Coimbra, J. S. d. R., Andrade, N. J., Cruz, R. S., Medeiros, E. A. A., et al. 2012. Zinc oxide nanoparticles: synthesis, antimicrobial activity and food packaging applications. Food Bioprocess Technology, 5: 1447-1464

Fàbrega, A., Madurga, S., Giralt, E., and Vila, J. 2009. Review Mechanism of action of and resistance to quinolones. Microbial Biotechnology, 2(1): 40–61

Fang, T. J., Tsai, H-C. 2003. Growth patterns of *Escherichia coli* O157:H7 in ground beef treated with nisin, chelators, organic acids and their combinations immobilized in calcium alginate gels. Food Microbiology, 20(2): 243–253

Faure, B., Salazar-Alvarez, G., Ahniyaz, A., Villaluenga, I., Berriozabal, G., De Miguel, Y.R., Bergström. L. 2013. Dispersion and surface functionalization of oxide nanoparticles for transparent photocatalytic and UV-protecting coatings and sunscreens. Science and Technology of Advanced Materials, 14: 023001

Fijalkowska, I. J., Schaaper, R. M., and Jonczyk, P. 2012. DNA replication fidelity in *Escherichia coli*: a multi-DNA polymerase affair. FEMS Microbiology Reviews, 36(6): 1105–1121

Firoozan, M. Gran, C. M., Duarte, J. A., and Tuite, M. F., 1990. Quantitation of read-through of termination codons in yeast using a novel gen fusion assay. Yeast, 7: 173-183.

Fischer, E., and Sauer, U. 2003. Metabolic flux profiling of *Escherichia coli* mutants in central carbon metabolism using GC-MS. European Journal of Biochemistry, 270(5): 880–891

Freiberg, C., Brötz-Oesterhel, H. 2005. Review: Functional genomics in antibacterial drug discovery. Drug Discovery Today, 10(13): 927–935.

Freiberg, C., Brötz-Oesterhel, H., and Labischinski, H. 2004. The impact of transcriptome and proteome analyses on antibiotic drug discovery. Current Opinion in Microbiology, 7(5): 451-459.

Freshney R.I. 1994. Culture of Animal Cells: A Manual of Basic Technique. 3rd Ed. WileyLiss. NewYork. USA.

Galván, I. J., Mir-Rashed, N., Jessulat, M., Atanya, M., Golshani, A., Durst, T., Petit, P., Amiguet, V. T., Boekhout, T., Summerbell, R., Cruz, I., Arnason, J. T., Smith, M. L. 2008. Antifungal and antioxidant activities of the phytomedicine pipsissewa, *Chimaphila umbellata*. Phytochemistry, 69: 738-746.

Galván Márquez, I. J., Akaku, J., Cruz, I., Cheetham, J., Golshani, A., and Smith, M. L. 2013. Disruption of protein synthesis as antifungal mode of action of chitosan. International Journal of Food Microbiology, 164(1): 108-112

Gibson, G. R., Roberfroid, M. B., 1995. Dietary modulation of the human colonic microbiotica: introducing the concept of prebiotics. Journal of Nutrition, 125: 1401 – 1412.

Golshania, A., Kolevb, V., Mironova, R., AbouHaidar, M. G., Ivanov, I. G. 2002. Enhancing Activity of ε in *Escherichia coli* and *Agrobacterium tumefaciens* Cells. Biochemical and Biophysical Research Communications, 269(2); 508-512.

González-Rodríguez, I., Gaspar, P., Sánchez, B., Gueimonde, M., Margolles, A., and Rute Neves, A. 2013. Catabolism of Glucose and Lactose in *Bifidobacterium animalis subsp. lactis*, Studied by ^{13}C Nuclear Magnetic Resonance. Applied and Environmental Microbiology, 79(24): 7628-7638

Goparaju, G. N., C., Satishchandran, C., Gupta, P. K. 2009. The effect of the structure of small cationic peptides on the characteristics of peptide-DNA complexes. International Journal of Pharmaceutics, 369(1-2): 162-169

Gottschalk, F., Sonderer, T., Scholz, R.W., Nowack, B. 2009. Modeled environmental concentrations of engineered nanomaterials (TiO_2, ZnO, Ag, CNT, fullerenes) for different regions. Environmental Science & Technology, 43: 9216–9222

Goy, R. C., de Britto, D., and Assis, O. B. G., 2009. A review of the antimicrobial activity of chitosan. Polimeros: Ciência e Tecnologia 19, 241-247.

Gyawali, R., and Ibrahim, S. 2014. Natural products as antimicrobial agents. Food Control, 46: 412-429.

Hardwiger, L. A., Kendra, D. F., Fristensky, B. W., and Wagoner, W., 1985. Chitosan both activates genes in plants and inhibits RNA synthesis in fungi. In: Chitin in Nature and Technology. Muzzarelli, R. A. A., Jeuniaux, C., Gooday, C. (eds.) Plenum Press, New York. P. 210.

Hardy, C. and N. Cozzarelli. 2002. Alteration of *Escherichia coli* Topoisomerase IV to novobiocin resistance. Antimicrobial Agents and Chemotherapy, 47: 941-7.

Hassan, A.A., Howayda, M.E., Mahmoud, H. H. 2013. Effect of Zinc Oxide Nanoparticles on the Growth of Mycotoxigenic Mould. Studies in Chemical Process Technology (SCPT) 1(4)

He, L., Liu, Y., Mustapha, A., Lin, M. 2011. Antifungal activity of zinc oxide nanoparticles against *Botrytis cinerea* and *Penicillium expansum*. Microbiological Research, 166: 207-215.

Helander, I. M., Mattila-Sandholm, T. 2000. Permeability barrier of the Gram-negative bacterial outer membrane with special reference to nisin. International Journal of Food Microbiology, 60: 153–161

Helander, I. M., Nurmiaho-Lassila, E.-L., Ahvenainen, R., Rhoades, J., Roller, S., 2001. International Journal of Food Microbiology 71, 235-244.

Higa, L. H., Schilrreff, P., Perez, A. P., Morilla, M. J., and Romero, E. L. 2013. The intervention of Nanotechnology Against Epithelial Fungal Diseases. Journal of biomaterials and tissue Engineering (3): 1-19.

Holt, K., and Bard, A. 2005. Interaction of silve (I) ions with the respiratory chain of *Escherichia coli:* an electrochemical and scanning electrochemical microscopy study of the antimicrobial mechanism of micromolar Ag. Biochemistry, 44: 13214-13223.

Hoon, S., Smith, A. M., Wallace, I. M., Suresh, S., Miranda, M., Fung, E., Proctor, M., Shokat, K. M., Zhang, C., Davis, R. W., Giaever, G., St. Onge, R. P., and Nislow, C. 2008.An integrated

platform of genomic assays, reveals small-moleculesbioactivities. Nature Chemical Biology, 4(8): 498-506.

Huang, Z., Zheng, X., Yan, D., Yin, G., Liao, X., Kang, Y., Yao, Y., Huang, D., Hao, B. 2008. Toxicological effect of ZnO nanoparticles based on bacteria. Langmuir, 24(8): 4140-4

Huber, L. A. 2003. Is proteomics heading in the wrong direction? Natural Reviews Molecular Cell Biology. 4: 74-80.

Hughes, D. 2003. Microbial Genetics: Exploiting genomics, genetics and chemistry to combat antibiotic resistance. Nature Reviews Genetics, 4(6), 432-441.

Hwang, I. S., Lee, J., Hwang, J. H. , Kim, K. J., Lee, D. G. 2012. Silver nanoparticles induce apoptotic cell death in *Candida albicans* through the increase of hydroxyl radicals. FEBS Journal, 279(7):1327-38.

Ivask, A., Juganson, K., Bondarenko, O., Mortimer, M., Aruoja, V., Kasemets, K., Blinova, I., Heinlaan, M., Slaveykova, V., Kahru, A. 2014. Mechanisms of toxic action of Ag, ZnO and CuO nanoparticles to selected ecotoxicological test organisms and mammalian cells in vitro: a comparative review. Nanotoxicology, 8(S1): 57-71

Ivask, A., Kurvet, I., Kasemets, K., Blinova, I., Aruoja, V., Suppi, S., Vija, H., Kakinen, A., Titma, T., Heinlaan, M., Visnapuu, M., Koller, D., Kisand, V., Kahru, A. 2014. Size-dependent toxicity of silver to bacteria, yeast, algae, crustaceans and mammalian cells *in vitro*. PLOSone 9(7): e102108

Jacoby, G. 2005. Mechanisms of Resistance to Quinolones. Oxford Journals Medicine & Health Clinical Infectious Diseases, 41(Supplement 2): S120-S126.

Jacobs, M. A., Alwood, A., Thaipisuttikul, I., Spencer, D., Haugen, E., Ernst, S., Will, O., Kaul, R., Raymond, C., Levy, R., Chun-Rong, L., Guenthner, D., Bovee, D., Olson, M.V., Manoil, C. 2003. Comprehensive transposon mutant library of *Pseudomonas aeruginosa*. Proceedings of the National Academy of Sciences oof the Unitated States of America, 100: 14339–14344

Jaime, M., Lopez-Llorca, L. V., Conesa, A., Proctor, M., Heisler, L. E., Gebbia, M., Giaever, G., Wetwood, J. T., and Nislow, C., 2012. Identification of yeast genes that confer resistance to chitosan oligosaccharide (COS) using chemogenomics. BMC Genomics 13: 267, 1-26.

Jessulat, M., Malty, R. H., Nguyen-Tran, D.-H., Deineko, V., Aoki, H., Vlasblom, J., Omidi, K., Jin, K., Minic, Z., Hooshyar, M., Burnside, D., Samanfar, B., Phanse, S., Freywald, R., Prasad, B., Zhang, Z., Vizeacoumar, F., Krogan, N. J., Freywald, A., Golshani, A., Babu, M. 2015. Spindle Checkpoint Factors Bub1 and Bub2 Promote DNA Double-Strand Break Repair by Nonhomologous End Joining. Molecular and Cellular Biology, 35(14), 2448–2463

Ji, S. L., Ye, C.H., 2008. Synthesis, growth mechanisms and applications of zinc oxide nanomaterials. Journal of Materials Science and Technology (24): 457-472.

Joo, N. E., Ritchie, K., Kamarajan, P., Miao, D., and Kapila, Y. L. 2012. Nisin, an apoptogenic bacteriocin and food preservative, attenuates HNSCC tumorigenesis via CHAC1. Cancer Med. 1, 295–305.

Juncioni de Arauz, L., Faustino Jozala, A., Gava Mazzola, P., and Vessoni Penna, T. C. 2009. Nisin biotechnological and applications: review. Trends in Food Science & Technology, 20: 146-154

Kamikawa, Y., Hirabayashi, D., Nagayama, T., Fujisaki, J., Hamada, T., Sakamoto, R., Kamikawa, Y., and Sugihara, K. 2014. *In vitro* antifungal activity against oral Candida species using a denture base coated with silver nanoparticles. Journal of Nanomaterials, volume 2014, article ID 780410, 6 pages

Kang, K.H., Shin, H.J., Park, Y.H., Lee, T.S. 1989. Studies on the antibacterial substances produced by lactic acid bacteria: purification and some properties of antibacterial substance "Bifilong" produced by *B. longum*. Korean Dairy Science, 1: 204–216

Kao, Y-Y., Chen, Y-C., Cheng, T-J., Chiung, Y-M., and Liu, P-S. 2012. Zinc Oxide Nanoparticles Interfere With Zinc Ion Homeostasis to Cause Cytotoxicity. Toxicological Sciences, 125(2): 462–472

Karaosmanoglu, K., Sayar, N.A., Kurnaz, I.A., Akbulut, B.S. 2014. Assessment of berberine as a multi-target antimicrobial: A multi-omics study for drug discovery and repositioning. OMICS A Journal of Integrative Biology, 18 (1): 42-53

Kasemets, K., Ivask, A., Dubourguier, H-C., Kahru, A., 2009. Toxicity of nanoparticles of ZnO, CuO and TiO_2 to yeast *Saccharomyces cerevisiae*. Toxicology in Vitro (23): 1116-1122

Kim, J. S., Kuk, E., Yu, K. N., Kim, J-H., Park, S. J., Lee, H. J., Kim, S. H., Park, Y,. K., Park, Y. H., Hwang, C-Y., Kim Y-K., Lee, Y-S., Jeong, D. H., Cho, M-H. 2007. Antimicrobial effect of silver nanoparticles. Nanomedicine: Nanotechnology, Biology and Medicine, 1: 95-101

Kim, K. J., Sung, W.s., Suh, B.K., Moon, S.K., Choi, J.S., Kim, J.G., Lee, D.G. 2009. Antifungal activity and mode of action of silver nano-particles on *Candida albicans*. Biometals, 22: 235-242

Kim, S., and Ryu D-Y. 2013. Silver nanoparticle-induced oxidative stress, genotoxicity and apoptosis in cultured cells an animal tissues. Journal of Applied Toxicology, 3(2): 78-89

Klaenhammer, T. R., 1988. Bacteriocin of lactic acid bacteria. Biochimie, 70: 337 – 349.

Kong, M., Chen, X. G., Xing, K., and Park, H. J., 2010. Antimicrobial properties of chitosan and mode of action: A state of art review. International Journal of Food Microbiology 144, 51-63.

Kopec, K. K., Bozyczko-Coyne, D. 2005. Target identification and validation in drug discovery: the role of proteomics, Biochemical Pharmacology, 69(8): 1133-1139.

Kozlowskia, H., Janicka-Klosb, A., Brasunb, J., Gaggellic, E., Valensinc, D., Valensinc, G. 2009. Copper, iron, and zinc ions homeostasis and their role in neurodegenerative disorders (metal uptake, transport, distribution and regulation). Coordination Chemistry Reviews, 253(21-22): 2665–2685

Kramer, N. E., Smid, E. J., Kok, J., Krujiff, B., Kuipers, O. P., Breukink E. 2004. Resistance of Gram-positive bacteria to nisin is not determined by Lipid II levels. FEMS Microbiology Letters, 239: 157–161

Krogan, N. J., Kim, M., Tong, A., Golshani, A., Cagney, G., Canadien, V., Richards, D.P., Beattie, B.K., Emili, A., Boone, C., Shilatifard. A., Buratowski, S., Greenblatt, J. 2003. Methylation of Histone H3 by Set2 in Saccharomyces cerevisiae Is Linked to Transcriptional Elongation by RNA Polymerase II. Molecular and Cellular Biology, 23(12), 4207–4218.

Kuhn, H-M., Meier-Dieter, U., Mayer, H. 1988. ECA, the enterobacterial common antigen. FEMS Microbiology Reviews, 4(3): 195-222.

Kumar, A., Beloglazova, N., Bundalovic-Torma, C., Phanse, S., Deneiko, V., Gagarinova, A., Musso, G., Vlasblom, J., Lemak, S., Hooshyar, M., Minic, Z., Wagih, O., Mosca, R., Aloy, P., Golshani, A., Parkinson, J., Emili, A., Yakunin, A. F., Babu, M. 2016. Conditional Epistatic Interaction Maps Reveal Global Functional Rewiring of Genome Integrity Pathways in *Escherichia coli.* Cell Reports, 14(3); 648-661

Kutsukake, K., Ohya, Y., and Iino, T. 1990. Transcriptional analysis of the flagellar regulon of *Salmonella* Typhimurium. Journal of Bacteriology, 172(2): 741-747

Le, A. T., Le, T. T., Nguyen, V. Q., Tran, H. H., Dang, D. A., Tran, Q. H., and Vu, D. L. 2012. Powerful colloidal silver nanoparticles for the prevention of gastrointestinal bacterial infections. Advances in Natural Sciences: Nanoscience and Nanotechnology, 3: 045007 (10pp)

LeBel, G., Piché, F., Frenette, M., Gottschalk, M., Grenier, D. 2013. Antimicrobial activity of nisin against the swine pathogen *Streptococcus suis* and its synergistic interaction with antibiotics. Peptides, 50: 19-23

Lee, J., Kim, K-K., Sung, W. S., Kim, J. G., Lee, D. G. The Silver Nanoparticle (Nano-Ag): a New Model for Antifungal Agents. 2010. The Silver Nanoparticle (Nano-Ag): a New Model for Antifungal Agents, Silver Nanoparticles, David Pozo Pérez (Ed.), ISBN: 978-953-307-028-5, InTech, DOI: 10.5772/8510. http://www.intechopen.com/books/silver-nanoparticles/the-silver-nanoparticle-nano-ag-a-new-model-for-antifungal-agents

Lee, J.-S., Chung, M.-J., & Seo, J.-G. 2013. *In Vitro* Evaluation of Antimicrobial Activity of Lactic Acid Bacteria against *Clostridium difficile*. Toxicological Research, 29(2): 99–106.

Lee Ligon, B. 2004. Penicillin: its discovery and early development. Seminars in Pediatric Infectious Diseases, 15(10): 52-57

Lemire, J., Harrison, J. J., and Turner, R. J. 2013. Antimicrobial activity of metals: mechanisms, molecular targets and applications. Nature Reviews Microbiology, 11(6): 371-384.

Li, W., Chen, C., Ye, C., Wei, T., Zhao, Y., Lao, F., Chen, Z., Meng, H., Gao, Y., Yuan, H., Xing, G., Zhao, F., Tang, X., Zhang, Y. 2008. The translocation of fullerenic nanoparticles into lysosome via the pathway of clathrin-mediated endocytosis. Nanotechnology, 19: 145102

Li, Z., Vizeacoumar, F. J., Bahr, S., Li, J., Warringer, J., Vizeacoumar, F. S., Min, R., VanderSluis, B., Bellay, J., DeVit, M., Fleming, A., Stephens, A., Haase, J., Lin, Z-Y., Baryshnikova, A., Lu, H.,Yan, Z., Jin, K., Barker, S., Datti, A., Giaever, G., Nislow, C., Bulawa, C., Myers, C., Constanzo, M., Gingras, A-G., Zhang, Z., Blomberg, A., Bloom, K., Andrews, B., and Boone, C. 2011. Systematic exploration of essential yeast gene function with temperature-sensitive mutants. Nature Biotechnology, 29(4), 361–367.

Lilly, J., & Camps, M. 2015. Mechanisms of Theta Plasmid Replication. Microbiology Spectrum, 3(1), PLAS–0029–2014.

Lipovsky, A., Nitzan, Y., Gedanken, A., and Lubart, R. 2011. Antifungal activity of ZnO nanoparticles- the role of ROS mediated cell injury. Nanotechnology 22, 1-5.

Luli, G. W., & Strohl, W. R. 1990. Comparison of growth, acetate production, and acetate inhibition of *Escherichia coli* strains in batch and fed-batch fermentations. Applied and Environmental Microbiology, 56(4): 1004–1011

Lv, J., Zhang, S., Luo, L., Han, W., Zhang, J., Yang, K., Christie, P. 2012.Dissolution and Microstructural Transformation of ZnO Nanoparticles under the Influence of Phosphate. Environmental Science & Technology, 46 (13), 7215-7221

Ma, P. L., Lavertu, M., Winnik, F.M. and Buschmann, M. D., 2009. New insights into chitosan-DNA interactions using isothermal titration microcalorimetry. Biomacromolecules 10, 1490-1499.

Makras, L., and De Vuyst, L. 2006. The in vitro inhibition of Gram-negative pathogenic bacteria by bifidobacteria is caused by the production of organic acids. International Dairy Journal, 16: 1049–1057

Mark D. Sutton, M. D., and Walker, G. C. 2001. Managing DNA polymerases: Coordinating DNA replication, DNA repair, and DNA recombination. Proceedings of the National Academy of Sciences, 98(15): 8342–8349.

Marlda, C. L., and Valvano, M. A. 1995. Genetic Analysis of the dTDP-Rhamnose Biosynthesis Region of the *Escherichia coli* VW187 (O7:K1) *rfb* Gene Cluster: Identification of Functional Homologs of *rfbB* and *rfbA* in the rff Cluster and Correct Location of the *rffE* Gene. Journal of Bacteriology, 177(19): 5539–5546

Massarsky, A., Trudeau, V.L., Moon, T.W. 2014. Predicting the environmental impact of nanosilver. Environmental Toxicology and Pharmacology, 38(3): 861-73.

Matsuki, T., Watanabe, K., Fujimoto, J., Miyamoto, Y., Takada, T., Matsumoto, K., Oyaizu, H., and Tanaka, R. 2002. Development of 16S rRNA-Gene-Targeted Group-Specific Primers for the Detection and Identification of Predominant Bacteria in Human Feces. Applied and Environmental Microbiology, 68(11): 5445–5451

Mayinger, P. 2012. Phosphoinositides and vesicular membrane traffic. Biochimica et Biophysica Acta - Molecular and Cell Biology of Lipids, 1821(8): 1104-1113

McMahon, H. T., and Gallop, J., 2005. Membrane curvature and mechanisms of dynamic cell membrane remodeling. Nature 438, 590-596.

Mellegård, H., Strand, S. P., Christensen, B. E., Granum, P. E., Hardy, S. P., 2011. Antibacterial activity of chemically defined chitosans: Influence of molecular weight, degree of acetylation and test organism. International Journal of Food Microbiology 148, 48-54.

Memarian, N., Jessulat, M., Alirezaie, J., Mir-Rashed, N., Xu, J., Zareie, M., Smith, M., Golshani, A. 2007. Colony size measurement of the yeast gene deletion strains for functional genomics. BMC Bioinformatics, 8: 117

Miller, B., and Tang, Y-W. 2009. Basic Concepts of Microarrays and Potential Applications in Clinical Microbiology. Clinical Microbiology Reviews: 22(4): 611-633.

Mir-Rashed, N., Cruz, I., Jessulat, M., Dumontier, M., Chesnais, C., Ng, J., Treyvaud, A. V., Golshani, A., Arnason, J. T., and Smith, M. L., 2010. Disruption of fungal cell wall by antifungal Echinacea extracts. Medical Mycology 48, 949–958.

Mitkova, A.V., Khopde, S. M., and Biswas, S. B. 2003. Mechanism and stoichiometry of interaction of DnaG primase with DnaB helicase of *Escherichia coli* in RNA primer synthesis. Journal of Biological Chemistry, 278: 52254-61.

Monaghan, R. L., and Barrett, J. F. 2006. Antibacterial drug discovery – Then, now and te genomics future. Biochemical Pharmacology, 71(7): 901-909

Mu, Q., David, C. A., Galceran, J., Rey-Castro, C., Krzemiński, Ł., Wallace, R., Bamiduro, F., Milne, S. J., Hondow, N. S., Brydson, R., Vizcay-Barrena, G., Routledge, M. N., Jeuken, J. J. C., and Broun, A. P. 2014. Systematic Investigation of the Physicochemical Factors That Contribute to the Toxicity of ZnO Nanoparticles. Chemical Research in Toxicology, 27 (4): 558–567

Mumberg, D., Müller, R., and Funk, M., 1994. Regulatable promoters of *Saccharomyces cerevisiae*: comparison of transcriptional activity and their use for heterologous expression. Nucleic Acids Research 22(25), 5767-5768.

Mussato, S. I., and Mancilha, I. M., 2006. Non-digestible oligosaccharides: A review. Carbohydrate Polymers, 68: 587 – 597.

Nanotech Project, 2014. Project on Emerging Nanotechnologies. Consumer Products Inventory,
http://www.nanotechproject.org/cpi (accessed 01.10.14)

Nasrollahi, A., Pourshamsian, Kh., Mansourkiaee, P. 2011. Antifungal activity of silver nanoparticles on some fungi. International Journal of Nano Dimension, 1(3): 233-239

Nel, A., Xia, T., Mädler, L., Li, N. 2006. Toxic Potential of Materials at the Nanolevel. Science 311, 622-627.

Niazi, J.H., Sang, B-I, Kim, Y. S., and Gu, M. G. 2011. Global gene response in *Saccharomyces cerevisae* exposed to Silver nanoparticles. Applied Biochemistry Biotechnology 26: 1278-1291

Nijman, S. 2015. Functional chemical genomics to uncover drug mechanism of action. Nature Chemical Biology 11(12), 942–948.

Nomura, T., Miyazaki, J., Miyamoto, A., Kuriyama, Y., Tokumoto, H., and Konishi, Y. 2013. Exposure of the yeast *Saccharomyces cerevisiae* to functionalized polystyrene latex nanoparticles: Influence of surface charge on toxicity. Environmental Science and Technology, 47: 3417-3423

Oh, M.K., Rohlin, L., Kao, K. C., Liao, J. C. 2002. Global Expression Profiling of Acetate-grown *Escherichia coli*. Journal of Biological Chemistry, 277: 13175-13183

Omidi, K., Hooshyar, M., Jessulat, M., Samanfar, B., Sanders, M., Burnside, D., Pitre, S., Schoenrock, A., Xu. J., Babu, M., Golshani, A. 2014 Phosphatase Complex Pph3/Psy2 Is Involved in Regulation of Efficient Non-Homologous End-Joining Pathway in the Yeast *Saccharomyces cerevisiae*. PLoS ONE 9(1): e87248.

Ortiz de Montellano, P. R., David, S. K., Ator, M. A., and Tew, D. 1988. Mechanism-Based Inactivation of Horseradish Peroxidase by Sodium Azide. Formation of meso-Azidoprotoporphyrin 1x7. Biochemistry, 27 (15): 5470–5476

Palanikumar, L., Ramasamy, S. N., Balachandran, C. 2012. Size-dependent antimicrobial response of zinc oxide nanoparticles. IET Nanobiotechnology vol 8(2): 111-117

Palma-Guerrero, J., López-Jiménez, J.A., Pérez-Berna, A.J., Huang, I.-C., Jansson, H.-B., Salinas, J., Villalain, N.D., and López-Llorca, L.V., 2010. Membrane fluidity determines sensitivity of filamentous fungi to chitosan. Molecular Microbiology 75, 1021-1032.

Parsons, A. B. , Geyer, R., Hughes, T. R., Boone, C. 2003. Yeast genomics and proteomics in drug discovery and target validation. Progress in Cell Cycle Research, 5: 159-66.

Parsons, A. B., Brost, R. L., Ding, H., Li, Z., Zhang, C., Sheikh, B., Brown, G. W., Kane, P. M., Hughes, T. R., and Boone, C., 2004. Integration of chemical-genetic and genetic interaction data links bioactive compounds to cellular target pathways. Nature Biotechnology 22, 62-69.

Payne, D. J., Gwynn, M. N., Holmes, D. J., Pompliano, D. L. 2007. Drugs for bad bugs: confroting the challenges of antibacterial discovery. Nature Reviews Drug Discovery, 6(1): 29-40.

Pearson, R. G. 1963. Hard and soft acids and bases. Journal of the American Chemical Society, 85: 3533-3539

Piccinno, F., Gottschalk, F., Seeger, S., Nowack, B. 2012. Industrial production quantities and uses of ten engineered nanomaterials in Europe and the world. Journal of Nanoparticle Research, 14: 1109–1119

Pokusaeva, K., Fitzgerald, G. F., van Sinderen, D. 2011. Carbohydrate metabolism in Bifidobacteria. Genes and Nutrition, 6(3): 285-306.

Porwollik, S., Santiviago, C. A., Cheng, P., Long, F., Desai, P., Fredlund, J., Srikumar, S., Silva, C. A., Chu, W., Chen, X., Canals, R., Reynolds, M., Bogomolnaya, L. Shields, C., Cui, P., Guo, J., Zheng, Y., Endicott-Yazdani, T., Yang, H-J., Maple, A., Ragoza, Y., Blondel, C. J., Valenzuela, C., Andrews-Polymenis, H., McClelland, M. 2014. Defined Single-Gene and Multi-Gene Deletion Mutant Collections in Salmonella enterica sv Typhimurium. PLoS ONE 9(7): e99820.

Quaranta, D., Krans, T., Santo, C. E., Elowsky, C. G., Domaille, D. W., Chang, C. J., & Grass, G. 2011. Mechanisms of Contact-Mediated Killing of Yeast Cells on Dry Metallic Copper Surfaces. Applied and Environmental Microbiology, *77*(2), 416–426.

Raafat, D., von Bargen, K., Haas, A., and Sahl, H. G., 2008. Insights into the mode of action of chitosan as an antibacterial compound. Applied and Environmental Microbiology 74, 3764-3773.

Rabea, E. I., Badawy, M., Stevens, C.V., Smagghe, G., and Steurbaut, W., 2003. Chitosan as antimicrobial agent: Applications and mode of action. Biomacromolecules 4(6), 1457-1465.

Riezman H. 1985. Endocytosis in yeast: several of the yeast secretory mutants are defective in endocytosis. Cell 40: 1001–1009.

Riley, M. A., 1998. Molecular mechanisms of bacteriocin evolution. Annual Reviews of Genetics, 32: 255 – 278.

Roemer, T., and Boone, C. 2013. Systems-level antimicrobial drug and drug synergy discovery. Nature Chemical Biology, 9(4): 222-231.

Rohde, J. R., Trinh, J., and Sadowski, I. 2000. Multiple signals regulate *GAL* transcription in yeast. Molecular and Cellular Biology, 20(11): 3880-3886

Rudi, K., Skulberg, O.M., Larsen, F., Jacoksen, K.S., 1997. Strain classification of oxyphotobacteria in clone cultures on the basis of 16S rRNA sequences from variable regions V6, V7 and V8. Applied Environmental and Microbiology, 63: 2593– 2599

Ruiz, B., Chávez, A., Forero, A., García-Huante, Y., Romero, Al., Sánchez, M., Rocha, D., Sánchez, B., Rodríguez-Sanoja, R., Sánchez, S., and Langley, E. 2010. Production of microbial secondary metabolites: regulation by the carbon source. Critical Reviews in Microbiology, 36(2), 146-167.

Saleh, A., El-Sayed, E.M. 2004. Isolation and characterization of bacteriocins produced by *Bifidobacterium lactis* BB-12 and *Bifidobacterium longum* BB-46. 9th Egyptian Conference for Dairy Science and Technology, Research Papers, Cairo, pp. 323–337

Sallam, K. I. 2007. Antimicrobial and antioxidant effects of sodium acetate, sodium lactate, and sodium citrate in refrigerated sliced salmon. Food Control, 18(5): 566–575.

Samanfar, S., Omidi, K., Hooshyar, M., Laliberte, B., Alamgir, M. D., Seal, A. J., Ahmed-Muhsin, E., Viteri, D. F., Said, K., Chalabian, F., Golshani, A., Wainer, G., Burnside, D., Shostak, K., Bugno, M., Willmore, W. G., Smith, M. L., and Golshani, A. 2013. Large-scale investigation of oxygen response mutants in *Saccharomyces cerevisiae*. Molecular Biology Systems, 9(6); 1351-1359

Samanfar B., Tan, le H., Shostak, K., Chalabian, F., Wu, Z., Alamgir, M., Sunba, N., Burnside, D., Omidi, K., Hooshyar, M., Galván Márquez, I., Jessulat, M., Smith, M.L., Babu, M., Azizi, A., Golshani, A. 2014. A global investigation of gene deletion strains that affect premature stop codon bypass in yeast, *Saccharomyces cerevisiae*. Molecular Biology Systems, 10(4):916-24.

Sánchez, S. N., and Königsberg, M. 2006. Using Yeast to Easily Determine Mitochondrial Functionality with 1-(4,5-Dimethylthiazol-2-yl)-3,5-diphenyltetrazolium Bromide (MTT) Assay. Biochemistry And Molecular Biology Education, 34(3): 209–212

Silver, L.L. 2007. Multi-targeting by monotherapeutic antibacterials. Nature Reviews Drug Discover, 6 (1): 41-55

Singh, S. B. 2014. Confronting the challenges of discovery of novel antibacterial agents. Bioorganic & Medicinal Chemistry Letters, 24(16), 3683-3689.

Šišková, K. M., Machala, L., Tuček, J., Kašlík, J., Mojzeš, P., and Zbořil, R. 2013. Mixtures of L-Amino Acids as Reaction Medium for Formation of Iron Nanoparticles: The Order of Addition into a Ferrous Salt Solution Matters. International Journal of Molecular Sciences, 14(10): 19452–19473.

Smith, A. M., Ammar, R., Nislow, C., & Giaever, G. 2010. A survey of yeast genomic assays for drug and target discovery. Pharmacology & Therapeutics, 127(2), 156–164.

Sobrino-Lopez, A., Belloso-Martin, O. 2008. Use of nisin and other bcteriocins for preservatio of dairy products. International Dairy Journal, 18: 329-343

Souza, H. K. S., Bai, G., Gonçalves, M. P., and Bastos, M., 2009. Whey protein isolate-chitosan interactions: A calorimetric and spectroscopy study. Termochimica Acta 495, 108-114.

Spellberg, B., Power, J., Brass, E., Miller, L. G., and Edwards, Jr. J. E. 2004. Trends in antimicrobial drug development: Implications for the Future.Clinical Infectious Diseases, 38(9): 1279-1286

Spring, D. R. 2004. Chemical genetics to chemical genomics: small molecules offer a big insight. Chemical Society Reviews, 34: 472-482

Stanfield, I., Akhmaloka, and Tuite, M. F., 1994. A mutant allele of the SUP45 (SAL4) gene of *Saccharomyces cerevisiae* shows temperature-dependent allosuppressor and omnipotent suppressor phenotypes. Current Genetics 27(5), 417-426.

Stevens, K., Sheldon, B. W., Klapes, N. A., and Klaenhammer, T. R. 1991. Nisin Treatment for Inactivation of *Salmonella* Species and Other Gram-Negative Bacteria. Applied And Environmental Microbiology, 57, (12): 3613-3615

Stiles, J., Penkar, S., Plocková, M., Chumchalová, J., Bullerman, L. B. 2002. Antifungal activity of sodium acetate and *Lactobacillus rhamnosus*. Journal of Food Protection, 65(7): 1188-91

Strober W. 1. 2001. Trypan blue exclusion test of cell viability. C*urrent Protocols* in *Immunology*. Appendix 3: Appendix 3B. doi: 10.1002/0471142735.ima03bs21

Su, H-L., Chou, C-C., Hung, D-J., Lin, S-H., Pao, I-C., Lin, J-H., Huang, F-L., Dong, R-X., J-J., Lin. 2009. The disruption of bacterial membrane integrity through ROS generation induced by nanohybrids of silver and clay. Biomaterials, 30: 5979-5987

Sudarshan, N. R., Hoover, D. G., and Knorr, D., 1992. Antibacterial action of chitosan. Food Biotechnology 6(3), 257-272.

Sutton, M. D., & Walker, G. C. 2001. Managing DNA polymerases: Coordinating DNA replication, DNA repair, and DNA recombination. Proceedings of the National Academy of Sciences of the United States of America, 98(15): 8342–8349.

Suzuki, T., Higashiyama, T., Takata, K. 1997. DNA Staining for Fluorescence and Laser Confocal Microscopy. The Journal of Histochemistry & Cytochemistry 45(1): 49–53, 1997

Swain, P., Nayak, S. K., Sasmal, A., Behera, T., Barik, S. K., Swain, S. K., Mishra, S. S., Sen, A. K., Das, J. K., Jayasankar, P. 2014. Antimicrobial activity of metal based nanoparticles against microbes associated with diseases in aquaculture. World Journal of Microbiology and Biotechnology, 30: 2491-2502

Tatusov, R. L., Fedorova, N. D., Jackson, J. D., Jacobs, A. R., Kiryutin, B., Koonin, E. V., Krylov, D. M., Mazumder, R., Mekhedov, S. L., Nikolskaya, A. N., Rao, B. S., Smirnov, S., Sverdlov, A. V., Vasudevan, S., Wolf, Y. I., Yin, J. J. and Natale, D. A., 2003. The COG database: an updated version includes eukaryotes. BMC Bioinformatics 4, 41

Tong, Z., Ni, L., Ling, J. 2014. Review: Antibacterial peptide nisin: A potential role in the inhibition of oral pathogenic bacteria. Peptides, 60: 32-40

Touré, R., Kheadr, E., Lacroix, C., Moroni, O., Fliss, I. 2003. Production of antibacterial substances by bifidobacterial isolates from infant stool active against *Listeria monocytogenes.* Journal of Applied Microbiology, 95: 1058–1069

Tran, S.-L., Puhar, A., Ngo-Camus, M., & Ramarao, N. 2011. Trypan Blue Dye Enters Viable Cells Incubated with the Pore-Forming Toxin HlyII of *Bacillus cereus*. PLoS ONE, 6(9), e22876. http://doi.org/10.1371/journal.pone.0022876

Tu, A-H. T., Tu. 2010. Transformation of Escherichia coli made competent by calcium chloride protocol. American Society for Microbiology Microbel Library. http://www.microbelibrary.org/component/resource/laboratory-test/3152-transformation-of-escherichia-coli-made-competent-by-calcium-chloride-protocol

Vamanu, E., and Vamanu, A. 2010. The influence of prebiotics on bacteriocin synthesis using the strain *Lactobacillus parcasei* CMGB16. African Journal of Microbiology Research, 4(7): 534-537.

Van der Meulen, R., Adriany, T., Verbrugghe, K., and De Vuyst, L. 2006. Kinetic Analysis of Bifidobacterial Metabolism Reveals a Minor Role for Succinic Acid in the Regeneration of NAD+ through Its Growth-Associated Production. Applied and Environmental Microbiology, 72(8): 5204–5210.

Vázquez-Muñoz, R., Ávalos-Borja, M., and Castro-Longoria, E. 2014. Ultrastructural analysis of *Candida albicans* when exposed to silver nanoparticles. PLOS ONE, 9(10): e108876

Ventura, M., Canchava, C., Fitzgerald, G., Gupta, R. S., van Sinderen, D. 2007. Genomics as a means to understand bacterial phylogeny and ecological adaptation: the case of bifidobacteria. Antonie van Leeuwenhoek 91:351–372.

Vidal-Aroca, F., Giannattasio, M., Brunelli, E., Vezzoli, A., Plevani, P., Muzi-Falconi, M., and Bertoni, G. 2006. One-step high-throughput assay for quantitative detection of b-galactosidase activity in intact Gram-negative bacteria, yeast, and mammalian cells. BioTechniques, 40: 433-440.

Von Ah, U. 2006. Identification of Bifidobacterium thermophilum RBL67 isolated from baby faeces and partial purification of its bacteriocin (Doctoral dissertation Thesis). Swiss Federal Institute of Technology. Zurich: p. 1–192. *e-collection.library.ethz.ch/eserv/eth:29373/eth-29373-02.pdf*

Wecke, T., and Mascher, T. 2011. Antibiotic research in the age of omics: from expression profiles to interspecies communication. Journal of Antimicrobial Chemotherapy, 66 (12): 2689-2704

Wiedemann, I., Benz, R., Sahl, H-G. 2004. Lipid II-Mediated Pore Formation by the Peptide Antibiotic Nisin: a Black Lipid Membrane Study. Journal of Bacteriology, 186(10): 3259-3261.

Wiederkehr, A., Meier, K.D., and Riezman, H. 2001. Identification and characterization of *Saccharomyces cerevisiae* mutants defective in fluid-phase endocytosis. Yeast 18: 759-773

Winzeler, E.A., Shoemaker, D.D., Astromoff, A., Liang, H., Anderson, K., Andre, B., Bangham, R., Benito, R., Boeke, J.D., Bussey, H., Chu, A.M., Bakkoury, M.E., Foury, F., Friend, S.H., Gentalen, E., Giaever, G., Hegemann, J.H., Jones, T., Laub, M., Liao, H., Liebundguth, N., Lockhart, D.J., Lucau-Danila, A., Lussier, M., M'Rabet, N., Menard, P., Mittmann, M., Pai, C., Rebischung, C., Revuelta, J.L., Riles, L., Snyder, M., Sookhai-Mahadeo, S., Storms, R. K., Veronneau, S., Voet, M., Volckaert, G., Ward, T., Wysocki, R., Yen, G. S., Yu, K., Zimmermann, K., Philippsen, P., Johnston, M., Davis, R. W., 1999. Functional characterization of *S. cerevisiae* genome by gene deletion and parallel analysis. Science 285, 901-906.

Wiseman, H., and Halliwell, B. 1996. Damage to DNA by reactive oxygen and nitrogen species: role in inflammatory disease and progression to cancer. Biochemical Journal, 313, 17-29.

World Health Organization WHO (2014) Antimicrobial resistance: a global report on surveillance

Xia, T., Kovochich, M., Liong, M., Mädler, L., Gilbert, B., Shi, H., Yeh, J. I., Zink, J. I., and Nel, A. E. 2008. Comparison of the Mechanism of Toxicity of Zinc Oxide and Cerium Oxide Nanoparticles Based on Dissolution and Oxidative Stress Properties. ACS Nano, 2(10): 2121–2134

Xu, T., Bharucha, N., and Kumar, A. 2011. Genome-wide Transposon mutagenesis in *Saccharomyces cerevisiae* and *Candida albicans*. Methods in Molecular Biology, 765: 207-224.

Yang, S.-C., Lin, C.-H., Sung, C. T., & Fang, J.-Y. 2014. Antibacterial activities of bacteriocins: application in foods and pharmaceuticals. Frontiers in Microbiology, 5, 241.

Yehia, R., and Ahmed, O.F. 2013. *In vitro* study of the antifungal efficacy of zinc oxide nanoparticles against *Fusarium oxysporum* and *Penicillum expansum*. African Journal of Microbiology Research, 7(9): 1917-1923.

Yildirim, Z., Winters, D. K., Johnson, M. G. 1999. Purification, amino acid sequence and mode of action of bifidocin B produced by *Bifidobacterium bifidum* NCFB 1454. Journal of Applied Microbiology, 86: 45–54

Yoonkyoung, P., Kim, M-H., Park, S.-C., Cheong, H., Jang, M-K., Nah, J-W., and Hahm, K-S., 2007. Investigation of the antifungal activity and mechanism of action of LMWS-Chitosan. J. Microbiology and Biotechnology 18, 1729-1734.

Yu, L., Castillo, L. P., Mnaimneh, S., Hughes, T. R., & Brown, G. W. 2006. A Survey of Essential Gene Function in the Yeast Cell Division Cycle. Molecular Biology of the Cell; 17(11), 4736–4747

Zakrzewska, A., Boorsma, A., Brul, S., Hellingwerf, J.K. and Klis, F.M., 2005. Transcriptional response of *Saccharomyces cerevisiae* to the plasma membrane-perturbing compound chitosan. Eukaryotic Cell 4, 703-715.

Zakrzewska, A., Boorsma, A., Delneri, D., Brul, S., Oliver, S.G. and Klis, F.M., 2007. Cellular processes and pathways that protect *Saccaromyces cerevisiae* cells against the plasma membrane-perturbing compound chitosan. Eukaryotic Cell 6, 600-608.

Zhang, L., Jiang, Y., Ding, Y., Daskalakis, N., Jeuken, L., Povey, M., O'Neill, A. J., York, D. W. 2010. Mechanistic investigation into antibacterial behaviour of suspensions of ZnO nanoparticles against *E. coli*. Journal of Nanoparticle Research, 12(5): 1625-1636

Zhang, L., Jiang, Y., Ding, Y., Povey, M., York, D., 2007. Investigation into the antibacterial behaviour of suspensions of ZnO nanoparticles (ZnO nanofluids). Journal of Nanoparticles Research, 9: 479-489

Zhang, T., Wang, L., Chen, Q. 2014. Cytotoxic Potential of Silver Nanoparticles. Yonsei Medical Journal, 55(2): 283–291.

Ziólkowska, N., Christiano, R., and Walther, T., 2012. Organized living: formation mechanisms and functions of plasma membrane domains in yeast. Trends in Cell Biology 22, 151-158.